The University Of Sheffield.

Hydrothermal Liquefaction of Lignocellulosic Biomass

By:

Nur Atiqah Nasir

The University of Sheffield
Faculty of Engineering
Department of Chemical and Biological Engineering

April 2019

A special dedication to:

My beloved and ever-inspiring late father Nasir Ali,
My lovely late mother Maryam Ahmad,

And all my brothers:

Nukman Nasir
Nasuha Nasir
Nasiruddin Nasir
Nuh Nasir
Nasreen Nasir

Acknowledgments

First and foremost, I would like to express my deepest gratitude and appreciation to my supervisor, Dr James McGregor for his attention, guidance, continues comments and patience throughout this PhD project.

I would like to convey my thanks to the technical staff in Department of Chemical and Biological Engineering; Adrian Lumby, Andy Patrick, Duncan Scofield, Usman Younis and Mark Jones who have been involve directly and indirectly in completing my research project. Also, thanks to Ali Al- Shathr, Cynthia Kartey, Ming Liu and all members in Catalysis Group, University of Sheffield that assisted me in completion of this PhD. I also thankful to Malaysian government and Universiti Sains Islam Malaysia (USIM) for the scholarship and financial support during my study time in Sheffield.

My personal appreciation to all my family members especially my sister in-law, Azmainie and all my brothers for their patient, love and the moral support, especially after our father had passed away; which I consider all of that as something beyond repayment. To those who helped me with advices and motivations (my cousin, Dalina and my housemate, Ejok) thank you. Last but not least, a special thanks to all my friends in Sheffield (Kamalliawati, Norfadhilah, Norhuda, Zati Aqmar and TCC's group) and in Malaysia (Salmiah and Sarina), who always kept me going in positive vibes.

Abstract

The introduction of a bio-refinery approach in producing bio-chemicals represents a potential opportunity to cover the increased demand for fine chemicals and reduce the societal dependence on fossil sources for petrochemicals. Valorisation of lignocellulosic material for the production of renewable chemicals has attracted much attention as such chemicals could significantly improve the economics of bio-refineries. The present work has investigated the conversion of brewer's spent grain (BSG), a raw material in the form of food industry wastes into value-added chemical and biofuels. BSG represent around 85% of the total by-products generated from the brewing industry and is available in large quantities throughout the year; however its primary application has been limited to animal feed. Despite this, due to its chemical composition, it has value as lignocellulosic rich material. In this thesis, raw BSG has undergone physical and chemical characterisation to determine the composition and selection of appropriate technologies for their utilisation. BSG contains a high moisture content (approx. 75 wt. %). As a consequence, any application towards utilisation of this waste needs to consider the best way to handle their moisture content. Hydrothermal liquefaction (HTL) is the thermochemical conversion of biomass by processing in a hot, pressurised water environment for sufficient time to break down the solid biopolymeric structure to predominantly liquid components. The potential of HTL to break down the lignocellulosic compounds was demonstrated by using both biomass model components (cellulose and lignin) and real biomass, BSG. However, due to the complex composition of real biomass, the product distribution obtained from BSG HTL is significantly different when compared to the biomass model. The most favourable processing condition identified based on both model and real biomass systems were found to be 250 ºC, 30 min reaction time and 80 barg. Further investigation on HTL shows, with the addition of methanol, ethanol and 2-propanol in direct liquefaction reaction, the conversion and water-soluble oil (WSO) yield increased significantly compared to the pure water system. The best conversion was obtained by a methanol-water solvent system at 82%, while 2-propanol-water system produces the highest WSO yield at 29%. Moreover, BSG biochar also shows a potential to be used directly as solid fuel without the need for significant modifications.

Table of Contents

List of Figure

List of Table

List of Abbreviation

BSG	- Brewer's spent grain
EtOH	- Ethanol
EF-BSG	- Extractive free BSG
FTIR	- Fourier- Transform Infrared
GC	- Gas chromatography
GCMS	- Gas chromatography mass spectroscopy
H_2SO_4	- Sulphuric acid
HHV	- Higher heating value
HMF	- Hydroxymethylfurfural
HTC	- Hydrothermal carbonisation
HTG	- Hydrothermal gasification
HTL	- Hydrothermal liquefaction
LA	- Levulinic acid
MeOH	- Methanol
NaOH	- Sodium hydroxide
TG	- Thermogravimetric
TGA	- Thermogravimetric analysis
TGA-DTA	- Thermogravimetric analysis-differential thermal analysis
PrOH	- Propanol
Ppm	- part permillion
SC	- Supercritical state
SCW	- Supercritical water
XRF	- X-ray fluoresence
WSO	- Water-soluble oil

CHAPTER 1

INTRODUCTION

Chapter 1: Introduction

1.0 Introduction

The world's energy use is complex and changing. Total energy use rises with the increasing population and economic activity, and technological and commercial innovations affect the type of energy used. As the result, the amount of energy used varies throughout the world depending on both, technology and available resource (BP, 2014). Technology development and industrialisation of mankind is growing rapidly every day, reaching a new method to make use of the resources, in order to provide better options for satisfying human needs. However, due to international phenomena such as climate change as a result of greenhouse emissions or fossil fuel shortages occurring are encouraging a divert towards sustainable development (Fernando *et al.*, 2006; Mohanty *et al.*, 2014). Alternative energy resources, which are cheap, renewable and do not cause pollution are highly needed to meet the current demand for energy. Therefore, renewable sources such as solar, wind, thermal, hydroelectric and biomass need to be alternated (Maity, 2015).

1.1 Renewable Sources: Biomass

An ideal source of renewable energy is one that can be replenished over a relatively short period of time or is essentially supply-free. Resources such as coal, natural gas and crude oil come from carbon dioxide, which was fixed by nature by photosynthesis several million years ago. They are of limited supply, they can not be replaced and therefore can not be renewed. Resources such as solar radiation, wind, tides and biomass are considered to be renewable sources that are not in danger of being over-exploited if properly managed. It is important to note, however, that while the first three resources can be used as a renewable energy source, biomass can be used to produce energy as well as chemicals and materials. (James H. Clark, 2011).

Biomass is a carbon neutral resource in its life cycle and can be converted into convenient solid, liquid and gaseous fuels through different conversion

processes (Özbay *et al.*, 2001). Biomass alone contributes to more than 50% of world's renewable energy (Maity, 2015) and been used to meet a variety of energy needs, including generating electricity, fuelling vehicles and providing process heat for industries (Bridgwater, 1999, 2003).

According to Demirbaş, (2001) and Saxena, Adhikari and Goyal(2009), biomass can be obtained from various sources and been categories as below:

i) Wastes: This category comprises wastes from agricultural production, process waste from agro industries, crop residues, etc.
ii) Standing forests: This comprises various intermediate products and residual wastes of different nature.
iii) Energy crops: This energy crop includes various edible and non-edible crops.

There is considerable political and social pressure nowadays to reduce pollution from industrial activities. Nearly all developed and underdeveloped countries try to adapt to this reality by modifying their processes in order to recycle their residues (Mussatto, Dragone and Roberto, 2006). Moreover, industrial ecology concepts and circular economy have been considered leading principle for 'zerowaste' society and economy where wastes are used as raw material for new products and applications. This is so called an industrial symbiosis (Ragauskas *et al.*, 2006), in which the goal is to use wastes from one sector as an input for other sectors as shown in Figure 1-1. Besides, many industrial waste have the potential to be reused into other production systems, e.g. bio-refineries (Forster-Carneiro *et al.*, 2013a) in which when comparing to other sources, wastes category would be the best and the most environmentally friendly sources for the biomass. This represents not only a resource problem but also an environmental and economic one, on top of being a moral challenge for the modern society nowadays.

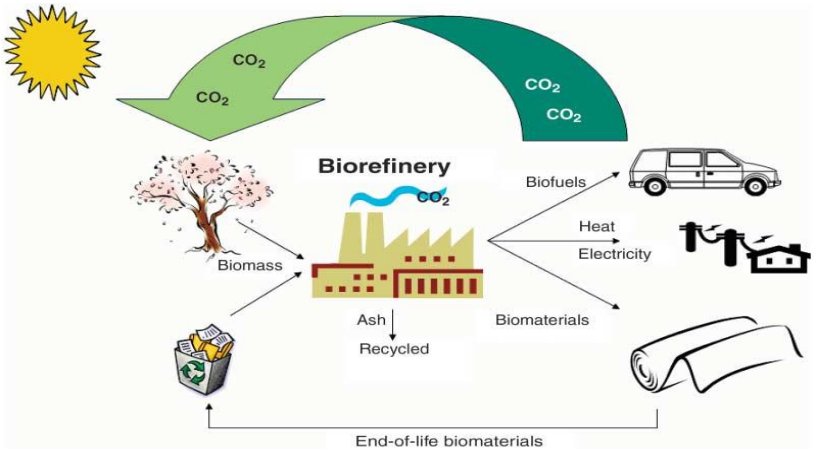

Figure 1-1: The fully integrated agro-biofuel-biomaterial-biopower cycle for sustainable technologies, adapted from The path forward for biofuels and biomaterials (Ragauskas et al., 2006).

1.1.1 Brewer's spent grain (BSG)

BSG is a low value by-product of the brewery industry and been produced in large quantity throughout the year (Aliyu and Bala, 2013; Malomo, 2013; Lynch, Steffen and Arendt, 2016). In the brewery process, the barley malt was partially liquefied and the produced liquor called wort was separated from the solid residues produce BSG as leftover product. The filtered liquor is subsequently brewed to beer, while BSG remain as by-product of this process which is currentlyeither disposed of to landfill/incinerated as waste or been used as animal feed due to its high sugar and protein content (Zhang and Wang, 2016). Breweries generate more than 250 million tonnes of wet BSG every year in the UK (Asad S.N. Mahmood *et al.*, 2013) and wet BSG contains a large amount of moisture, typically 67-81 (w/w%). Because of its high content of moisture and fermentable sugars, BSG is a very unstable material and is susceptible to rapid deterioration due to microbial activity (Fărcaş *et al.*, 2014). Therefore, is an urge to find a way for develop value-added end-used for this by-product.

1.2 Hydrothermal liquefaction (HTL)

HTL is as wet thermal process at relatively moderate reaction conditions; temperature below 420°C and pressure between 10 and 30MPa (Anselmo Filho and Badr, 2004; A. a. Peterson *et al.*, 2008) which converts biomass into biofuels mainly

in a liquid form) bio-oil. HTL work properly with feedstock with high moisture content, then, drying process as pre-treatment is not necessary as in gasification or pyrolysis. Pre-treatment is a bottleneck in the waste conversion since drying process typically takes large quantity of energy and time thereby making HTL technology an attractive option for biomass utilization. Additionally, the product of HTL is a bio-oil with less oxygen content and higher heating value in comparison with other processes (Zhu *et al.*, 2009).

The above indication provides sufficient arguments to foster research and development in the conversion of waste biomass to biofuels through the HTL process as a reliable way to address the new energy supply challenges. Converting waste biomass by HTL is one of the approaches for alternative processes that can potentially be used in near future as promising technology in fulfil the need of energy demand.

1.3 Objectives of the research

The ultimate goal of this research is contribute to the development for conversion of industrial biomass waste into valuable chemicals and fuel. BSG waste was used as a case study and were undergone HTL process. The aim will be accomplish by meeting the following objectives:

1. To characterise the raw BSG in order to understand their physical properties and chemical composition as lignocellulosic biomass.
2. To study the HTL reaction conditions using model biomass components; cellulose and lignin as single and binary model reaction system.
3. To compare the liquid product distribution in HTL between model system and real biomass system, BSG.
4. To investigate the effect of alcoholic solvent in direct liquefaction process based on conversion, water-soluble oil (WSO) yield and biochar product.
5. To determine the properties and potential used for BSG biochar as solid fuel.

CHAPTER 2

LITERATURE REVIEW

Chapter 2: Literature review

2.0 Introduction

Current growing industrialisation and motorisation of the world has led to a steep rise in demand for petroleum-based fuels. It is necessary to develop renewable resources in order to produce biofuels and biochemical for economic and sustainable development due to over-consumption of petroleum sources (Lee, Hamid and Zain, 2014). The European Union has already approved environmental abuse legislation and has begun to make greater efforts to find environmentally friendly materials based on natural resources (Isikgor and Becer, 2015). Hence, the alternative solutions in developing sustainable energy and fine chemicals should come from renewable natural resources; which will decrease the current dependence on fossil resources, and fixed the negative impact due to greenhouse gas (GHG) emission associated with their use (Brennan and Owende, 2010; Borugadda and Goud, 2012). Climate change is currently believed to be the most pressing global environmental issue (Atabani *et al.*, 2012) and as the result, it have stimulated the search for alternative sources which is GHG mitigation and carbon neutral (Kumar *et al.*, 2016).

2.1 Biomass: A renewable feedstock

Biomass refers to material of biological origin and can be derived from growing plant or from animal manure (Babu, 2008). Compare to other sources for renewable energies, biomass and biomass derived material was described as "sleeping giant" due to its high worldwide availability, associated with limited valuation (Déniel *et al.*, 2016). Biomass has been labelled as an abundant carbon neutral renewable source that can reduce CO_2 emissions and atmospheric pollution. Biomass plant derived was estimated to be produce about 1.3×10^{10} metric tons per annum which is energetically equivalent to about two-thirds of the world's energy requirement (Ganesh D. Saratale, 2012). The biomass materials been generated from available atmospheric CO_2, water and sunlight through biological photosynthesis process and represent a renewable and cheap sources for a renewable feedstock.

However, the sustainability on production of fuels and chemicals from biomass has been greatly debated; there are critical concerns regarding the sustainability of current production of bioethanol, which relies on starch and sugar crops. For example, in 2015, Brazil and the United States produced approximately 70% of the global biofuel supply which primarily use sugarcane and corn as based for the bio-ethanol, respectively (GBEP, 2007; Araújo *et al.*, 2017). These production may lead in competition with food and feed industries for the use of biomass and agricultural land, giving rise to ethical implications(Cherubini, 2010). Lignocellulosic feedstocks have crucial advantages over other biomass supplies in this manner because they are the non-edible portion of the plant and therefore, they do not interfere with food supplies(Nigam and Singh, 2011). Large amounts of lignocellulosic materials are generated from waste materials mainly from agricultural residues, forestry product and industrial and municipal waste (Gallezot, 2012; Iqbal, Kyazze and Keshavarz, 2013; Van Rossum *et al.*, 2014). In overall, the use of lignocellulosic biomass can maximize economic and environmental benefits, while minimizing waste and pollution (Briens, Piskorz and Berruti, 2008; Isikgor and Becer, 2015).

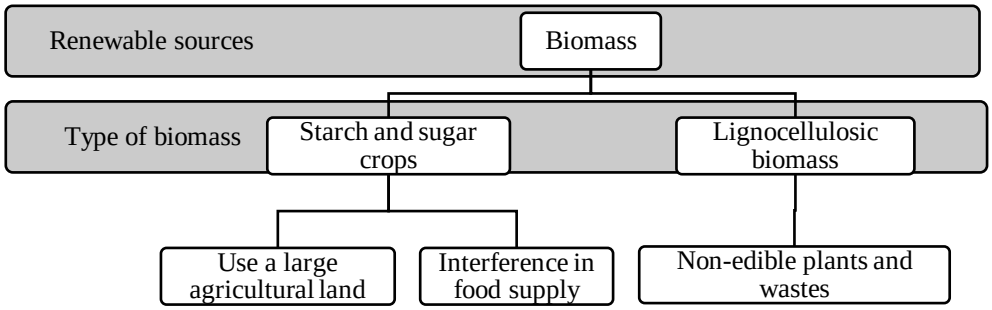

Figure 2-1: Summarize on two types of biomass feedstocks; starch and sugar crops and lignocellulosic biomass.

2.1.1 Lignocellulosic biomass resources

Lignocellulosic biomass differs from other alternative energy sources because the resource is varies and their utilisation to product stream are through many conversion processes (Demirbaş, 2001). In the context of lignocellulosic materials, it constitute the most abundant bio-chemicals on earth (A. a. Peterson *et al.*, 2008). According to Kang *et al.*, (2014) approximately 150EJ/J of energy are available in lignocellulosic materials, therefore, they could provide a sustainable source for

low-cost biofuel production (Sun and Cheng, 2002; Nagy, 2009). There are several resource groups of lignocellulosic materials; (i) agricultural residues (palm trunk and empty fruit bunch, corncobs, wheat straw, sugarcane bagasse, corn stover, coconut husks, wheat rice, and empty fruit bunches); (ii) forest residues (hardwood and softwood); (iii) energy crops (switch grass); (iv) food wastes; and (v) municipal and industrial wastes (waste paper and demolition wood) (Lee, Hamid and Zain, 2014). In current work, three general lignocellulosic resources were discussed, namely agricultural waste (Section 2.1.1.1), forest woody feedstock (Section 2.1.1.2) and municipal and industrial waste (Section 2.1.1.3).

2.1.1.1 Agricultural waste

An agricultural waste is an important category of live-stock sources with great potential application in bio-refineries and is not opposed to the availability of food. Agricultural waste can be refers to any lignocellulosic residue produced by agri-food industries in their daily operations, such as roots, stalks, bark, bagasse, leaves, straw residues, seeds, and animal residues (Forster-Carneiro *et al.*, 2013b). The available amount of agro-residues is estimated to be 1010 Mt. globally, which corresponds to an energy value of 47 EJ (Gabrielle *et al.*, 2007). The most abundant lignocellulose agricultural residues are corncobs, corn stover, wheat, rice, barley straw, sorghum stalks, coconut husks, sugarcane bagasse, switchgrass, pineapple and banana leaves can be produce every year (Demain *et al.*, 2005). Apart from environmental point of view, agricultural residues help to prevent unsustainable tree cutting which reduce the phenomenon of deforestation (Limayem and Ricke, 2012; Achinas and Euverink, 2016). Because of their unique chemical composition, abundant availability, renewable nature and low cost, agricultural waste materials are economical and environmentally friendly as biomass feedstock (Bhatnagar and Sillanpää, 2010).

2.1.1.2 Forest woody feedstock

Compared with agricultural biomass, woody biomass as a feedstock has many advantages in terms of production, harvesting, storage, and transportation biomass for conversion (Zhu and Pan, 2010). In addition, due to high lignin content and low

ash composition, forest biomass represents a valuable feedstocks for energy utilization (Zhu and Pan, 2010; Achinas and Euverink, 2016). Figure 2-2 simplified the type of forest biomass sources consisting mainly of residue or by- products from manufacturing processes, biomass plantation and tree and branches residues. Woody biomass from forestlands and intensively managed plantations can be sustainably produced in large quantities in many regions of the world(Zhu, Pan and Zalesny, 2010). According the taxonomical division, the woody material can be classifies into two broad categories which is softwoods and hardwoods (Limayem and Ricke, 2012; Achinas and Euverink, 2016). Softwoods originate from conifers and gymnosperm trees and have lower densities compared to hardword and grow faster. Gymnosperm trees mostly come from evergreen species such as pine, cedar, spruce, cypress, fir, hemlock and redwood. In the meantime, the hardwoods are mostly deciduous and angiosperm trees. They are found mainly in the northern hemisphere, including trees like oak, willow, cottonwood, poplar and aspen.

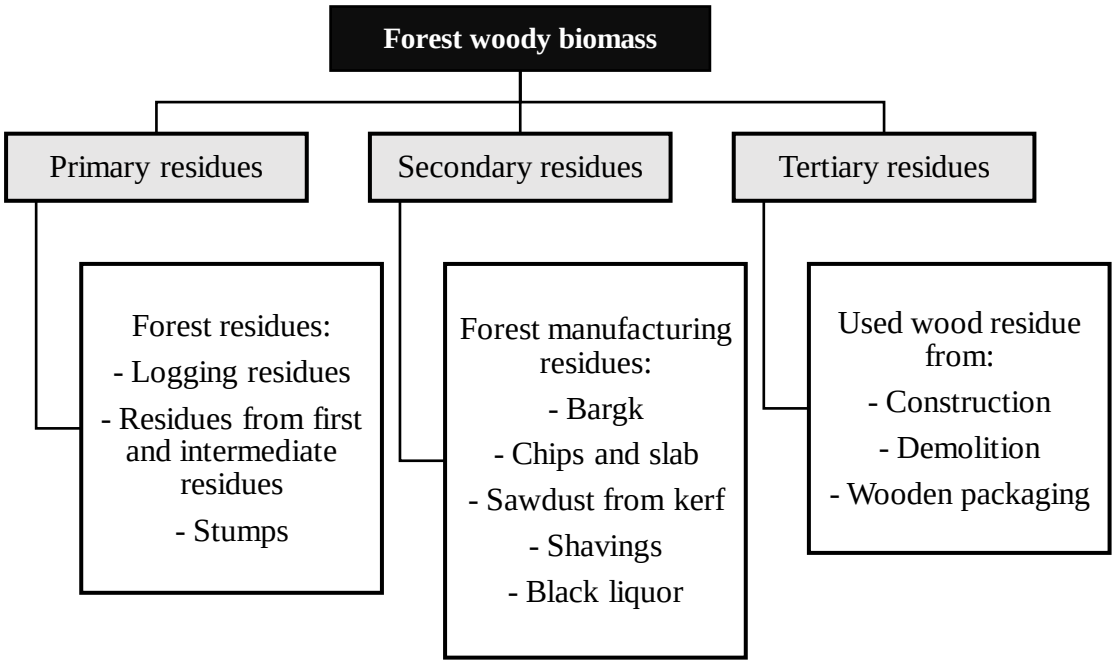

Figure 2-2: Different type of forest biomass that can be supplied globally, adapted from Achinas and Euverink, 2016.

2.1.1.3 Municipal and industrial waste

Municipal and industrial wastes is also a prospective way to produce biofuel or bio-chemical (Achinas and Euverink, 2016). These materials can originate either from residential or non-residential sources. The utilisation of this waste limits environmental problems associated with the garbage household disposal, food-processing by-products, processing papers, black liquors and pulps (Limayem and Ricke, 2012). A significant volume of the industrial waste is discharged to public sewers, streams, lakes, landfills, and other sinks at great cost to the industry and/or the community that accepts these effluents; i.e. pulp and paper industry and brewery factory.

The pulp and paper industry had processes a huge quantities of lignocellulosic waste materials (Iqbal, Kyazze and Keshavarz, 2013). Most of the resources of pulp and paper fibre are plant materials obtained from trees or agricultural crops. These plant materials are harvested directly from wood, straw, bamboo or residuals from other manufacturing processes (sawmill wood chips, sugarcane bagasse fiber, cotton linter, etc), fibres recovered from recycle paper or paperboard and second hand cloth (Gupta, 2007; Nigam and Singh, 2011). There are three major processing steps are involve in paper production, i.e. i) pulping, ii) bleaching and finally iii) paper production. Throughout this process, different types of solid waste and sludge are generated as by-product which obtained at different production processes (Bajpai, 2015) and example of the wastes are summarize in Table 2-1. With an increasing demand for paper, the experts are wondering on waste management in this industry; with the reality that paper will still be produce to fulfil the demand.

Table 2-1: Solid waste generated from paper mills in paper and pulp industry adapted from Bajpai, (2015).

Rejects
The rejects from recovered paper are impurities and consist of lumps of fibres, staples and metals from ring binders, sand, glass and plastics and paper constituents as fillers, sizing agents and other chemicals. Rejects also have a relatively low moisture content, significant heating values, are easily dewatered and are, generally, incinerated or disposed of in landfills. Screen rejects are produced during filtration steps with screens with very small slots to remove pulp possibly containing stickies that might disturb the production process and quality of end product. Screen rejects have a high content of cellulose fibre
Deinking sludge
This residue contains mainly short fibres or fines, coatings, fillers, ink particles (a potential source of heavy metals), extractive substances and deinking additives. It is normally reused in other industries (e.g. cement, ceramics), or is incinerated, even though it has a poor heating value. Deinking sludge is generated during recycling of paper (except for packaging production). Separation between ink and fibres is driven by "flotation" process, where foam is collected on the surface of flotation cells. The generated deinking sludge contains minerals, ink and cellulose fibres (that are too small to be withhold by filters)
Primary sludge
This sludge is generated in the clarification of process water by kidney treatments, e.g. dissolved air flotation. The sludge consists of mostly fines and fillers depending on the recovered paper being processed and it is relatively easy to dewater. This sludge can be reincorporated into the process for board industry, but for high grade products can be incinerated, dumped or, otherwise, mixed with deinking or secondary sludge
Secondary or biological sludge
This sludge is generated in the clarifier of the biological units of the wastewater treatment, and it is either recycled to the product (board industry) or thickened, dewatered and then incinerated or disposed of in landfill. Secondary sludge volumes are lower than those corresponding to the primary sludge, since most of the heavy, fibrous or inorganic solids are removed in the primary clarifier. Secondary sludges are often difficult to handle (due to a high microbial protein content), and such solids need to be mixed with primary sludge to permit adequate dewatering

Besides, brewing industry also generates a large amounts of by-products and wastes in each beer processing stages, such as water, brewery spent grain (BSG), spent hops, yeast and etc. High volumes of waste material are discharged with every brew; an example of waste from small scale brewery is listed in Table 2-2. From the table, it can be seen that BSG and water are the most extensive problems (Thomas and Rahman, 2006) with 3.4 million tonnes of BSG from this industry are produced in the EU every year (Stojceska *et al.*, 2008). A typical small brewery brewing 1500 litres three times a week and produce around two tons of spent grain in a week. Meanwhile, for large regional breweries, 1,000HL beer per day been produce with 40 tons BSG per day need to be remove (Thomas and Rahman, 2006). Currently the basic utilisation of this waste are in form of animal fodder or compost to the landfill (Sežun *et al.*, 2011; Asad S.N. Mahmood *et al.*, 2013; Malomo, 2013). However,

these plant-derived waste co- products are known to contain significant amounts of valuable components, which remain unexploited waste in the current processes; i.e. lignocellulosic rich materials (Stojceska *et al.*, 2008; Mussatto *et al.*, 2010; Waters *et al.*, 2012; Mussatto, 2014). Besides, because if its high moisture and fermentable sugar content, BSG becomes an environmental problem after a short time (7-10 days) (El-Shafey *et al.*, 2004).

Table 2-2: Brewery waste products from small scale production adapted from Thomas and Rahman, (2006)

Material	Volume per HL 4% abv beer	Source / origin	Brewing use	Destination(s)	Difficulties
Water	3 – 10 HL	Mains or bore hole	Product, cleaning, heating and cooling	Product, Effluent discharge	Chemical composition from acids & alkalis
Spent grain	14 Kg dry wt	Barley and other cereal malts	Source of sugars for fermentation	Agricultural	Hygiene, odour, High BOD
Spent hops	0.166 Kg dry wt	Hop flowers	Bitterness and other flavours	Agricultural	Anti microbial, unpalatable to animals
Trub	0.350 Kg dry wt	Precipitation from wort	Unwanted by product	Effluent discharge	High BOD and TSS
Yeast	3 Kg dry wt	Previous brew	Fermentation	Effluent discharge	High BOD, and TSS
Caustic and acid cleaners		Chemical suppliers	Cleaning	Effluent discharge	Acidity effects on effluent
Waste beer	Variable	Contamination Production errors	Nil	Low value sales or effluent discharge	High BOD

Briefly, in beer-brewing, the process are starts with the production of the wort. Wort is a sugar-rich solution that will be used in the subsequent fermentation stage to produce ethanol. To obtained wort, the milled barley malt is mixed with water in a mash tun and the temperature of mash slowly increased from 37 to 78 ºC to promote the enzymatic hydrolysis of malt constituents (Fărcaş *et al.*, 2014). At this stage, the malt starch were convert into fermentable (mainly maltose and maltotriose)

and non- fermentable (dextrins) sugars, meanwhile, proteins from the barley malt are also partially degraded during this stage into polypeptides and amino acids (Mussatto, 2014). This enzymatic conversion stage (mashing) produces sweet liquid known as wort (Fărcaş *et al.*, 2014). At the end of this process, the insoluble undegraded part of the barley malt grain, also known as BSG is obtained in mixture with the wort (Fillaudeau, Blanpain-Avet and Daufin, 2006). The wort is filtered through the BSG bed formed at the bottom of the mash tun and is transferred to the fermentation tank (Mussatto, 2014). The wort will be fermented into beer while BSG is obtained as a by-product of this process (Lynch, Steffen and Arendt, 2016). Figure 2-3 simplified the above process and show an example of BSG waste. Details on BSG and potential application on this waste as lignocellulosic material were further elaborate in Section 2.3.

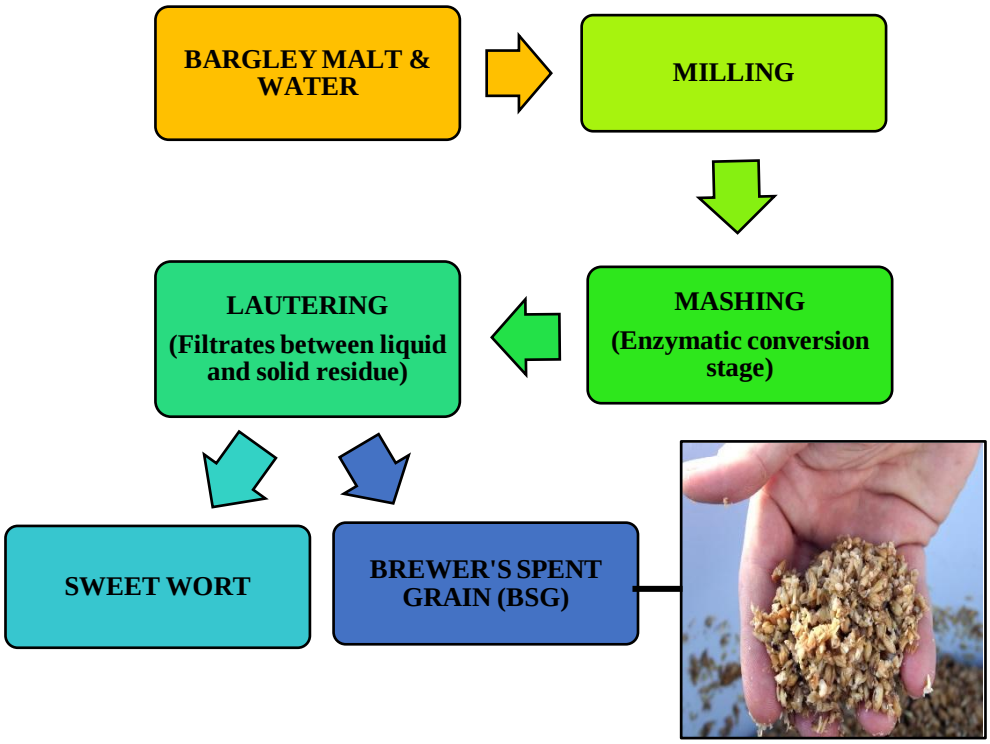

Figure 2-3: The general process in beer-brewing for production of beer and produce BSG as by-product.

2.1.2 Composition of lignocellulosic biomass

The chemical composition of lignocellulosic biomass are varies depending on the specific needs of the plants. Cellulose, hemicellulose and lignin are the three main components of lignocellulosic source, and the proportion of these components in a fiber depending on the age, fiber sources and the extraction conditions used to obtain the fiber (Reddy and Yang, 2005). Table 2-3 show an example of chemical composition for lignocelluloic materials based on their general resources and common substrate.

Table 2-3: Cellulose, hemicellulose and lignin composition in common lignocellulosic materials adapted from Lee, Hamid and Zain, (2014)

Types of biomass	Lignocellulosic substrate	Cellulose (%)	Hemicellulose (%)	Lignin (%)
Agriculture waste	Corncobs	45	35	15
	Wheat straw	30	50	15
	Barley straw	33–40	20–35	8–17
	Corn stover	39–42	22–28	18–22
	Nut shells	25–30	25–30	30–40
Energy crops	Empty fruit bunch	41	24	21.2
	Switch grass	45	31.4	12
Forestry waste	Hardwood stems	40–55	24–40	18–25
	Softwood stems	45–50	25–30	25–35
	Leaves	15–20	80–85	0
Industrial waste	Waste papers from chemical pulps	60–70	10–20	5–10
	Organic compound from wastewater solid	8–15	0	0

Cellulose, a β(1–4)-linked chain of glucose molecules is the main component lignocellulosic material which sometimes also been referred as cellulosic biomass. Hemicellulose present in nearly similar fraction of cellulose, is composed of various 5- and 6-carbon sugars such as arabinose, galactose, glucose, mannose andxylose. Lignin is composed of three major phenolic components, namely of p-coumaryl alcohol (H), coniferyl alcohol (G) and sinapyl alcohol (S). The ratio of these three components in the biomass are varies between different plants, wood tissues and cell wall layers. The lignocellulosic components; cellulose, hemicellulose and lignin are form a structure called microfibrils, which are organised into macrofibrils that mediate structural stability in the plant cell wall (Rubin, 2008). Figure 2-4 provides a schematic illustration for the main lignocellulosic components.

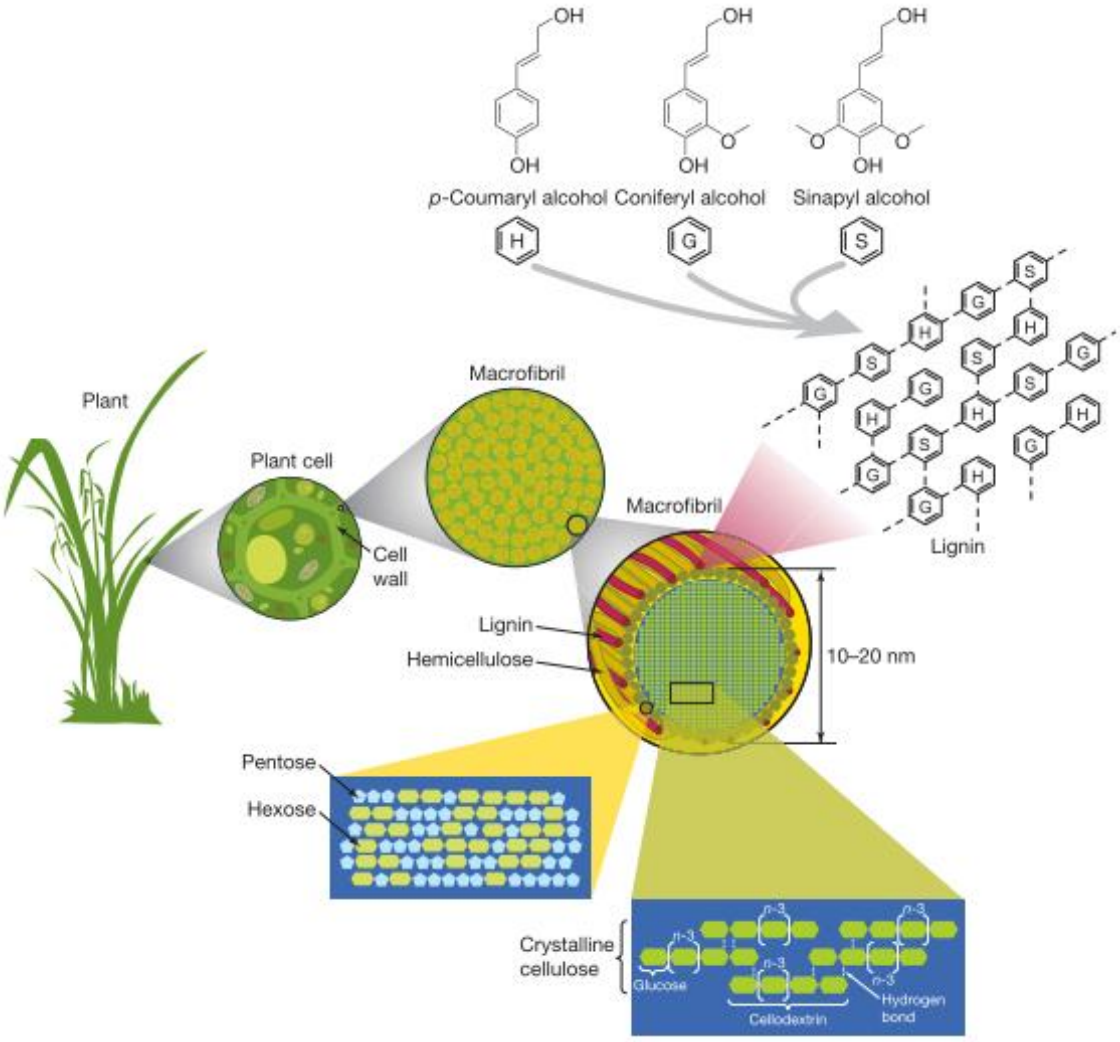

Figure 2-4: Structure of lignocellulosic materials; comprised of cellulose, hemicellulose and lignin adapted from Genomics of cellulosic biofuels (Rubin, 2008).

2.1.2.1 Cellulose

Cellulose is the major component of lignocellulosic biomass, and almost half of the organic carbon in the biosphere is estimated to be present in the form of cellulose. Cellulose is the structural basis of plant cells and the most important and abundant natural substance (Zheng, Tao and Xie, 2013); which usually exists as long thread like fibres called microfibrils. The amount of cellulose influences the properties, economics of fibre production and the utility of the fibre. For example, higher cellulose content in fibres are more preferable for textile, paper and other fibrous applications. Meanwhile, fibre with higher hemicellulose content would beneficial in producing ethanol and other fermentation products because

hemicellulose is relatively easily hydrolysable into fermentable sugars (Reddy and Yang, 2005). Therefore, the value for the cellulosic materials are largely determine by their end use applications (Reddy and Yang, 2005).

However, it is difficult to convert the cellulose into end product because cellulose is insoluble in water and in most organic solvents under mild conditions. Cellulose is insoluble in water because of its low-surface-area crystalline form held together by hydrogen bonds (Yu, Lou and Wu, 2008). Furthermore, since cellulose contains various kinds of C–O and C–C bonds, the precise cleavage of specific C– O and/or C–C bonds for the production of specific chemicals is a challenging task (Deng, Zhang and Wang, 2015).

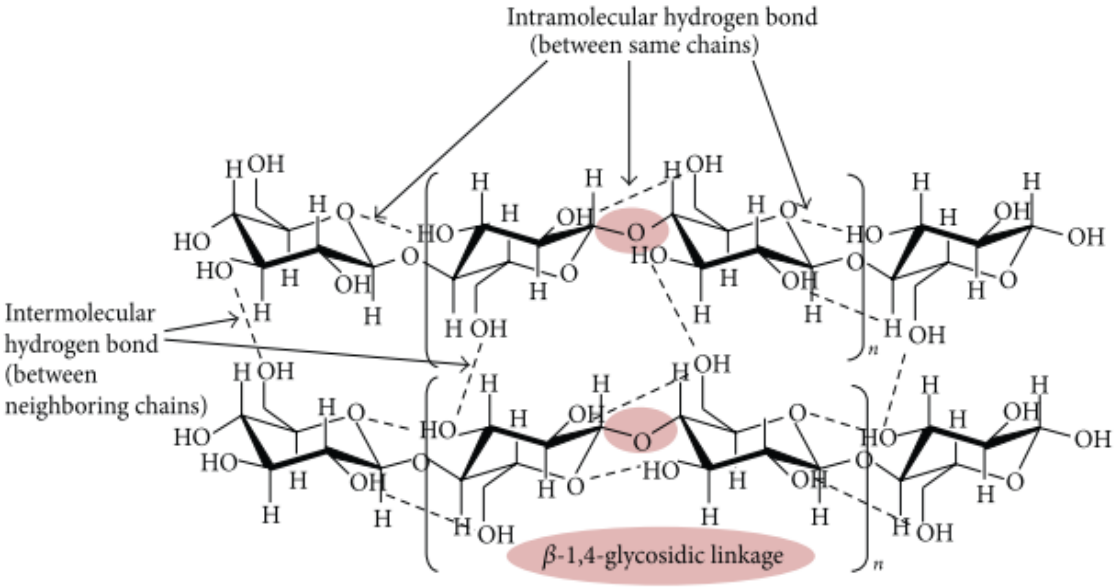

Figure 2-5: Chemical structure of cellulose chain connected together by β-1,4 -glycosidic bonds and strong hydrogen bonds adapted from Lee, Hamid and Zain, (2014).

2.1.2.2 Hemicellulose

Hemicellulose is the second most common polysaccharide in nature and accounts for about 15−35% of lignocellulose, depending on the biomass type and source (Pavlovič, Knez and Škerget, 2013). Hemicellulose was estimated to account for approximately 22% of softwood, 26% of hardwood and 30% of various agricultural residues (Ganesh D. Saratale, 2012). Compared to cellulose, hemicellulose is short, highly branched polymer consisting of five-carbon (C5) and

six-carbon (C6) sugars monomer such as glucose, xylose, mannose, galactose and arabinose and uronic acids (Pasangulapati *et al.*, 2012). Due to its structure and branched nature, hemicellulose is amorphous and relatively easy to hydrolyse to its monomer sugars compared to cellulose (Yu, Lou and Wu, 2008). Hemicellulose is insoluble in water at low temperature. However, hemicellulose hydrolyse at a temperature lower than cellulose; which at elevated temperature their solubility are rendered (Harmsen and Huijgen, 2010).

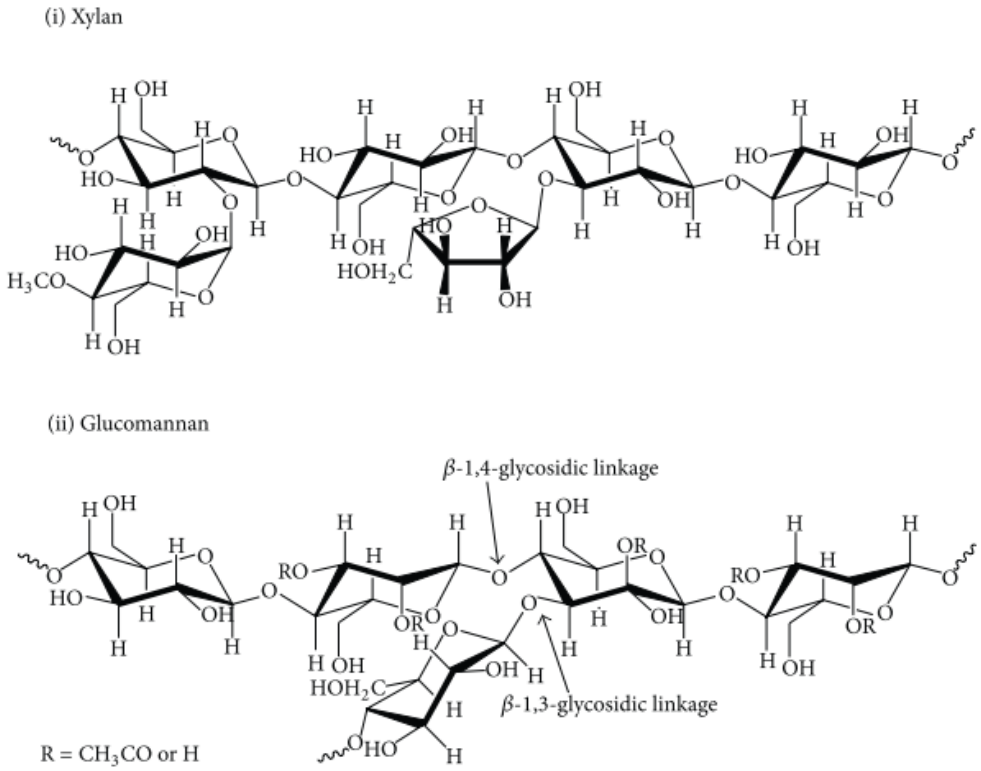

Figure 2-6:Chemical structure of xylan and glucomannan; the most existing biopolymer present in hemicellulose fraction adapted from Lee, Hamid and Zain, (2014).

2.1.2.3 Lignin

Lignin is widely found in plants and its production ranks after cellulose, making it the most abundant renewable organic resources with aromatic characteristics in nature (Cao *et al.*, 2018). Lignin is a complex and non-crystalline three-dimensional network of phenolic polymers, which widely exist in higher plant cells. Lignin is the most invasive component of the plant cell wall, given its role in providing tensile strength to the plant. It is prevalently bonded to hemicellulose, which helps stabilize all three biopolymers, and thereby enhances the rigidity of the

wall (Laskar *et al.*, 2013). Compared to other biopolymers, lignin is a polymer network resulting from the dehydrogenated radical polymerisation of monolignols (e.g. p-coumaryl-, coniferyl- and sinapyl-alcohols), connected through carbon–carbon and ether connections (Boeriu *et al.*, 2004). Lignin accounts for about 15–40% of the dry weight of lignocellulosic biomass and represent as one of the main components in plants (Cao *et al.*, 2018). There are two types of lignin are recognized nowadays: native lignin, which is naturally present in biomass; and technical lignin, which is thoroughly isolated from biomass by different processes (Pavlovič, Knez and Škerget, 2013). For current work, kraft lignin was used as lignocellulosic biomass model compound. The kraft pulping process is the dominant global process for industrial chemical modification of lignin to produce kraft lignin. During this treatment, the hydroxide and hydrosulfide onions react with the lignin, causing the lignin polymer to fragment into smaller water/alkali-soluble fragments (Chakar and Ragauskas, 2004). The presences of these hydroxyl groups increase the hydrophilicity of the lignin and lignin fragments.

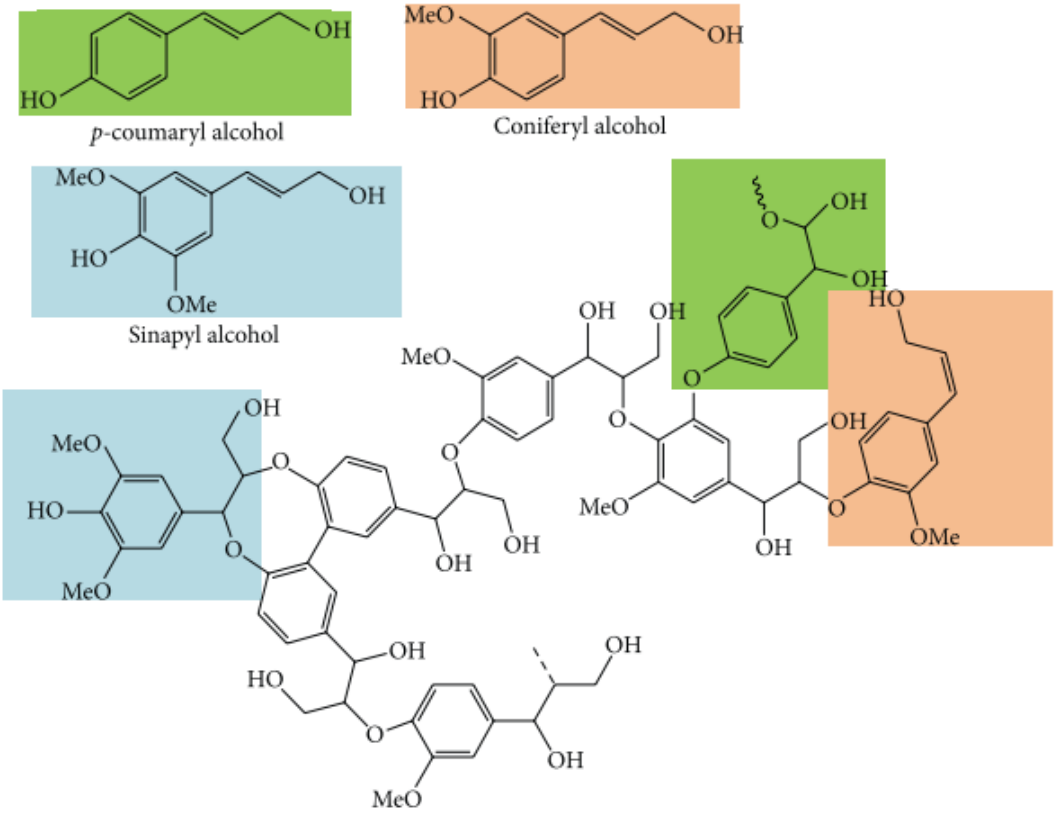

Figure 2-7: Chemical structure of lignin (p-coumaryl alcohol, coniferyl alcohol and sinapyl alcohol) adapted from Lee, Hamid and Zain, (2014).

2.2 Biomass conversion technologies

Lignocellulosic biomass is a potential renewable resources which can be used directly or indirectly to produce numerous biological and chemical products (Iqbal, Kyazze and Keshavarz, 2013). Biomass can be converted into product streams using a number of different processes. The choice of conversion process depends on different factors; biomass feedstock type and properties, end-used requirements, environmental standards and economic conditions (Saxena, Adhikari and Goyal, 2009a). According to Mckendry, (2002), biomass can be converted into three main types of 'bio-product':

i) Electrical/ heat energy
ii) Transport
iii) Chemical feedstock

In general, conversion of biomass can be divided into two main technologies; i) biochemical technologies which degrades biomass with enzymes and microorganisms, and ii) thermochemical conversion technologies which using heat to breakdown the biomass polymer (McKendry, 2002b; Tekin, Karagöz and Bektaş, 2014). For biochemical process, the conversion were divided into three process options; aerobic and anaerobic degradations, fermentation, and enzymatic hydrolysis. Meanwhile, within thermo-chemical conversion four process options are available: combustion, gasification, pyrolysis and hydrothermal processing (McKendry, 2002b; Saxena, Adhikari and Goyal, 2009b; Canabargro *et al.*, 2013; Tekin, Karagöz and Bektaş, 2014).

Hydrothermal processing is a thermochemical conversion that can be used to produce liquid, gaseous and solid products from biomass (Tekin, Karagöz and Bektaş, 2014; Kruse and Dahmen, 2015). Hydrothermal processing can be divided into three different processing depending on the temperature and pressure conditions, namely hydrothermal gasification (HTG), hydrothermal carbonisation (HTC) and hydrothermal liquefaction (HTL) (Kruse and Dahmen, 2015). The summaries on biomass conversion technology are shown in Figure 2-8.

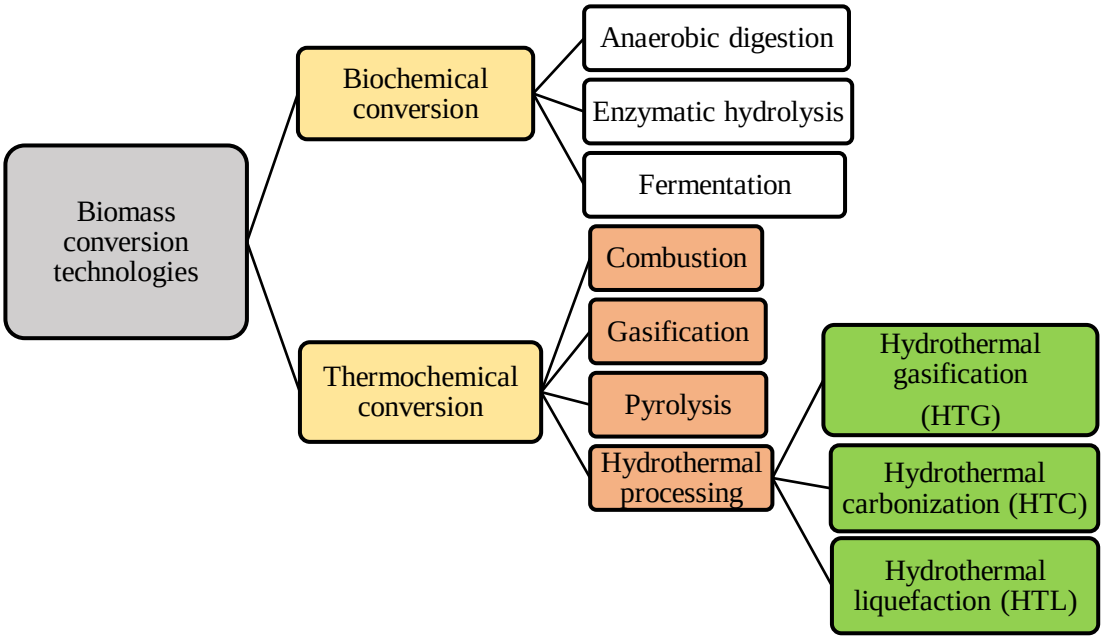

Figure 2-8: Biomass conversion technology for lignocellulosic biomass summarize from McKendry, (2002), Tanger et al., (2013), Tekin, Karagöz and Bektaş, (2014) and Kruse and Dahmen, (2015).

2.2.1 Biochemical conversion

The degradation of biomass through biochemical processes occurs naturally. The most common types of biochemical processes are aerobic and anaerobic degradations, enzymatic hydrolysis, and fermentation; and these processes are performed by micro-organisms and bacterial enzymes (Tekin, Karagöz and Bektaş, 2014). Anaerobic digestion is the use of micro-organism to break down the feedstock by releasing heat, hydrogen sulphide, methane, and carbon dioxide. These processes take places under specific conditions of hydrogen gas and need longer reaction time. The main disadvantage of this process is that micro-organisms and bacterial enzymes need to have an ideal condition to proceed with. The microbes are sensitive to changes in the feedstock, especially the presence of anti- microbial compounds, and variation of reactor conditions. Due to these, they require constant circulation of the reactor fluid, and a constant operating temperature and pH during the processes (Sumit Sharma *et al.*, 2014).

Fermentation is the process in which yeast were used to convert the biomass into sugar and subsequently ethanol and other useful chemicals. The conversion of

starch and sugar-based raw materials into bio-ethanol by fermentation is also used for commercial purposes. However, due to the presence of long-chain polysaccharide molecules, the conversion of lignocellulosic biomass (such as wood and grasses) is more complex. These molecules requires acid or enzymatic hydrolysis before the resulting sugars can be fermented to ethanol (McKendry, 2002b). The use of fermentation to degrade lignocellulosic biomass therefore increase the cost of processing and is not preferred commercially (Tekin, Karagöz and Bektaş, 2014).

2.2.2 Thermochemical conversion

Thermochemical conversion technologies are based on the thermal breakdown of biomass to produce valuable chemicals and fuel. These processes do not necessarily produce useful energy directly, in which under controlled temperature and oxygen conditions, the original biomass feedstock may be converted into more convenient forms of energy carriers, such as producer gas, oils or methanol (Sumit Sharma *et al.*, 2014). Thermochemical conversion technologies include combustion, pyrolysis, gasification and hydrothermal processing.

2.2.2.1 Combustion

Biomass combustion is one of the earliest and fastest method for human energy use. This process has been adapted as experimental technologies to produce liquid transportation fuels and chemical feedstocks (Saxena, Adhikari and Goyal, 2009a). Currently, the direct combustion of biomass continues to be the dominant pathway for bioenergy in worldwide (Bridgwater, 2003; Gaul, 2012). During biomass combustion, hot gases were produces at temperatures around 800–1000 ºC. Meanwhile, for complete combustion, the heat was produce as a result of the oxidation of carbon- and hydrogen-rich biomass to CO_2 and H_2O. Any type of biomass can be burned, however in practice, only feedstock with a moisture content < 50 % are applicable for a feasible biomass combustion process (McKendry, 2002b). Due to these condition, the biomass with high moisture content need to go for pre-dried process before been introduced to the process. Details on chemical kinetics of combustion process are complex and imperfect combustion will result in the release of intermediate compounds. This intermediate may resulted in

environmental air pollutants such as CH_4, CO, with sulfur and nitrogen content cause the emission of SO_x and NO_x (Tanger *et al.*, 2013).

2.2.2.2 Pyrolysis

One of the promising routes in converting biomass feedstock is through pyrolysis process. The pyrolysis technology can convert biomass into solid (charcoal), liquid (tar and other organics, such as acetic acid, acetone and methanol) and gaseous products (H_2, CO_2, CO). These products offer possible alternate sources of energy. Pyrolysis is a process by which a biomass feedstock is thermally degraded in the absence of oxygen/air (Babu, 2008). The pyrolysis can be divided into three subclasses, namely conventional pyrolysis (slow pyrolysis), fast pyrolysis and flash pyrolysis which depending on different operating conditions. Details on the operating parameters for pyrolysis processes are given in Table 2-4.

Table 2-4: Range of main operating parameters for pyrolysis processes.

Parameters	**Conventional pyrolysis**	**Fast pyrolysis**	**Flash pyrolysis**
Temperature (K)	550-950	850-1250	1050-1300
Heating rate (K/s)	0.1-1.0	10-200	< 1000
Particle size (mm)	5-50	<1	<0.2
Solid residence time (s)	450-550	0.5-10	<0.5

Conventional pyrolysis is defined as the pyrolysis that occurs under a slow heating rate and a long residence time of hot vapour (W.-H. Chen *et al.*, 2014). Longer residence time of hot vapour tailored to larger portions of char and non-condensable gas in the products (Arni, 2018). Fast pyrolysis of biomass occurs at much higher temperature and heating rate than slow pyrolysis. The main constituent of this process, pyrolytic-oil, contains 75–80 wt. % polar organics and 20–25 wt. % H_2O and has a yield of 65–70 wt. % of total product output along with char and gas as the by-products (Ail and Dasappa, 2016). One of the major disadvantages of these pyrolytic oils includes the presence of high content of O_2 and H_2O, which makes them low quality fuels compared to regular hydrocarbon fuels (Zhang *et al.*, 2007).

Flash pyrolysis differs strongly from the conventional pyrolysis which performed slowly with massive pieces of wood. Flash pyrolysis was conducted at high heating rate using small particle size of feedstock which gives mostly gaseous products due to its operating condition (Babu, 2008).

2.2.2.3 Gasification

Gasification is the exothermic partial oxidation of biomass with optimised process conditions for high yields of CO, H_2, CH_4, and CO_2 – rich gaseous products (syngas or producer gas). Syngas can be upgraded to liquid fuels such as Diesel and gasoline by Fischer–Tropsch (FT) synthesis and large scale gasification - FT production facilities are in use in South Africa (SASOL) (Alonso, Bond and Dumesic, 2010). Gasification process occurs in a number of sequential steps and Figure 2-9 illustrates the biomass gasification technology:

i) drying process to evaporate moisture content in feedstock
ii) pyrolysis process to produce gas, vaporised tarts or oils and a solid char residue
iii) gasification or partial oxidation of the solid char, pyrolysis tars and pyrolysis gases

Pyrolysis reaction generally takes place at much faster rate than gasification during the process; this latter is used determine the rate for gasification process. The pyrolysis product which is gas, liquid and solid then react with the oxidising agent, usually air to produce permanent gases of CO, CO_2, H_2, and lower hydrocarbon gas quantities. Char gasification is the interactive combination of several gas–solid and gas–gas reactions. This interaction will oxidise the solid carbon to carbon monoxide and carbon dioxide, and hydrogen is generated through the water gas shift reaction. The gas–solid reactions of char oxidation are the slowest and limit the overall rate of the gasification process (Bridgwater, 2003). One of the challenges of gasification is to manage the higher molecular weight volatiles that condense into tars; these tars are both a fouling challenge and a potential source of persistent environmental pollutants such as polycyclic aromatic hydrocarbons (Milne and Evans, 1998)

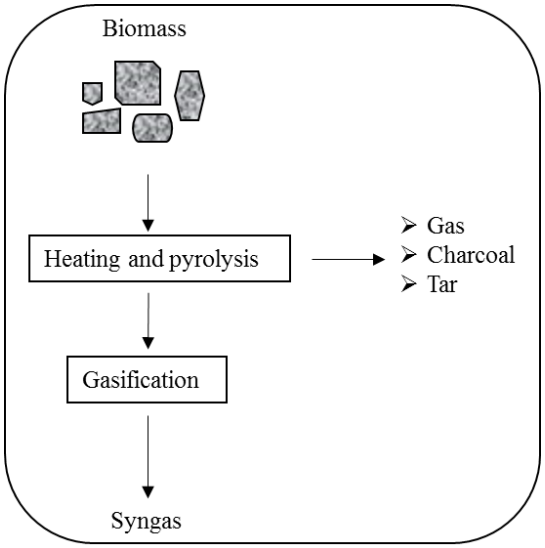

Figure 2-9: Schematic diagram for biomass gasification adapted from Canabargro et al., (2013)

2.2.2.4 Hydrothermal processing

Biomass conversions through hydrothermal processes are one of the promising techniques to produce renewable solid, liquid/tarry or gaseous fuels which conducted in liquid water as reaction medium. The main advantage of hydrothermal processing is that wet biomass, typically with 70 wt. % or more moisture content can directly introduce to the reaction without need for drying process. Drying of biomass to optimal water contents below 10 wt. %, as necessary for "dry" biomass conversion processes, involve substantial amounts of energy. Therefore, compare to other three thermochemical processes discussed above; combustion, pyrolysis and gasification, hydrothermal conversions offers an attractive option to extend the resource for biomass to bio-based production (Pavlovič, Knez and Škerget, 2013; Tekin, Karagöz and Bektaş, 2014; Kruse and Dahmen, 2015).

Depending on the processing temperature and pressure, hydrothermal processing can be divided into three main regions namely carbonisation, liquefaction and gasification and was shown in Figure 2-10. The pressure-temperature phase diagram for pure water is superimposed in a same figure with regard to the liquid–vapour co-existence behaviour. Water can exist in three phases: solid, liquid, and gas. Below water's critical point, the vapour pressure curve separating the liquid and vapour phase ends at the critical point (Tc = 373 °C, Pc = 22.1 MPa). Beyond the

critical point, the properties of water can be changed without any phase transition (Kumar, Olajire Oyedun and Kumar, 2018).In general, hydrothermal carbonisation take place at relatively low temperature (≤ 200) and saturated pressure (2–10 MPa) for several hours (Nizamuddin *et al.*, 2017). Meanwhile, for hydrothermal conversion via liquefaction pathways, the reaction generally occurs at temperature about 200 and 370ºC, with pressures between about 4 and 20 MPa, sufficient to keep the water in a liquid state (sub- critical water). At higher temperature and pressure than critical point of water, the free-radical reaction pathway dominates; this condition is favourable for hydrothermal gasification (HTG) which take place at supercritical water condition (Kruse, 2009).

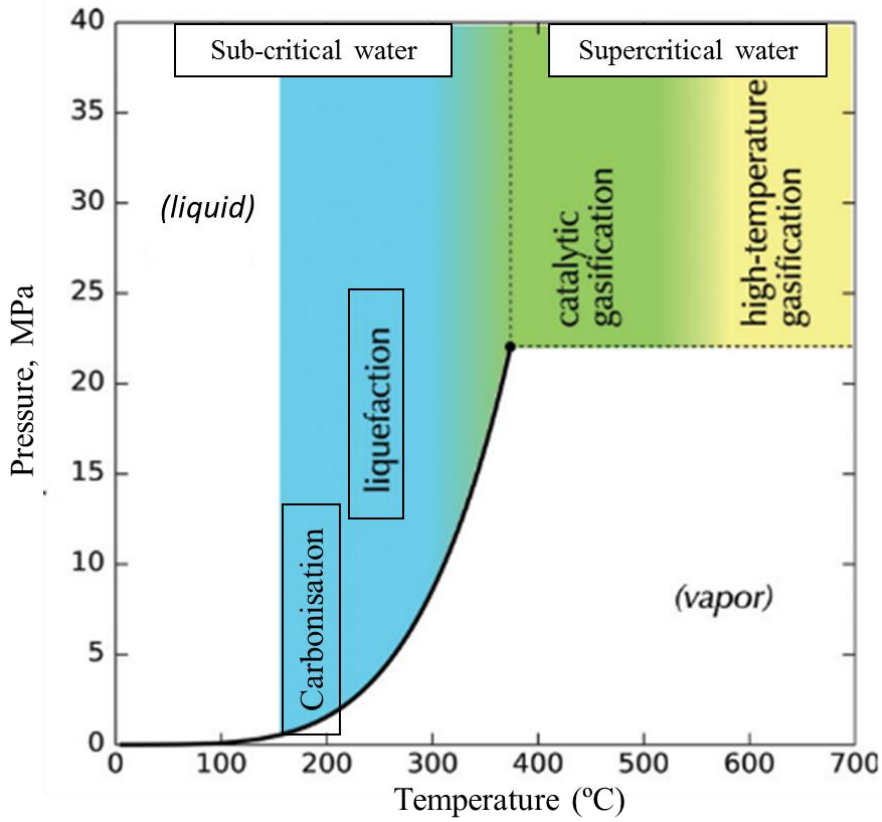

Figure 2-10: Overview of different hydrothermal biomass conversion processes region referenced to the pressure-temperature phase diagram of water adapted from Peterson et al.,(2008) and Kruse and Dahmen,(2015).

Hydrothermal processes are chemical reaction in water; due to that, the chemical processes are influenced by behaviour of water depending on reaction conditions. The pressure-temperature phase diagram for pure water are shown in Figure 2-11, which indicate the behaviour of water; density, static dielectric constant,

and ion dissociation constant (Kw) as the function of temperature. For example, increases temperature from 25 °C to 375°C at 30MPa, enormous changes in solvation behaviour of water occur where it transforms from a polar, highly hydrogen-bonded solvent to behaviour in more typical of a non-polar solvent like hexane (A. a. Peterson *et al.*, 2008). Besides, the dielectric constant of water decreases quickly when the temperature increases. When the thermal energy increases, the shared electron by oxygen and hydrogen atoms tends to circulate more evenly and the electro- negativity of the oxygen molecule is reduced(Zhang, 2010). For example, when temperature increases from 25 °C to 450° C, the dielectric constant value decreases from about 80 to less than 2. In addition of that, the dissociation of water dramatically increases with the increase of temperature. Water dissociates into H^+ and OH^- ions during hydrolysis. As can be seen from Figure 2-11, the ion product (Kw) first increases from 10^{-14} to 10^{-11} just below 350 ºC and then decreases by five orders of magnitude or more above 500 ºC (A. a. Peterson *et al.*, 2008).

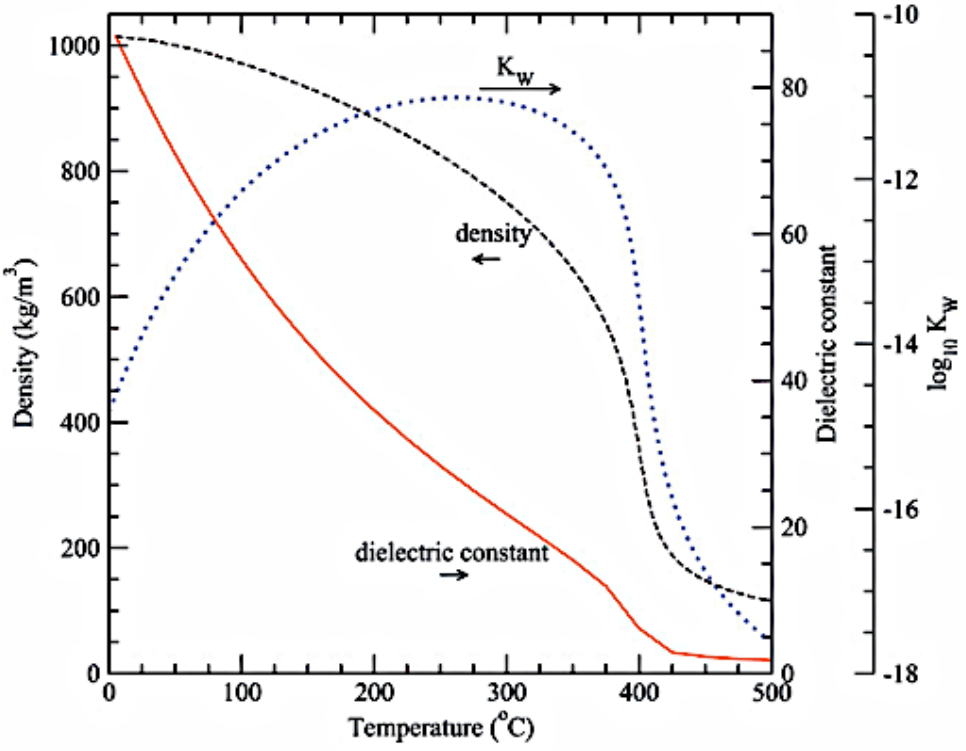

Figure 2-11: Density, static dielectric constant, and ion dissociation constant (Kw) of water at 30 MPa as a function of temperature. The dielectric constant ofwater drops drastically as water is heated, and approaches that of a (room-temperature) non-polar solvent at supercritical conditions (image and data adapted from Peterson et al.,(2008))

2.2.2.4.1 Hydrothermal carbonisation (HTC)

Hydrothermal carbonization (HTC) process converts biomass into a value-added product (solid fuel) at a comparatively low temperature (≤ 200 ºC) and saturated pressure (2–10 MPa) for several hours (Tekin, Karagöz and Bektaş, 2014; Olajire Oyedun and Kumar, 2018). HTC, also known as hydrous or wet pyrolysis, also can be defined as the carbonization of biomass heated in water under autogenous pressure and temperatures in the lower region of liquefaction process (subcritical conditions) (Álvarez-Murillo *et al.*, 2016). At this condition, the carbohydrates are completely solved after hydrolysis and polymerize subsequently to a product called "HTC-coal" (Kruse and Dahmen, 2015).

During HTC process, a liquid, gas and a solid carbonaceous phase, hydrochar are obtained; depending on the raw material and processing condition, the product distribution are varies (Álvarez-Murillo *et al.*, 2016). HTC is widely used to convert lignocellulosics into solid hydrochars, which have better physico-chemical characteristics than raw feedstock (Kumar, Olajire Oyedun and Kumar, 2018). According to Titirici and Antonietti, (2010) the hydrothermal carbonization reaction takes place in three important steps: (1) dehydration of the carbohydrate to (hydroxymethyl)-furfural; (2) polymerization towards polyfurans; (3) carbonization via further intermolecular dehydration. The proposed mechanism for hydrothermal carbonization process is shown in Figure 2-12.

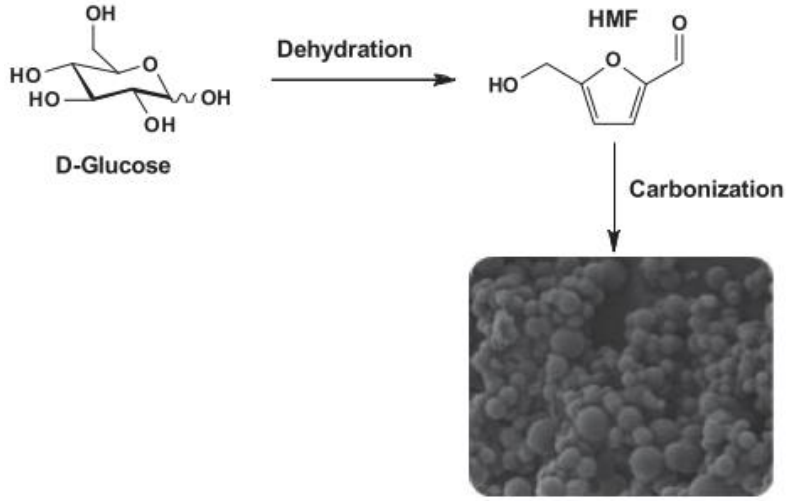

Figure 2-12: Proposed mechanism of hydrothermal carbonisation from D-glucose adapted from Tekin, Karagöz and Bektaş, (2014).

2.2.2.4.2 Hydrothermal gasification (HTG*)*

The main idea of HTG process is to take advantage from the special properties of near- and supercritical water as solvent and their presence as reaction partner (Kruse, 2009). The supercritical state (SC) refers to the zone of high temperature and pressure at the critical point at which water will acts as both a reactant and a catalyst. At this condition, water properties such as the ionic product, density, viscosity, and dielectric constant show large variations. Supercritical water (SCW) is an excellent solvent for most homogeneous organic reactions due to high miscibility and the absence of any phase boundaries (Kumar, Olajire Oyedun and Kumar, 2018). Under pressurised hot water, HTG breaks down biomass into its liquid components and then into its gaseous components. Water acts not only as a solvent but also as a reactant at near critical/supercritical conditions. Biomass rapidly undergoes hydrolysis under subcritical and supercritical conditions. Under supercritical water conditions, the dissolution of reactive species caused by decomposition of biomass prevents the formation of biochar, thereby ensuring a high gas yield (Tekin, Karagöz and Bektaş, 2014)

Biomass decomposition chemistry is very complex. During hydrothermal gasification, biomass decomposes into lower molecular weight compounds by hydrolysis reactions. High temperatures break the bonds of components in the biomass enabling the formation of gases, such as H_2, CH_4, CO and CO_2. Figure 2-13 depicts the simplified process flow for the conversion of biomass to gaseous products via aqueous intermediate compounds under hydrothermal conditions (Güngören Madenoğlu *et al.*, 2016) . However, the disadvantage of HTG might be the fact that so much water has to be heated up. The heat necessary to reach, e.g. 600 ºC may exceed the energy content of the biomass at water content higher than 80% (g/g). This means that a heat exchanger is required and the efficiency of this heat exchanger is crucial to the overall energy efficiency in the gasification process (Kruse, 2009). Fortunately, high-pressure heat exchangers are compact and relatively efficient. However, due to high operating parameters, the major drawback of HTG is the high investment costs are required.

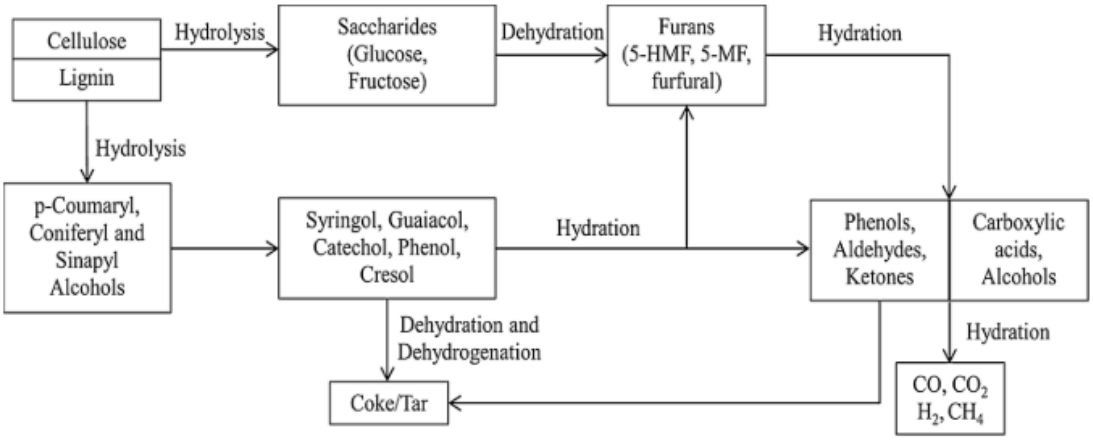

Figure 2-13: Simplified mechanism for conversion of cellulose/lignin to gaseous products through aqueous intermediates at hydrothermal conditions of water adapted from Güngören Madenoğlu et al.,(2016).

2.2.2.4.3 Hydrothermal liquefaction (HTL)

HTL is the thermochemical conversion of biomass into liquid fuels by processing in a hot, pressurised water environment for sufficient time to break down the solid biopolymeric structure to mainly liquid components. Hydrothermal technologies are broadly defined as chemical and physical transformations in medium-temperature (200–400°C), with high-pressure (5–40 MPa) water (A. Peterson *et al.*, 2008). The HTL of total biomass yields a range of different products including bio-crude oil, aqueous dissolved chemicals, solid residue, and gas. HTL product yields and properties vary significantly according to the feedstocks processed as well as the reaction conditions employed (Jazrawi *et al.*, 2015). Although the product distribution in bio-oil varies with the composition of the raw material and process conditions, the same groups of compounds are detected in almost all HTL bio-oils (Pavlovič, Knez and Škerget, 2013). The liquid oils contain a range of chemicals including carboxylic acids, alcohols, aldehydes, esters, ketones, sugars, lignin-derived phenols, furans, etc. (Stöcker, 2008).

At present, HTL and pyrolysis are two principle thermochemical conversion technologies to upgrade biomass feedstocks to biofuels (Kruse and Dahmen, 2015; Zhu *et al.*, 2015). Xu (2014) have proposed the bio-oil platform in bio refinery and it was illustrated in Figure 2-14.

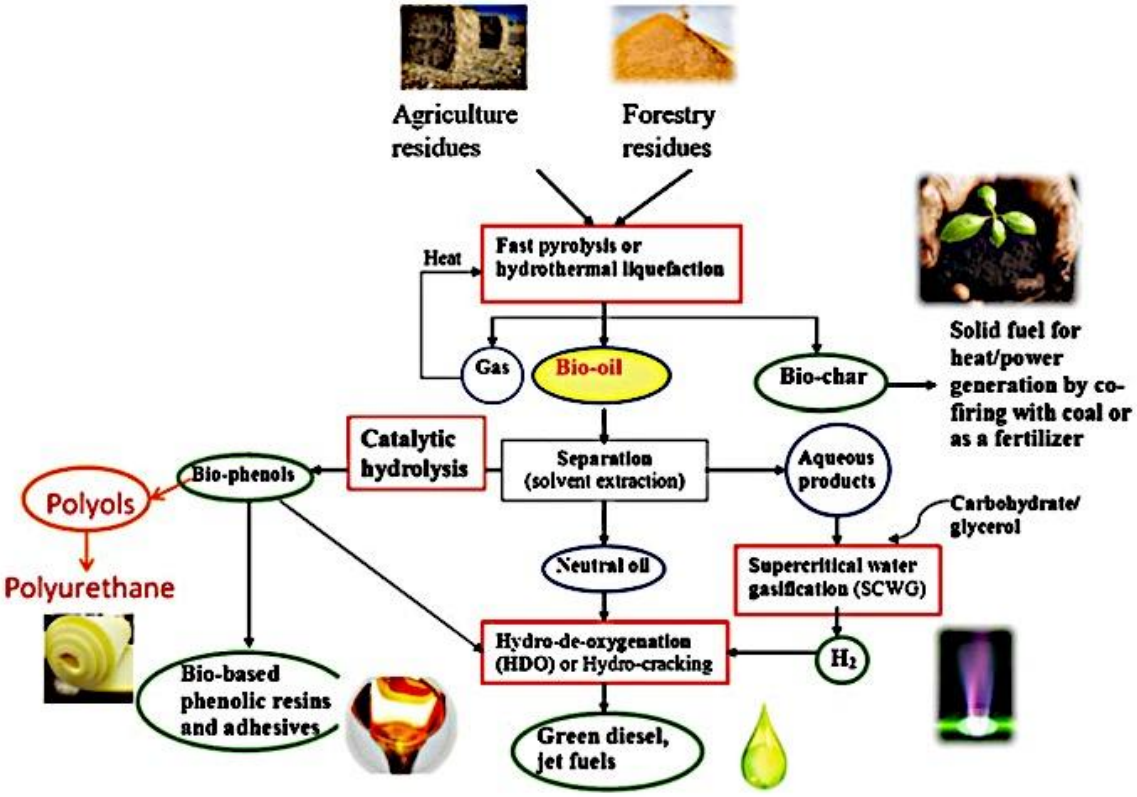

Figure 2-14: Bio-oil platform bio refinery proposed by Xu (2014) and currently under investigation.

However, compared with bio-oil from fast pyrolysis, bio-crude obtained from HTL have a better properties, i.e. lower moisture content, lower oxygen/carbon and consequently higher heating value (HHV) of about 30-36 MJ/kg (Demirbas, 2011). According to Kruse and Dahmen, (2015), in order to obtained high yields of pyrolysis oil (60 wt. %), the reaction must be conducted at very short reaction time and high temperature around 500 – 600 ºC. This oil is an intermediate product and longer reaction time would lead to production of gas and solid char. As a consequence, very fast heating-up (ca. 1000 K/s) and rapid cooling down of the vapours formed during pyrolysis must be carried out. In contrast, this is not necessary in HTL process; no further reactions to solid or gaseous products occur at lower reaction temperature. They also reported that during flash pyrolysis the solid yield is usually in the range of 20 wt. %., however during HTL, no solid product is formed (Kruse and Dahmen, 2015).

Most of the biomass sources are wet, and their moisture content can be at the range up to 95wt. %. In most methods for biomass upgrading, the feed must be dried before processing (Akia, Yazdani and Motaee, 2014). HTL reaction takes place in subcritical water as the reaction medium; thus biomass feedstock can be treated directly without the need for energy-consuming drying process (Zhu *et al.*, 2015; de Caprariis *et al.*, 2017). Water also has a lower dielectric constant, lower viscosity, and a higher ionic product than normal water in subcritical condition. The combination of these factors results in higher solubility of organic compounds and increased reaction rates of base and acid-catalysed reactions (Laine, 2015). In turns, these properties make subcritical water as an excellent medium for converting biomass-derived organic molecules into value-added liquid products (Kruse and Dinjus, 2007). On top of that, the density, dissociation and solubility of water change significantly with higher temperature and greatly affect co-existing reaction and rate of reaction. By controlling the temperature of the HTL reaction, the desired reactions to liquid biofuels production can be shifted. Overall, HTL offers an advantage and flexible technology in utilising various biomass feedstocks to produce liquid biofuel compare to other thermochemical method. Current study focuses on the HTL of brewer's spent grain (BSG) as lignocellulosic biomass.

2.3 Brewers spent grain (BSG): A case study

Barley grain is rich in starch and proteins and consists of the germ (embryo), the endosperm (comprising the aleurone and starchy endosperm) and the grain coverings; as the main components. The grain cover can further be divided into the seed coat, the pericarp layers and the husk as shown in Figure 2-15. The pericarp is waterproof and waxy, and the seed coat acts as a semi-permeable membrane. The pericarp–seed coat interface effectively defines the exterior and the interior of the kernel (Mussatto, Dragone and Roberto, 2006). The husk provides external grain protection, and is a multi-layered, dead tissue consisting mainly of lignocellulosic cell walls, but also contains small amounts of proteins, resins and tannins (Lewis and Young, 1995; VenturiniFilho and Cereda, 2001).

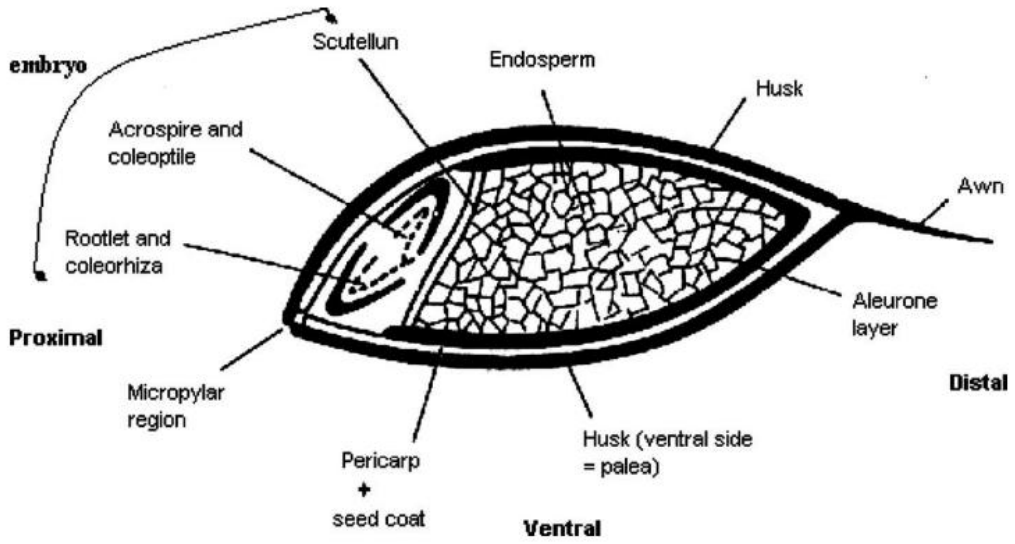

Figure 2-15: Schematic representation of a barley kernel in longitudinal section (adapted from Lewis and Young, 1995).

BSG consists mainly of the seed coat-pericarp-husk layers covering the original barley grain. The starchy endosperm and walls of empty aleurone cells may also remain in BSG, depending on the malting process. The starch content will be negligible, and some residues of hops introduced during mashing will be present depending on the brewing regime used. The main components of BSG will therefore be the husk–pericarp–seed coat walls, which are rich in cellulose and non-cellulosic polysaccharides and lignin, and may contain some protein and lipid (Mussatto, Dragone and Roberto, 2006). Although BSG is well known to be rich in sugars, proteins and minerals, the chemical composition of this material may vary significantly due to a variety of factors, including cereal variety, harvest time, type of hops added, the malting and mashing regime, and whether adjuncts were used during brewing (Mussatto, 2014; Lynch, Steffen and Arendt, 2016).

As mention above, BSG is rich in sugar and proteins but in general, BSG is considered as a lignocellulosic material rich in protein and fibre, which account for around 20% and 70% of its composition, respectively. Analyses of BSG conducted by Kanauchi et al. (2001), Mussatto and Roberto (2005) and Fukuda et al. (2002) are summarising in Table 2-5which proved that BSG as a lignocellulosic material.

Table 2-5: Chemical composition of brewers' spent grain (BSG) and germinated barley foodstuff (GBF)

Component (% dry wt)	BSG[a]	BSG[b]	GBF[a]	GBF[c]
Cellulose	25.4	16.8	8.9	9.1
Lignin	11.9	27.8	8.2	6.7
Arabinoxylan	21.8	28.4	17.0	19.2
Protein	24.0	15.2	46.0	48.0
Lipid	10.6	Nd	10.2	9.2
Ash	2.4	4.6	2.0	2.0

[a]FromKanauchi et al. (2001)
[b]FromMusatto and Roberto (2005)
[c]From Fukuda et al. (2005)
Nd, no determined

Since BSG is rich in sugars and proteins, the main and quickest alternative to eliminate this industrial by-product has been as animal feed. However, due to its of its low cost, large availability throughout the year and valuable chemical composition, BSG ia a raw material of interest for application in different areas. Many efforts have been made over the past decade to reuse BSG, taking into account the incentive that has been given to recycle the wastes and by-products generated by this industrial activity (Thomas and Rahman, 2006; Aliyu and Bala, 2013; Asad S N Mahmood *et al.*, 2013; Caetano *et al.*, 2013). Thus, compared to other industries, the brewing industry tends to be more environmentally friendly (Ishiwaki et al., 2000).

2.3.1 Potential application of BSG

The road to sustainability in the brewing industry has considerable potential due to the high volumes of waste material discharged with every brew. While BSG which are the major brewery by product and contain significant energy resources from their organic contents, they have some major difficulties in a sustainable energy balance which are: high water content, high nutrient content and handling difficulties (Thomas and Rahman, 2006). Despite of that, energy recovery from BSG has been considered as viable relative to thermochemical and biological process and several

alternatives had been proposed for BSG use in energy production, including in ethanol production, biogas production, and also thermochemical conversion (pyrolysis, combustion). The production of energy from BSG is been drive by the energy crisis that the world is currently experiencing (Mussatto, 2014).

Thermochemical conversion technologies such as pyrolisis and combustion of biomass material are one of the promising alternative methods to generate energy from BSG. With the net and gross calorific values of 18.64 and 20.14 MJ kg^{-1} dry mass respectively of BSG (Russ et al., 2005), and its reflect BSG as an interesting raw material to produce energy by combustion. The combustion process of BGS need pre-drainage of spent grain to moisture content lower than 550 g kg^{-1}. The heat generated by combustion of the BSG could be used to support the energetic demand of breweries in a brewery-integrated system(Mussatto, 2014). Nevertheless, combustion of BSG will generates the emission of particles and toxic gaseous emitted during combustion of dried BSG contain nitrogen and SOx(S.I. Mussatto et al., 2006; Weger et al., 2014) and it is crucial to take a special care when performing the combustion of BSG in order to minimizes this problem.

An alternative possibility for energy production from BSG is by anaerobic fermentation. Several studies have reported the possibility of producing biogas from BSG (Ezeonu & Okaka, 1996; Sežun et al., 2011) by this method and it is been considered especially suitable for obtaining thermal energy in breweries with few disadvantages towards environmental effects. Research conducted by (Ezeonu and Okaka, 1996), evaluated the process kinetic and digestion efficiency of biogas anaerobic batch fermentation of BSG which resulted in the production of biogas with a total yield of 3476 cm^3 per 100 g BSG after 15 days of digestion. Nonetheless, the biogas production from BSG is hindered by the presence of lignin and it is at the same time the limiting step for the complete degradation of the substrate (Sežun *et al.*, 2011). This inhibition is not prevented even by submitting BSG to mechanical, thermochemical or chemical pre-treatments. The biogas production from BSG is therefore a research area that merits great attention in order to develop a stable production process.

During the last decade, an interest in established a competitive process for ethanol production led to an significant impact of research in this area due to BSG was considered as a promising raw material for this application(White et al., 2008). Currently, ethanol production is at high levels for worldwide demanding and corn is main raw material used for this purpose. However, since feedstock is an essentially food, this scenario need an urge to change. Being evaluated in different kinds of processes, BSG had been considered owing a great potential to produce ethanol due to high content of hemicelluloses and cellulose fraction(White, Yohannan and Walker, 2008; Xiros and Christakopoulos, 2009). BSG are rich source of lignocellulose, such as the hemicellulose and cellulose which may be converted to fermentable sugar for production of bioethanol. For the production of ethanol, some pre-treatment may involve for example ultrasonication,acid treatment, enzymatic hydrolysis, or microwave digestion, in which need to be consider as main challenge for industrial sector nowadays(Mussatto, 2014). The pre-treatment steps for the raw material areessentialto make the extraction of glucose from cellulose easier and for ensuing use as a carbon source for fermentation process.

Recent research on BSG was done by Mahmood *et al.*, (2013) using a commercial reforming catalyst in a catalytic reforming reactor directly coupled to a batch fixed bed pyrolysis reactor. It is proved that BSG can produce high yield of bio- oil together with gas product by using thermochemical conversion. However, either the combustion or pyrolysis, both of these technologies require pre-dried out before the rest of the waste can go for the reaction, which would entail higher energy and longer reaction times. Liquefaction conversion, which is a thermal process at relatively moderate reaction conditions (temperature below 400°C and pressure between 1 and 30MPa, generally in the presence of a catalyst) offers a great potential to be applied for conversion of BSG.

2.4 Conclusion

The energy content in biomass or the waste products from harvesting or processing of biomass could be diverted into renewable energy and biofuels. The conversion of biomass to potential product stream can be achieved primarily via biochemical and thermochemical processes. The thermochemical processes is a

promising technology that can convert biomass to valuable products and suitable for different industrial applications.

The gasification and pyrolysis processes are complex and depends on several factors such as composition of lignocellulosic material, heating rate and moisture content. Most of the biomass sources are wet, and their moisture content can be at the range up to 95 wt. %. Due to this, the biomass feedstock needs to go for drying stages before been introduced to the biomass upgrading process. It should be noted that the final cost of bio-products not just based on the price of the starting feedstock, but it also depends heavily upon the processing cost. The latter may be decreased by reducing the number of synthesis steps and improving their yields, but a judicious choice of biomass conversion strategy could be essential to achieve a cost-effective development of biomass utilisation towards bio-products (Gallezot, 2012).

Hydrothermal technologies have ability to process high moisture content biomass waste without prior dewatering. This technology processing can be divided into three main process namely hydrothermal carbonisation, hydrothermal liquefaction and hydrothermal gasification; depending on the processing parameter. In current work, the study will focus on hydrothermal liquefaction reactions using BSG to produce liquid biofuel and valuable chemicals. Current applications of BSG are basically limited to animal feeding because of its high protein and fiber content or simply as landfill. Due to these, developing a new technique to utilise this agro-industrial by-product is a great interest since BSG is produced in large quantities throughout the year.

CHAPTER 3

RESEARCH METHODOLOGY: EXPERIMENTAL WORK AND ANALYTICAL TECHNIQUES

Chapter 3: Research methodology

3.0 Introduction

In this chapter, the liquefaction process including both the reactor set-up and experimental procedure is presented. Section 3.1 discusses the experimental set-up and reaction protocol, Section 3.2 on product identification and Section 3.3 elaborate additional characterisation technique employed in current work and theoretical principle underlie in those characterisations instrument is explained.

3.1 Liquefaction reaction set-up and procedure

The liquefaction reaction was studied using both model biomass (Chapter 5) and real lignocellulosic biomass (Chapter 6 and Chapter 7). The catalytic effect on liquefaction was also investigated to improve the reaction selectivity and efficiency. All liquefaction experiments were conducted in the same experimental set-up described in Section 3.1.1 by applying the method in Section 3.1.2. Depending on the type of biomass and parameter investigated, the methodology underwent small modifications, which are explainedin the corresponding chapters.

3.1.1 Reactor set-up

The equipment used for the HTL reaction of lignocellulosic biomass is shown in Figure 3-1, and the experiment set-up schematic diagram is illustrated in Figure 3-2. The main apparatus used for HTL is a stainless steel autoclave (Parker Autoclave Engineers) with the magnetically driven impeller (Figure 3-1-a). The capacity of the autoclave was 100 mL, and it was equipped with a cooling system. The cooler system works to avoid overheating of the mixer engine. The heating coat was used to heat the vessel, and the temperature will be controlled by SOLO Temperature Controller model 4842 (Figure 3-1-b) which connected to the reactor. The SOLO Controller also provides the setting for mixer speed. The pressure was measured by two different devices: i) pressure gauge with a range from 1 barg to 350 barg and ii) pressure transducer model PX319-3KG5V provided by Omega. Lastly, the system was also connected to the helium cylinder tank using a 1/8 inch stainless

steel tube. Helium gas was used as the reaction medium in liquefaction reaction to avoid the vaporisation of water, solvent or any liquid products present during the reaction.

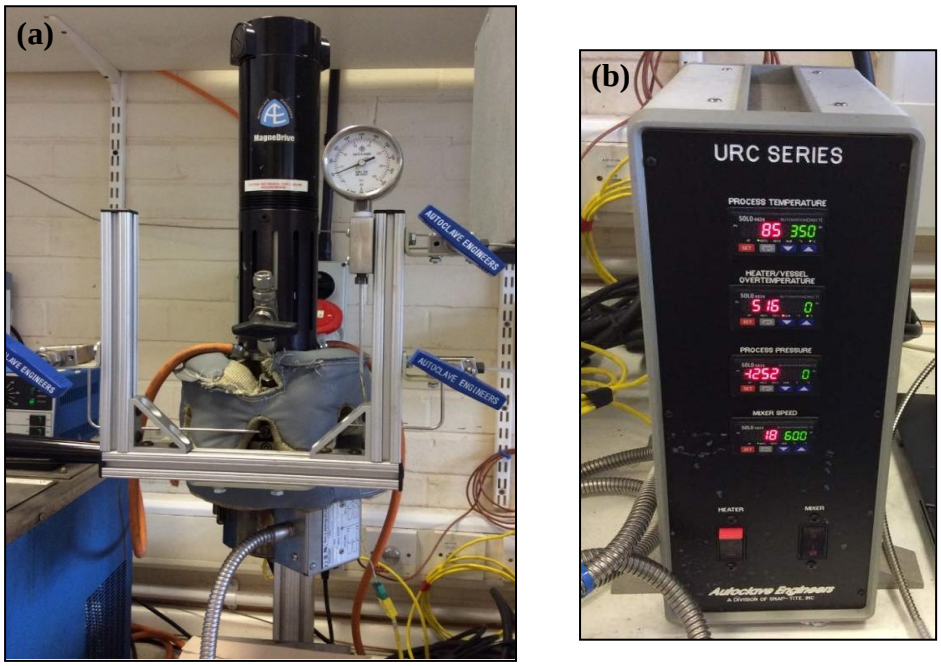

Figure 3-1: Photo of a) autoclave (Parker Autoclave Engineers) equipped with the cooling system and b) SOLO Controller used for liquefaction reaction.

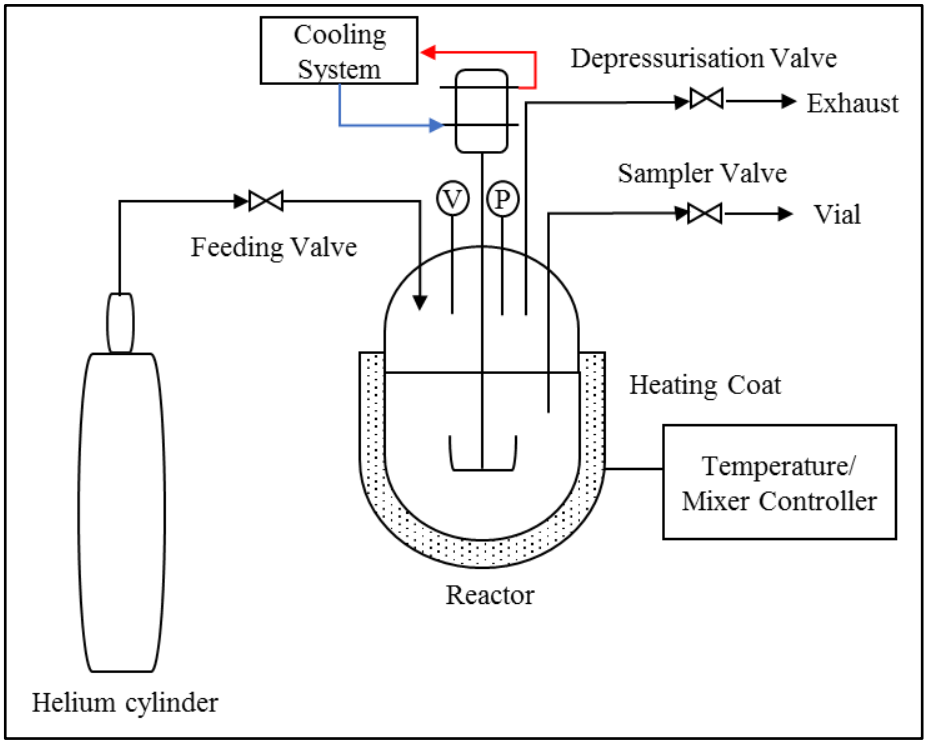

Figure 3-2: Schematic diagram of the liquefaction reaction set-up.

3.1.2 Experimental procedure

Initially, the reactor was loaded with biomass and solvent (Figure 3-3), depending on the parameter investigated. For example, in Chapter 5, the type of biomass is a cellulose model and lignin model while in Chapter 6 and Chapter 7, BSG was used as the biomass sources. In most cases, distilled water was used as solvent indicate by HTL reaction. However, in Chapter 6, the effect of solvent in liquefaction was investigated and, methanol, ethanol and 2- propanol employed as the solvent.

The second step was to pressurise with helium (99.99% purity, BOC). To displace any air present the reactor; helium was passed through the reactor for 3 minutes. After that, the depressurisation and sampling valve was closed,and the reactor was loaded with 30 barg of helium. The initial reading in both pressure gauge and pressure transducer were recorded,and after 15 minutes, the reactor was heated to the desired temperature. The waiting time before setting the temperature is important, prior to monitor for any leaking of gas or pressure drop. The vessel was heated using a heating jacket, and the mixer was activated when the desired temperature reached. The mixer was set at 500 rpm and the reaction time started as the mixer was switched on.

After the reaction time was completed, the temperature controller and mixer were stopped. The reactor was immediately cooled down by quenching in ice bath until the temperature reached 25 ºC. After cooling to room temperature, the pressure inside the vessel was released through the depressurisation valve. After each run, the gas was vented. The gas products were not analysed in this work as the main interest is the liquid-mixture products. Finally, the autoclave was opened, and the reaction mixture was removed prior to product determination.

Figure 3-3: Photo of 100 mL vessel used in the autoclave reaction system for current work.

3.2 Product determination

The solid-liquid mixture was separated by filtration through Whatman No.1 filter paper and under vacuum. The soluble fraction was taken as a liquid product, and the solid remain called residue. The liquid product was further analysed to determine the product composition, and for the solid residue, it was used to calculate the conversion for the reaction. The determination on residue and conversion were explained detail in Section 3.2.3.

3.2.1 Liquid product

The liquid sample was subjected to product analysis using gas chromatography-mass spectroscopy (GCMS). Depending on the biomass used, the liquid sample might undergo the second filtration using a 0.2 μm pore size Captiva Premium Syringe Layered Filter (Agilent). This second filtration is to ensure that none of the solid residues remains in the liquid phase to avoid blockage of the GCMS column in later analysis.

The GC analyser used in current research is Shimadzu GCMSQP2012SE device, which equipped with MS detector. It was operated by lab Solutions software which includes the NIST MS Search version 2.0 library with mass spectra of numerous match compound. The column used is HP-INNOWAX and the characteristics of the column employed are presented in Table 3-1.

Table 3-1: Characteristic of the column used for analysis of liquefaction sample by GCMS

Type of column:	**HP-INNOWAX**
Column length:	30 m
Internal diameter:	0.25 μm
Film thickness:	0.2 μm
Maximum temperature:	260 °C

3.2.1.1 Gas chromatography (GC)

GC is a versatile separation technique employed for volatile and thermally stable organic compounds. Widespread utilisation of a variety of detectors has exponentially expanded the dimensions of GC among which mass selective detection is one of the most popular. MS provides a basic elemental and structural composition of organic molecules (Kanaujia et al., 2014). When two separate techniques such as GC and MS are successfully combined to form gas chromatography-mass spectrometry (GCMS), the advantages become obvious. GC can separate many volatile and semi-volatile compounds but not always selectively detect them whereas MS can selectively detect many compounds but not always separate them (Sneddon et al., 2007).

A gas chromatograph is composed of five elements namely gas inlet, injector, column, detector and the data system which illustrates in Figure 2.3. The GC instrument procedure starts by injecting the sample into the inlet where it is volatilised , and a representative portion is carried onto the column by the carrier gas. Then, the sample components are separated by differential portioning in the stationary and mobile phased in the column section. Finally, the separated sample components elute from the column into the detector where some physic-chemical parameter is detected and a signal produced. This signal is then amplified and sent to the data system where the chromatogram is electronically constructed.

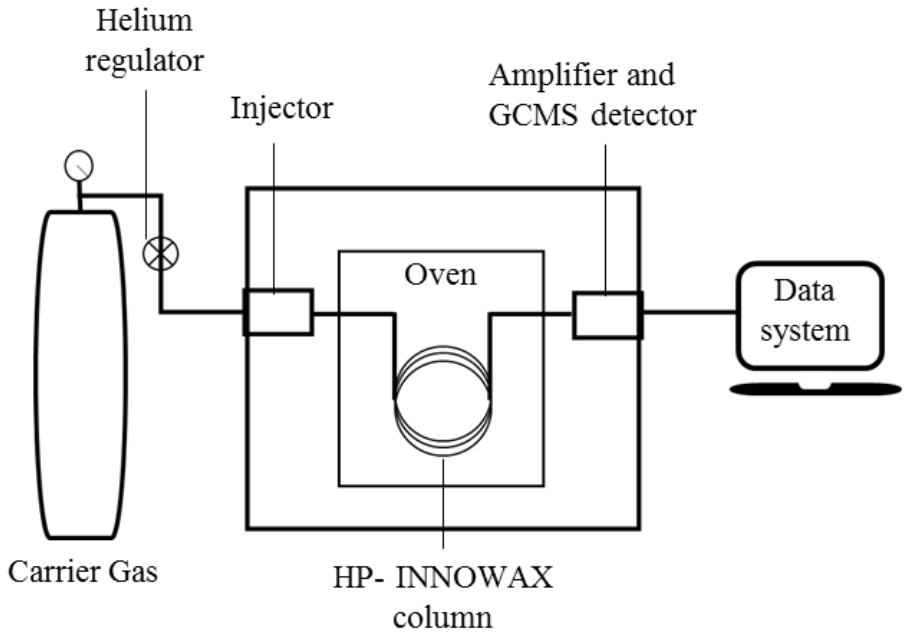

Figure 3-4: Basic components of a Gas Chromatograph-Mass Spectrometer Detector (GCMS) instrument.

3.2.1.2 Mass spectrometer (MS) detector

Mass spectrometry is an analytical technique that analyses gaseous ions by their mass-to-charge (m/z) ratio (Sneddon, Masuram and Richert, 2007). Mass spectrometry is an analytical technique that can determine precisely the atomic or the molecular weight of atoms or molecules once they have been ionised. The operation of a typical MS consists of the introduction of the sample into an ion source where the sample compounds are ionised. There are four crucial components in a mass spectrometer namely i) sample introduction, ii) the source where ionisation occurs, iii) mass analyser and iv) the detector (Hopfgartner, 2008). A representation of a typical MS system can be observed in Figure 3-4. Mass spectrometry can analyse many different types of sample that range from gas, solid or liquid.

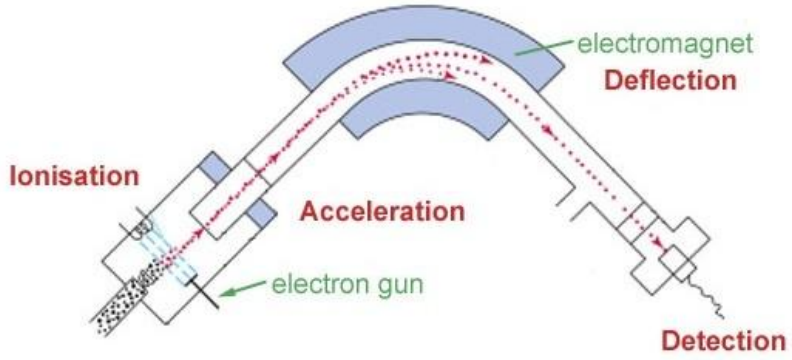

Figure 3-5:Diagram of a typical mass spectrometer configuration (Scienceaid, 2014).

3.2.1.3 HP- INNOWAX column

The column used in current research is HP-INNOWAX, and its characterisation is listed in Table 3-1. The column oven was used to control oven temperature (Skoog*etal.*,2007) for better product separation. The separation mode in this instrument was temperature programming which the column temperature was increased either continuously or in steps as separation proceeds for the sample has a wide boiling range. For better separation of the product obtained, the column temperature program was developed, and the method is illustrated in Table 3-2. The method used was set by referring to the work done by Lyu et al., (2015). The temperature was programmed with an initial temperature of 50°C.The temperature was then increased to 90°C at 10°C min^{-1}. At the second stage of temperature programming, the temperature was increased at 4°C min^{-1} from 90 °C to 120 ºC. At the final stage of the temperature programming, the temperature was increased from 120 ºC to 230ºC by 10°Cmin^{-1} and was held for 10 minutes. The total run time through this programme was 37.25 minutes.

Table 3-2: The program of the column oven temperature for chromatographic analysis of liquefaction sample by GCMS

Temperature rate (°C/min)	Final temperature (°C)	Hold time (min)
-	50	2
10	90	0
4	120	0
8	230	10

The amount of sample injected was 0.3 µL and was injected using an autosampler. The concentration of the product obtained was determined by re-calibrating the data with the standard calibration.

3.2.2 Product calibration

Calibration standards were prepared to quantitatively determine the concentration of the compound in the liquid product. GCMS calibration curves were prepared using the method detailed in Table 3-2. The compounds calibrated were: guaiacol (≥ 99, Sigma-Aldrich), 4 -ethyl-guaiacol (99%, Sigma-Aldrich), phenol (>99.5 %, Sigma Aldrich), furfural (99%, Sigma-Aldrich), levulinic acid (99%, Sigma- Aldrich), 5-HMF (99%, Sigma-Aldrich), glycerol (99%, Sigma-Aldrich),2-pyrrolidinone (99%, Sigma-Aldrich) and acetic acid (> 99 %, Acros Organics).

Calibration standards with different concentrations were prepared by series of dilutions of the stock solution. The quantity of compound used for the preparation of the stock solution was selected based on their solubility in water, and this concentration solution should be in the concentration range for the target compound. Details on dilution for the stock solution are presented in Table 3-3. The product concentration was measured using linear regression as follows:

$$y = mx + C$$

Where;

y = area of reactant or products under the peak curve

m = is the gradient or products calibration curve

x = the products concentration

C= point at which the line crosses the y-axis

Table 3-3: Dilutions employed for the preparation of standard calibration using a stock solution of liquid products

Stock solution (mL)	Solvent (mL)	Total volume (mL)
0.1	1.0	1.1
0.2	1.0	1.2
0.3	1.0	1.3
0.4	1.0	1.4
0.5	1.0	1.5

For each compound, the procedure was applied twice with different concentration for stock solution, and the resultant calibration curves were plotted in linear regression graph. The regression equation for the quantification of liquid products was the obtained using calibration curves. The calibration graph was shown in Figure 3-6 until Figure 3-14.

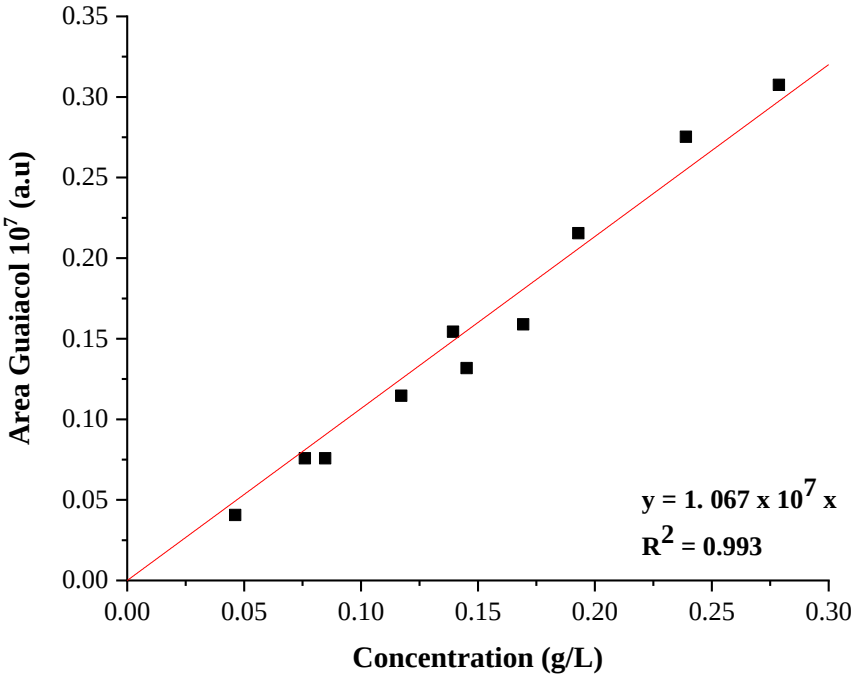

Figure 3-6: Calibration curve for guaiacol / 2- methoxy phenol with the value for linear concentration regression, y = 1.067 x 10^7x

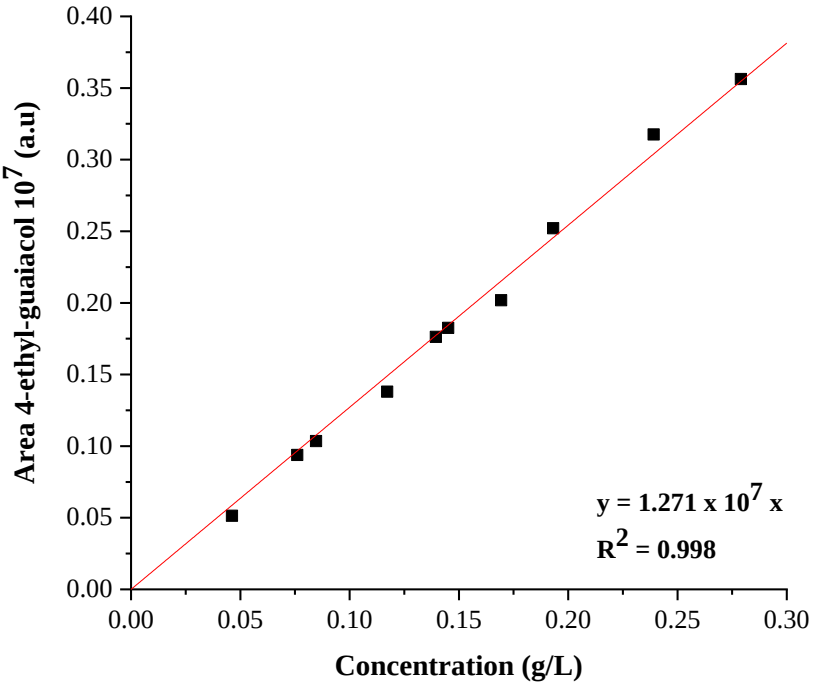

Figure 3-7: Calibration curve for 4 - ethyl- guaiacol / 4 - ethyl-2- methoxy phenol with value for concentration linear regression, $y = 1.271 \times 10^7 x$

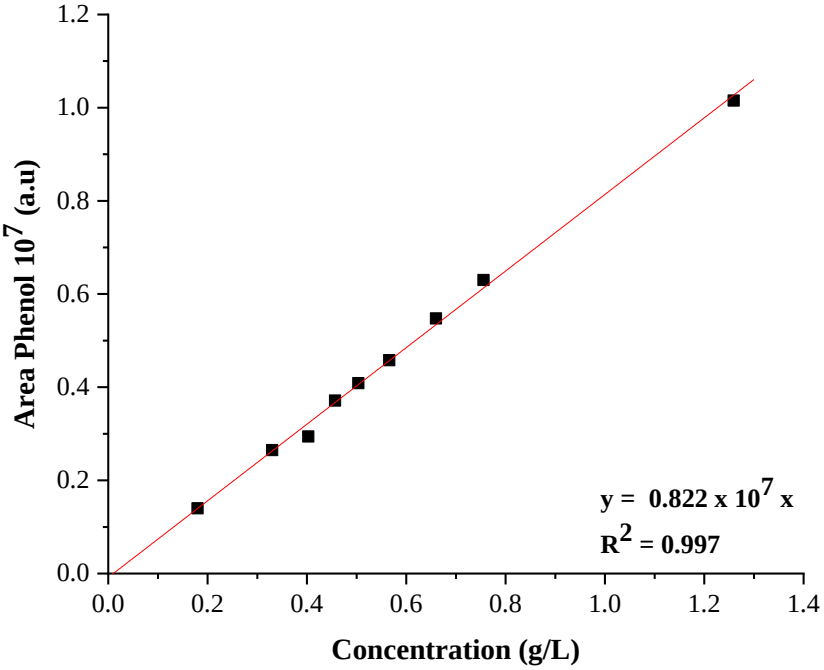

Figure 3-8: Calibration curve for phenol with the value for linear concentration regression, $y = 0.822 \times 10^7 x$

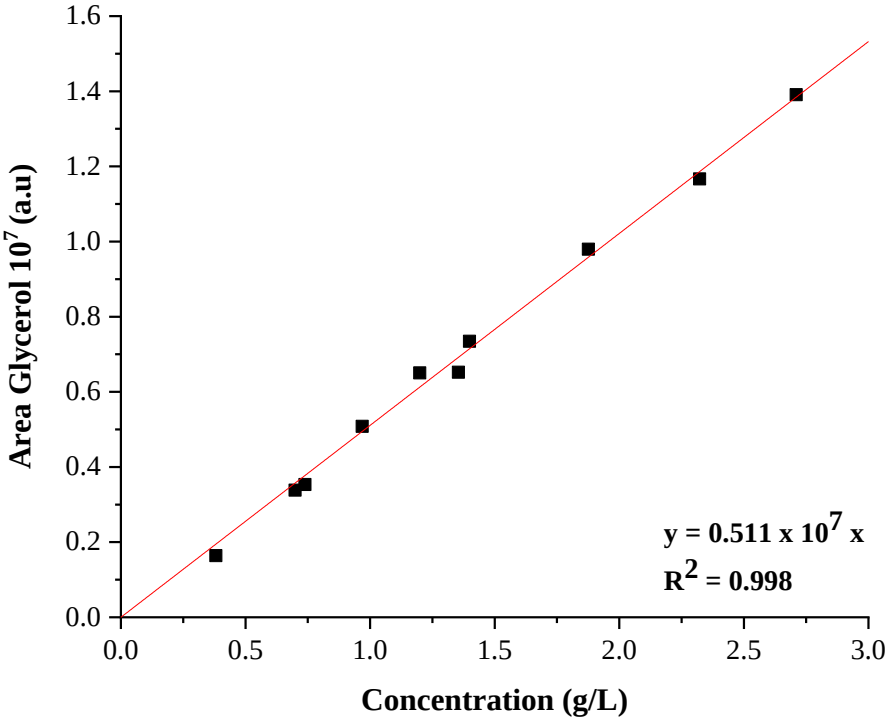

Figure 3-9: Calibration curve for glycerol with the value for linear concentration regression, $y = 0.511 \times 10^7 x$

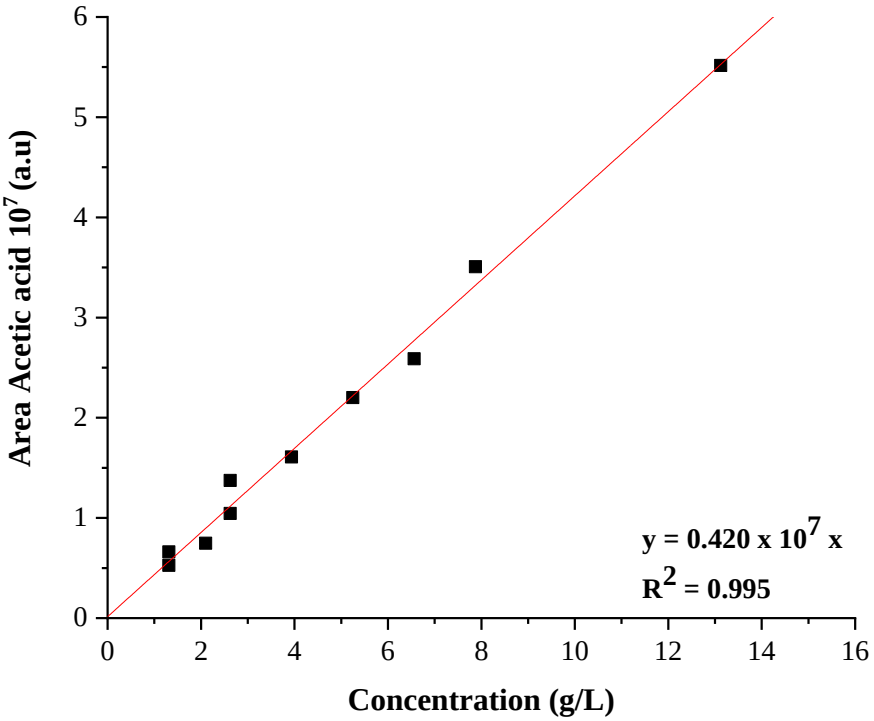

Figure 3-10: Calibration curve for acetic acid with the value for linear concentration regression, $y = 0.420 \times 10^7 x$

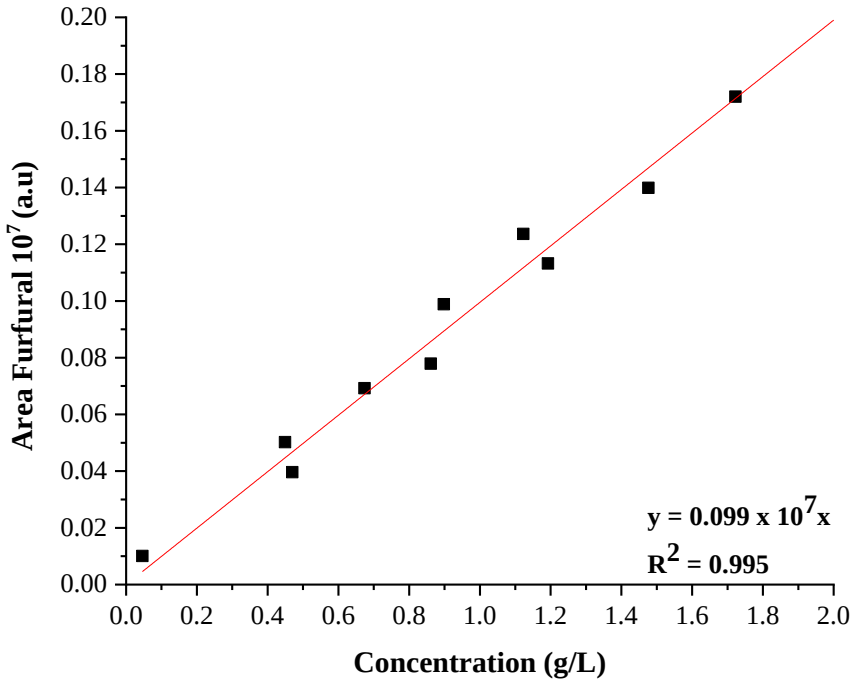

Figure 3-11: Calibration curve for furfural with the value for linear concentration regression, $y = 0.099 \times 10^7 x$

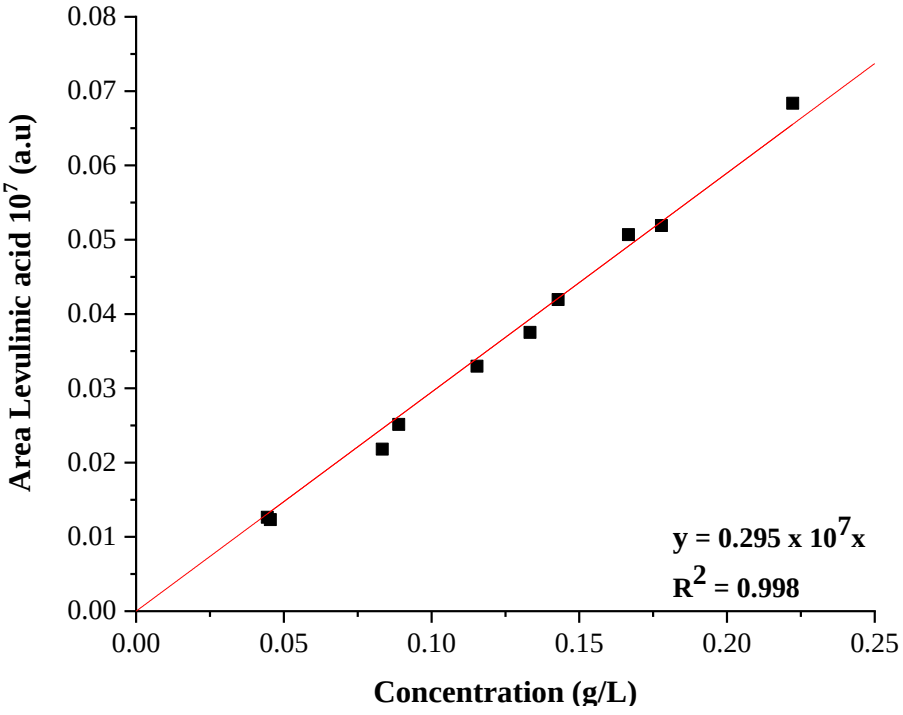

Figure 3-12: Calibration curve for levulinic acid (LA) with the value for linear concentration regression, $y = 0.295 \times 10^7 x$

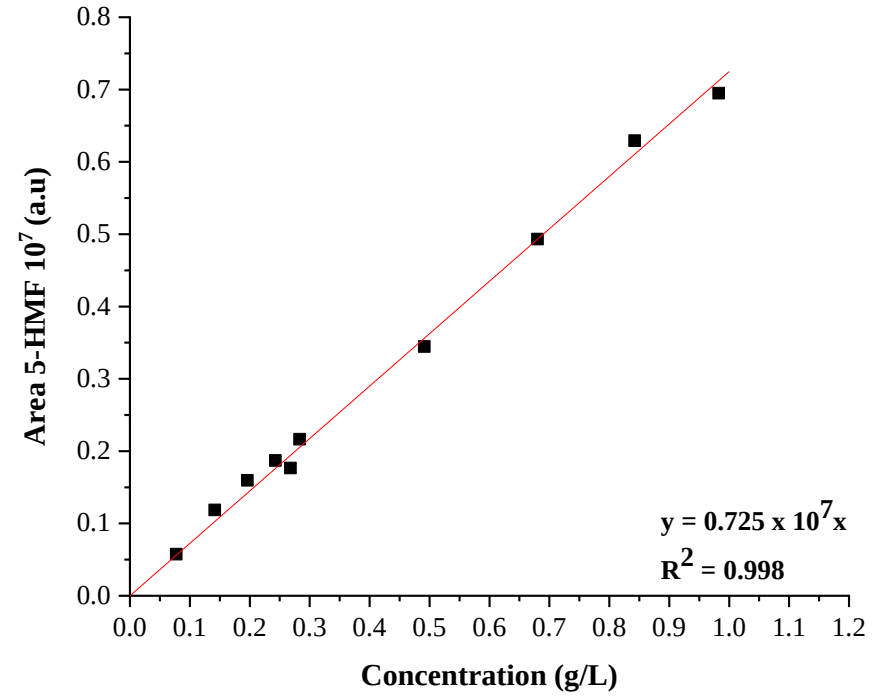

Figure 3-13: Calibration curve for 5-HMF with the value for linear concentration regression, y = 0.725 x10^{7}x

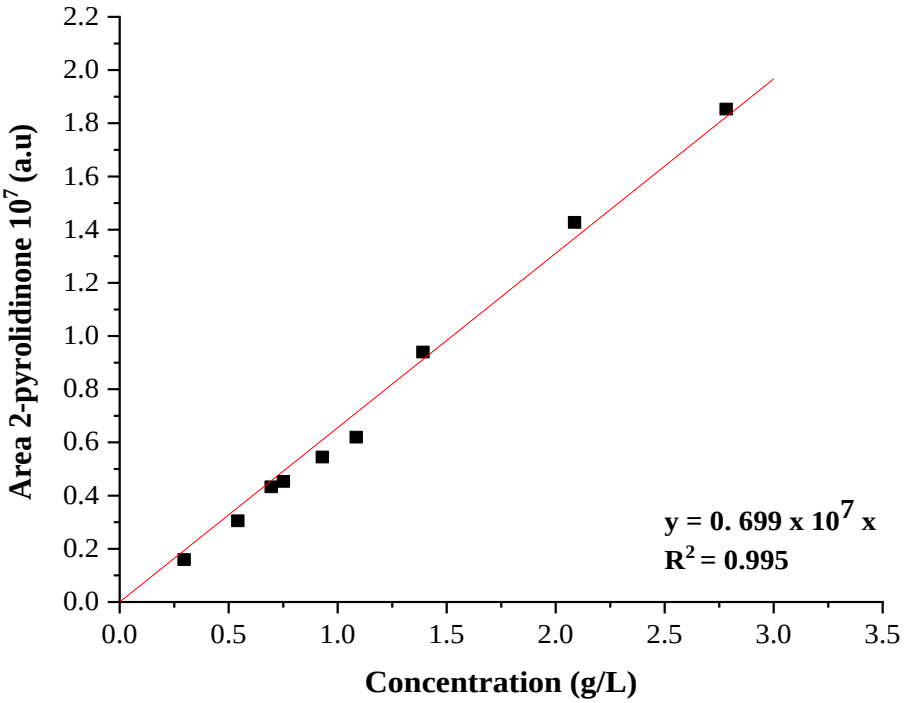

Figure 3-14: Calibration curve for 2-pyrrolidinone with the value for linear concentration regression, y = 0.699 x 10^{7}x

3.2.3 Solid residue and definition of conversion

Liquefaction is a thermo-chemical process that converts biomass into a liquid product, bio-oil (Stöcker, 2008). Thus, the focus on current work is the liquid obtained resulted from liquefying product of feedstock. However, throughout the process, there is a solid residue present after the reaction. The remaining solid was dried at 105 ^{o}C in an oven for 24 h to obtain the constant weight. The determination of residue yield and conversion were defined as the weight percentage of the biomass input (Nazari *et al.*, 2015) and was calculated as follow:

$$\textbf{Residue yield } \% = \frac{\text{weight of residue}}{\text{weight of the biomass input}} \text{ x } 100\%$$

$$\textbf{Conversion } (\%) = 100 - \text{Residue } (\%)$$

3.3 Characterisation techniques

The biomass and liquefaction products were subjected to several characterisation techniques to study their chemical and physical properties. The data from these characterisations are useful to understand the relationship between the properties of biomass and the product in the liquefaction reaction. In this research, the characterisation techniques used are thermogravimetric analysis-differential thermal analysis (TGA-DTA), Fourier-transform infrared (FTIR) spectroscopy, C, H and N elemental analyser (FLASH 2000), X-ray fluorescence (XRF) and bomb calorimetry. In the current section, brief theoretical principles behind the characterisation techniques used in current work are explained.

3.3.1 Thermogravimetric analysis- differential thermal analysis (TGA-DTA)

Thermogravimetric analysis is a technique in which the mass of substances is monitored as a function of temperature or time. Additionally, the sample specimen is also subjected to a controlled atmosphere during the temperature programme (Perkin Elmer, 2004). A TGA consists of a micro sample pan that is supported by a precision balance. The pan is placed inside the furnace and is heated or cooled during the experiment. The microbalance is connected to the

thermal analysis processing system to get a plot of weight loss versus temperature. A sample purge gas controls the sample environment. This gas may be inert or a reactive gas that flows over the sample andexits through an exhaust.

In the present work, TGA-DTA was used to study the thermal properties of biomass and solid residue obtained after the liquefaction reaction. The TG and DTA curves for the samples were obtained by TGA 4000 simultaneous thermal analyser up to 1000 °C. Two thermograms were obtained from this instrument, the TGA thermogram indicating the weight loss and energy loss and the DTA thermogram indicating the absorption or evolution of heat. For analysis, the sample in the form of powder was placed in an alumina covered crucible, while an empty crucible being the reference. In current work, nitrogen was used as an inert gas, and the air was set as an active gas. The temperature used was in the range of 30 ºC and 950 ºC, with constant heating rate and gradually isothermic programme depending on the research parameter.

3.3.2 ATR-Fourier – Transform Infrared (ATR-FTIR) spectroscopy

Infrared spectroscopy is a technique based on the vibrations of the atoms of a molecule. An infrared spectrum is commonly obtained by passing infrared radiation through a sample and determining what fraction of the incident radiation is absorbed in particular energy. The energy at which any peak in an absorption spectrum appears corresponds to the frequency of vibration of a part of a sample molecule.

Fourier- transform infrared (FTIR) spectroscopy is based on the idea of the interference of radiation between two beams to yield an interferogram. The latter is a signal produced as a function of the change of path length between the two beams. The two domains of distance and frequency are interconvertible by the mathematical method of Fourier- transformation. The basic component of the FTIR spectrometer is shown schematically in Figure 3-15. The radiation emerging from the source is passed through an interferometer to the sample before reaching a detector. Upon amplification of the signal, in which high-frequency contributions have been eliminated by a filter, the data are converted to digital by an analogue-to-digital converter and transferred to the computer for Fourier- transformation (Stuart, 2004).

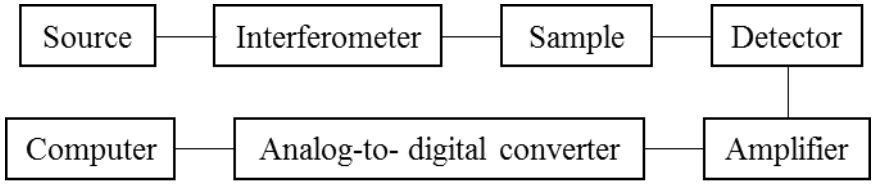

Figure 3-15: A basic component of an FTIR spectrometer

ATR-FTIR analysis for was conducted employing a Shimadzu IRAfiinity-1S. Spectra were collected over the range 400 to 4000 cm^{-1} with a resolution of 4 cm^{-1}. Through this technique, the functional group present BSG and the solid residue was measured,and for extracted cellulose and lignin, the spectrum obtained were compared with their commercial compound.

3.3.3 X-rayFluorescence (XRF)

X-ray spectrochemical analysis is based on the fact that the chemical elements emit characteristic radiation when subjected to appropriate excitation. When a sufficiently energetic X-ray photon interacts with an atom, several phenomena take place. One interaction involves the transfer photon energy to one of the electrons of the atom (for example, a K shell electron) resulting in its ejection from the atom (Figure 3-16). The distribution of the electron in the ionised atom is then out of equilibrium and within short time reach such electron turns to the normal state, by the transition of an electron from outer shells (excited state) to inner shells. The electron drops to the lower energy state by releasing a fluorescent X-ray. The energy of this X-ray is equal to the specific difference in energy between two quantum states of the electron. The measurement of this energy is the basis of XRF analysis.

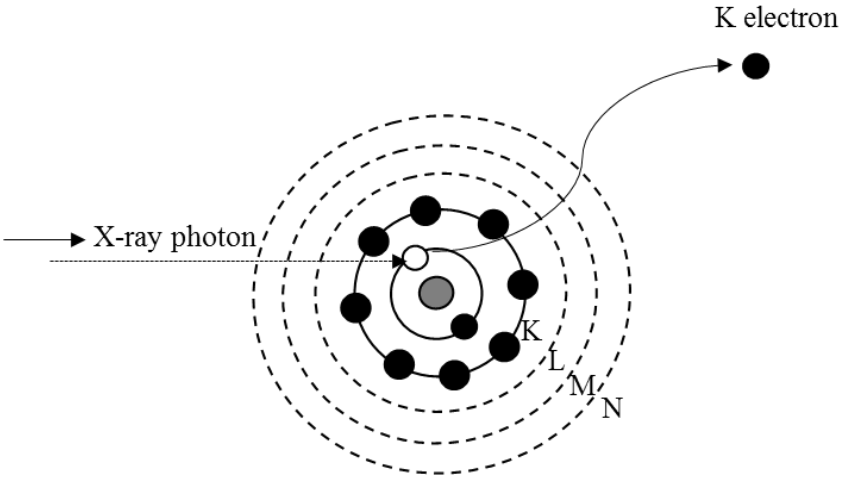

Figure 3-16: Ionization of the K shell by an incident x-ray photon

In current work, PANalyticalZetium (XRF) instrument was used to determine the metallic and minerals element in BSG samples. The basic working principles in XRF spectrometer are shown in Figure 3-17. The BSG sample used for XRF analysis is a powder. The sample was prepared prior analysis by place a single sheet of round Mylar foil as a based in sample cell. The BSG powder then were poured to the sample cell with at least 4 mm depth and ensure the based was fully covered. Then, the sample cell was transferred into solid metal cup and was placed into sample trays inside PANalyticalZetium (XRF) instrument. The sample was thenanalysed and the data obtained represent the metallic and minerals element in BSG samples in term of weight percentage (wt. %) and also ppm.

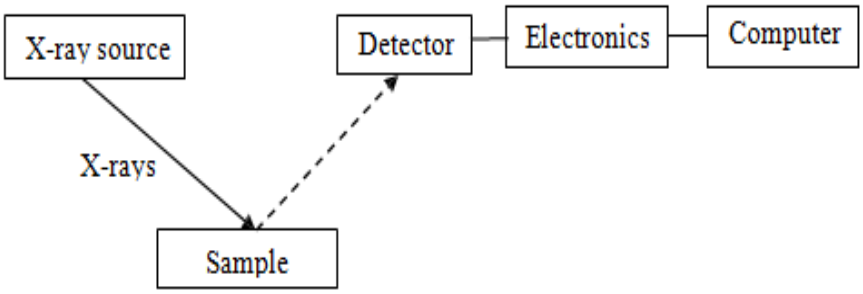

Figure 3-17: Schematic of a simplified wavelength dispersive x-ray spectrometer

3.3.4 C, H and N elemental analysis

The elemental analyser is composedof an autosampler that can run a sequence of samples, a combustion chamber (furnace), a GC column, and a TCD to detect the elements eluted from the GC column. The instrument is usually used to measure the percentage of the C, N, H, and S in solid or liquid samples. The carrier gas used is usually He, while pure O_2 is used as the combustion gas.

In this work, the ultimate analysis of BSG, lignocellulosic composition and char properties was determine using a Flash 2000 organic elemental analyser (Thermo Scientific) fitted with a MAS 200R carousel auto sampler for solids. A sample of 2-3 mg was introduced to the instrument using tin capsules (CE instruments). Afterwards, the sample was burned off in the presence of pure oxygen in the instrument furnace seated at 900 °C. The combustion products were analysed using a GC column and then detected by the TCD. The carrier gas employed was He at a flow rate of 130 mL min^{-1}. The instrument was calibrated using a calibration standard that has a known percentage of C, N, H, and S. The data were collected as elemental weight percentage using Eager Xperience software version 1.1.

CHAPTER 4

A CASE STUDY: CHARACTERISATION OF BREWER'S SPENT GRAIN (BSG)

Chapter 4: Characterisation of BSG

4.0 Introduction

The identification of physical and chemical characteristics is the most crucial step in determining the selection of appropriate technologies for biomass utilization (Vassilev *et al.*, 2010). A complete understanding of both physical and chemical characteristics of BSG will determine the properties, quality and potential application of this waste. In this chapter, three types of characterisation methods have been used on raw BSG. The first stage is the BSG pre-treatment, which involves the determination of the moisture content and the ball milling process. The second stage of the BSG characterisation will focus on the chemical characteristic of BSG using FTIR, proximate and ultimate analysis. The third stage then focuses on the components of BSG, which are cellulose and lignin. In this final stage, the BSG went through several degradation processes to break the polymer structure down before extracting its main components. Ranges of thermal and spectroscopic characterisation techniques were also employed in this stage and comparisons of the quality, structure, and nature of the extracted components with their respective commercial compounds were made.

4.1 Experimental procedures

4.1.1 Materials

The materials used in this work were ethanol (Sigma – Aldrich, ≥ 99%), sodium acetate anhydrous (Sigma – Aldrich, ≥ 99%), sodium chloride (missing supplier), acetone (Alfa Aeser, 99.5%), sulphuric acid (Sigma – Aldrich, percentage), sodium hydroxide (Sigma – Aldrich, 97+%), distilled water (produced in an Elga reservoir of 75 L), microcrystalline cellulose (Avicel® PH-101, Sigma Aldrich), and kraft lignin (Low sulfonate content lignin, Sigma Aldrich).

4.1.2 Stage one- BSG pre-treatment

In the current work, BSG underwent two stages of pre-treatment; drying and ball milling. Dry BSG was obtained in the first stage of pre-treatment and in the second stage, BSG power was obtained.

The procedure used to determine the moisture content of the raw BSG was adopted from Samuelsson, Burvall, and Jirjis (2006)and British Standard BS EN 14774-3:2009 (Asad S N Mahmood *et al.*, 2013) and involved using oven drying in air. The experiments used samples of the material as received and measured to 0.1 g accuracy. For this analysis, approximately 5 g of raw BSG were measured and placed into the evaporator glassware with the oven temperature set at 105 ºC. Four replicates of raw BSG samples were prepared for each batch of the drying process. BSG was dried to a constant weight, which was accomplished within 24 h drying time. The weight difference between the raw BSG and the dry BSG was calculated and gave the moisture content of the samples.

Prior to chemical analysis (FTIR, proximate and ultimate analysis), the raw BSG was subjected into two stages of pre-treatment, which were drying and milling. The drying process must be conducted before the milling process. Bargakat, de Vries and Rouau (2013) investigated the effect of the moisture content on the milling process. They concluded that a lower moisture content produced finer particles of the biomass, which results in a more accurate analysis of the data. Furthermore, the grinding energy also decreased significantly as the moisture content was reduced.

The milling process was conducted using a Retsch PM100 planetary ball mill. The grinding bowl and the supporting disc of the planetary ball mill rotated in opposite directions which produced corresponding centrifugal forces. As a result of this, a friction effect was produced by the movement of the milling balls down the inside wall of the bowl (Suryanarayana, 2001).

Figure 4-1 shows a schematic depicting the ball motion inside the ball mill. As a consequence of the friction, the material was milled into a coarser powder. With continuous cycles of the milling process, finer or nanoscale powder was produced.

In this work, 10 g of dry BSG were used in the milling process. The process was set up to run for a grinding time of 15 minutes, at speed 500 rpm with1 minute of interval breaks. The BSG powder obtained following this process was subjected to the characterisation of proximate and ultimate analysis.

(a) 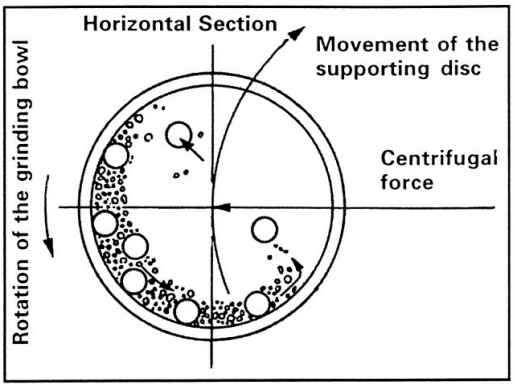

(b) 

Figure 4-1: (a) Schematic depicting the ball motion inside the ball mill. Image adapted from (Suryanarayana, 2001) and (b) BSG powder obtained after the milling process

4.1.3 Stage two – FTIR, proximate and ultimate analysis of BSG

4.1.3.1 FTIR analysis

FTIR has previously been used for the successful compositional analysis of lignocellulosic biomass (Tucker *et al.*, 2001; Xu *et al.*, 2013). Generally, different functional groups correspond to different components of the IR spectrum; therefore, the spectral features can be used to determine the structure of the biomass. For analysis, approximately 50mg of the BSG powder wereplaced in a diamond-composite ATR sample cell. Then, the sample was pressed with a spring-loaded anvil until it was tightly compressed against the diamond surface. Mid-IR spectra were collected in the range 4000 to 400cm^{-1} with a resolution of 4cm^{-1} using Shimadzu IRAfiinity-1S.

4.1.3.2 Proximate analysis method

The proximate analysis conducted was adapted from the work presented by Garcia *et al.*, (2013) and Carrier, Loppinet-Serani and Denux, (2011). They both applied thermal analysis as a proximate analysis method and have successfully proved that TGA can be applied to determine biomass composition. Thermal analysis can be defined as methods that measure the property of substances when subjected to a controlled temperature. In this work, thermal decomposition of BSG was applied and predominantly focused on the moisture, volatile matter, fixed carbon and ash content. Data obtained was used to calculate several parameters using the equations indicated in Table 4-1 (Anukam *et al.*, 2017).

Table 4-1: Equation parameters used for proximate analysis determination from the TGA curve of BSG.

Parameter	Equation
Moisture content	$\left(\frac{([\boldsymbol{Initial\ Mass}] - [\boldsymbol{Dry\ Mass}])}{[\boldsymbol{Initial\ Mass}]}\right)\mathbf{x\ 100}$
Volatile matter content	$\left(\frac{([\boldsymbol{Volatile\ Mass}])}{[\boldsymbol{Initial\ Mass}]}\right)\mathbf{x\ 100}$
Fixed carbon	$\left(\frac{[\boldsymbol{Fixed\ carbon\ mass}]}{[\boldsymbol{Initial\ Mass}]}\right)\boldsymbol{x}\ \mathbf{100}$
Ash	$\left(\frac{[\boldsymbol{Ash\ mass}]}{[\boldsymbol{Initial\ Mass}]}\right)\boldsymbol{x}\ \mathbf{100}$

For this analysis, 20-25 mg of BSG powder were measured and analysed using the TGA instrument analyser; the PerkinElmer TGA4000. The initial parameters used for this analysis were a flow rate of 20.0 ml/min of nitrogen and 40.0 ml/min of oxygen heating of 30 to 50 ºC/min, with the temperature been held for several stages until the temperature reached 950 ºC.

The moisture content was determined by the weight loss at a temperature close to 100 ºC to 110 ºC, while the volatiles content was indicated by the mass evolved between a temperature of 110 ºC to700 ºC (Saldarriaga *et al.*, 2015). At a temperature of 900 ºC, the gas flow was switched from nitrogen to oxygen to allow the full combustion of carbon-containing species (CO_x, C_xH_y and tars) and char oxidation (Garcia *et al.*, 2013), which leads to the determination of the fixed carbon content.

In some other works, the fixed carbon content was determined by the differences between moisture, volatiles and ash (Tanger *et al.*, 2013). However, the effect of ash on the fixed carbon content produces a possible limitation in determining a stable fraction. This is due to the decreasing measured weight of ash leading to inflated values for the fixed carbon determined via subtraction. (Crombie *et al.*, 2013). Due to this fact, the fixed carbon content in this work was determined based on mass loss through the combustion process. Finally, after heating the sample to approximately 950 ºC, the remaining mass in the crucible was considered to be only ash and represented the same value as indicated by the differences of moisture, volatiles and fixed carbon. In conclusion, the ash content represents the inorganic part of the biomass left after complete combustion (Garcia, 2012).

4.1.3.3 Ultimate analysis method

BSG was subjected to elemental analysis using two methods; firstly, the C,H, N and S components of BSG were measured using FLASH 2000,and secondly, the metallic and mineral components were determined using XRF. FLASH 2000 measured the nuclear properties of BSG through mass spectroscopy. The XRF used the electronic properties of the components as basis for the analysis. By combining both methods, all the individual elements present in the BSG were identified apart from oxygen.

In most cases, the amount of oxygen was determined by subtracting the sum of the amount of C,H,N, and S from 100% (Nanda *et al.*, 2013; Mussatto, 2014; Anukam *et al.*, 2017), but there are some disagreements to this approach, mostly coming from different opinions on whether or not to include the percentage of ash. The analysis of C, H, N, S was done through complete combustion in an active

atmosphere and the sample was reduced to a group of gases such as CO_2,H_2O, N_2 and SO_2, which permitted the simultaneous determination of carbon, hydrogen, nitrogen, and sulphur in the organic material (García *et al.*, 2012). This mode of analysis did not detect the presence of ash which is generally indicated by inorganic material. Many authors included the ash when calculating the oxygen value which can be obtained from the proximate analysis (Gai *et al.*, 2015; Jazrawi *et al.*, 2015; Nazari *et al.*, 2015). In this work, the oxygen percentage in BSG was determined by considering the ash and was calculated by the difference between 100 and the sum of C, H, N and ash, assuming negligible sulphur content. The equation used is as follows:

$$O = 100 - (C + H + N + ash) \qquad \textit{Equation 4-1}$$

4.1.4 Stage three-Determination of BSG composition

4.1.4.1 Soxhlet extraction procedure

The extractive content of BSG was determined in accordance with Tappi 204 cm- 97 (Technical Association of Pulp and Paper Industry, 1997)by using Soxhlet extraction. Firstly, 5 g of dry BSG was measured and was put in to the extraction thimble before been placed inside a Soxhlet glass filter. 150 mL of ethanol was used as a solvent and was placed in the receiving flask on the Soxhlet apparatus. The Soxhlet apparatus was assembled with a condenser to avoid any evaporation of the solvent. The reflux temperature was set at 78-80ºC (boiling point of ethanol) for 12 h in order to optimize the removal of the extraction content of BSG. When the reflux time was reached, the heating plate was turned off, and the apparatus was cooled to room temperature. After 30 minutes, the thimble was removed from the Soxhlet glass filter, and the BSG was placed into the evaporator glassware before being dried in the oven at a temperature of 105 ºC for 3 h. The extractive content was calculated by the mass loss of the dry BSG sample before and after the extraction process. The BSG obtained after this process was called *extractives-free BSG* (*EF* - BSG) and was used for determination of the BSG composition.

4.1.4.2 Cellulose extraction procedure

The hemicellulose and cellulose composition of BSG was extracted from *EF-BSG* using two stages, as adapted from Carrier, Loppinet-Serani, and Denux (2011). The first stage was to obtain the holocellulose from *EF-BSG* in which the ideal holocellulose should only contain cellulose and hemicellulose. The second step was to hydrolyse and degrade the hemicellulose from holocellulose and therefore, the solid that remained should represent the cellulose content of BSG.

The first stage in obtaining holocellulose was to add 4 g of *EF- BSG* to 160 mL of sodium acetate solution (1 M), and heat the mixture at the temperature of 75 ºC for 6 h using a hot plate. After 3 h of heating, 4 mL of sodium chloride (1M) was added, and the heating was continued for another 3 h. The use of this solution was to allow the degradation of lignin present in *EF- BSG*, which then led to the remaining solid being *lignin free BSG* (Rodríguez-Gutiérrez *et al.*, 2014). After that, the mixture was cooled down and filtered using vacuum filtration. 500 mL of distilled water was used to wash the solid residue obtained and the solid residue was then placed into evaporator glassware. The solid was dried in the oven at the temperature of 105 ºC for 24 h; the weight of the solid residue obtained after the drying process represented the holocellulose content.

The second stage involved the extraction of the cellulose from the holocellulose and was conducted following the procedures as suggested by Carrier, Loppinet-Serani, and Denux (2011). By definition, the cellulose obtained in this work was the α-cellulose in which the residue of holocellulose insoluble in 17.5 wt.% NaOH solution. Firstly, the holocellulose obtained from the first extraction was added to 100 mL of NaOH with a concentration of 17.5 wt. %. Then, the mixture was stirred at 200 rpm for 30 minutes at room temperature. After the contact period ends, the solid residue was filtered and washed with 400 mL of distilled water. The residue was then put in to the beaker and then15 mL of 10 wt. % acetic acid solution was added to optimize the holocellulose hydrolysis. Finally, the solid residue was filtered and washed with 500 mL of hot water and was dried at 105 ºC for 24 h. The dry solid residue represented the cellulose content of BSG. The hemicellulose content was determined gravimetrically by the weight difference

between the holocellulose and the cellulose obtained. Throughout the process, the hemicelluloses were more readily hydrolysed compared with the cellulose because of its branched and amorphous nature.

4.1.4.3 Lignin extraction procedure

The lignin content of the current BSG samples was determined in accordance with Tappi T222 om-88 (Tappi, 2011) and the extracted lignin is known as “Klason lignin". This method was used with the objective of retrieving the acid-insoluble lignin contained in the biomass (Chimica and Uni, 2010).

The first step in extracting the lignin involves mixing 1 g of *EF- BSG* with 15 mL of 72 wt. % H_2SO_4. The mixture was stirred at 200 rpm for 2 h at room temperature. This step was to hydrolyse and solubilise the carbohydrate content of the BSG (Carrier, Loppinet-Serani and Denux, 2011). After 2 h, 560 mL of distilled water was added to the mixture, and this reduced the H_2SO_4 to 3 wt. %. The diluted sample was further boiled at the temperature of 100 ºC for the next 4 h. The mixture was then separated using vacuum filtration, and the lignin which was the solid residue was washed using distilled water until it reached a neutral pH. Finally, the solid was placed into the evaporator glassware and dried in the oven at the temperature of 105 ºC for 24 h. The solid residue obtained following this process represented the lignin content of the BSG.

4.2 Results and discussions

4.2.1 The moisture content of raw BSG

BSG used in this work was a wet residue type, which was obtained after separation from the wort during the lautering stage (Poerschmann *et al.*, 2014). This insoluble waste was composed of a husk-pericarp barley grain together with minor fragments of endosperm (Mussatto *et al.*, 2010). The grains were dark brown in color and wet (El-Shafey *et al.*, 2004), which may have resulted from the leftover wort that remained in the grain during the filtration stage. The shape of the spent grain was non-uniform and ripped which may have been due to the grinding process of the malt prior to mashing (Mussatto, 2014). The spent grain was also sticky and clammy

which may have been caused by the incomplete conversion of starch into maltose during the mashing process (Iserentant, 1995). Figure 4-2 shows the BSG used in this research. It was used in the experimental work without any pre- treatment or modification, except those mentioned in the previous sections.

Figure 4-2: Photo of the wet residue type of raw BSG used in this study.

It is known that raw BSG has high moisture content; therefore it is essential to measure the exact amount of moisture present in this waste. The determination of the moisture content in raw BSG will reveal the amount of water associated with this waste. This step is also useful to calculate the solid content/ conversion on one consistent basis (i.e., dry weight basis).

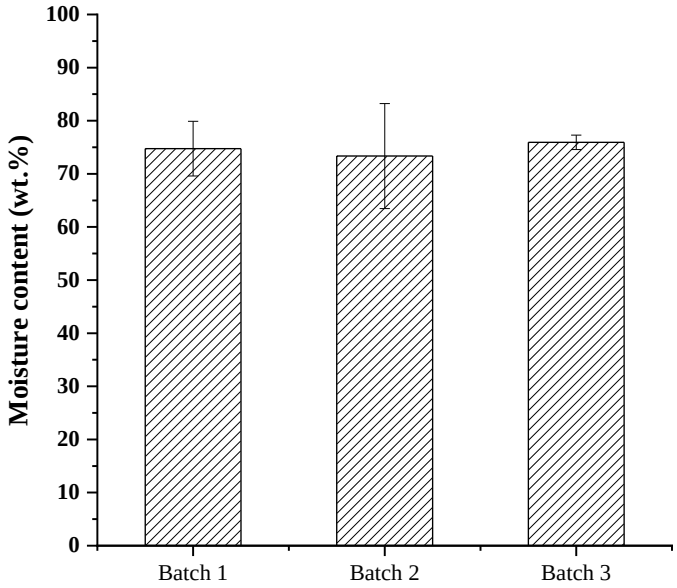

Figure 4-3: Weight percentage (wt. %) of moisture content in raw BSG used in current experimental work.

As shown in Figure 4-3, the mean value for the moisture content of the BSG is 74.7wt. % with the relative standard deviation of 3.2 %.Based on these results, the moisture content represents about three quarters of the raw BSG weight, which is in agreement with the findings reported by other researchers studying wet BSG. Mussatto, Dragone and Roberto (2006) stated that wet BSG from a lauter tun contained about 77-81% (w/w) of moisture. Moreover, Fărcaş *et al.*, (2014) also wrote that wet spent grain contained about 70 to 80% water content. El-Shafey *et al.*, (2004) claimed that wet BSG was a perishable product (difficult to preserve under environmental conditions) due to its high moisture content (75–80%). Due to the fact that raw BSG contains high moisture and sugar, the BSG easily deteriorates through microbial activity leading to difficulties in storing, transporting and handling (El-Shafey *et al.*, 2004; Weger *et al.*, 2014). This highlights the importance of finding a way to make the most out of this waste by maximising the use of their high moisture content.

4.2.2 Characterisation of BSG

Another critical factor that needs to be considered when utilising this waste is its chemical characteristics; the selection of the biomass conversion technology depends on the nature and composition of the biomass (Kumar, Olajire Oyedun and Kumar, 2018). Section 4.1.3.1.2.2 will focus on the chemical characterisation of BSG based on the FTIR spectroscopy and the proximate and ultimate data.

4.2.2.1 FTIR spectra of BSG

ATR- FTIR spectroscopy was employed in this study to obtain information regarding the type of functional group and polymer present in the solid waste. The IR spectrum of the BSG is as shown in Figure 4-4 with the value for each significant peak was labelled.

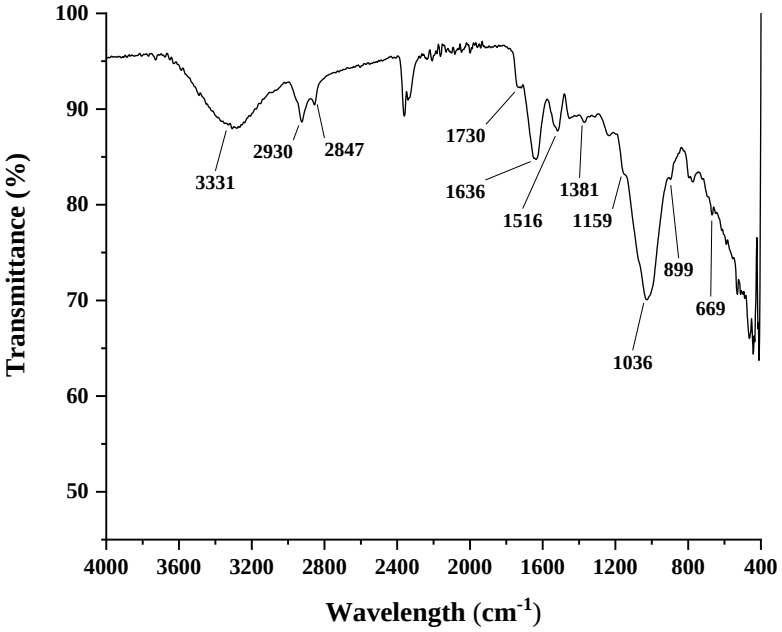

Figure 4-4: FTIR spectra of BSG used in this experimental study and their respective wavenumber.

From the figure, it is shown that the most prominent peak is around 1036 cm^{-1} which may be due to C-O, C=C and C-C-O deformation or stretching vibrations of the different polymers in the BSG. This is a common feature for lignocellulosic biomass but most notably in the spectra for cellulose (Fan, Dai and Huang, 2012). The peaks which appear in the region between 1300 cm^{-1} and 1636 cm^{-1} mainly represent the lignin polymer band which originate from C-H bending and aromatic C-C stretching (Nanda *et al.,* 2013). The stretching of the carbonyl group at 1730 cm^{-1}in the spectrum represents the ketone, aldehyde or carboxylic acid, mainly from hemicelluloses (Sills and Gossett, 2012). There is a strong broad band which appears around 3331 cm^{-1}, which is attributed to different O–H stretching modes. According to Nanda *et al.,* (2013) the intramolecular hydrogen bond in a phenolic group in lignin is observed at around 3568–3577 cm^{-1}. While, for cellulose, the intramolecular hydrogen bond vibration appears at around 3432 cm^{-1}or at 3342 cm^{-1}. Based on these observations, it can be deduced that the BSG spectrum shows typical peak of lignocellulosic materials which are cellulose, hemicellulose and lignin. Details of each peak and their associated polymer present in the BSG are summarised in Table 4-2.

Table 4-2: FTIR absorbance band and polymer present in BSG according to the literature (M.Schwanninnger, 2004)[a], (Kubo and Kadla, 2005)[b] and (Sills and Gossett, 2012)[c]

Wavenumber (cm^{-1})	Functional group/ Band assignment	Polymer present in biomass
669	C-H out of a plane	Cellulose[a]
899	COC, CCO and CCH deformation and stretching	Cellulose[a]
1036	C-O, C=C and C-C-O stretching	Cellulose[a], hemicellulose[c]lignin[b]
1159	C-O-C asymmetrical stretching	Cellulose[a], hemicellulose[c]
1381	C-H bending	Cellulose[a], hemicellulose[c]lignin[b]
1516	Aromatic C-C ring stretching	Lignin[b]
1636	Aromatic C-C ring stretching	Lignin[b]
1730	Ketone/aldehyde C=O stretch	Hemicellulose[c]
2847	Tertiary CH group	Lignin[b]
2930	C-H stretching	Cellulose[a], lignin[b]
3331	OH- stretching	Cellulose[a], lignin[b]

4.2.2.2 Proximate and ultimate analysis of BSG

The proximate analysis determined by TGA methods separates the biomass into four categories. These are namely; moisture, volatile matter, fixed carbon and ash based on their weight loss (Tanger *et al.*, 2013). Figure 4-5 shows the TG and DTG curves with three significant slopes representing the pyrolytic degradation and decomposition behavior of the BSG used in this study. Similar curves were also found in other biomass that were subjected to TGA analysis (Nanda *et al.*, 2013; Anukam *et al.*, 2017); the initial weight loss was due to their moisture content while the final weight loss was due to the volatile matter caused by the degradation of the fibrous material in the biomass.

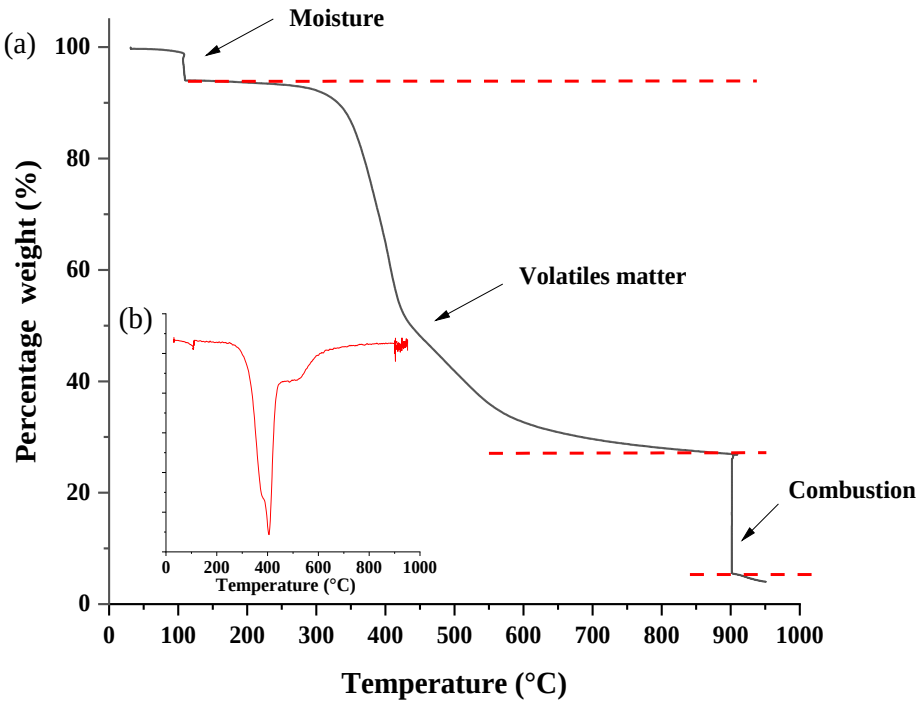

Figure 4-5: (a) TGA and (b) DTG curves of BSG from proximate data analysis conducted using thermogravimetric analysis at a temperature range of 30 ℃ to 950℃.

This characterisation was repeated three times and the results obtained are presented as mean values with a standard deviation. The moisture content is 5.52 ± 0.7 wt.%, and the volatiles represent 68.62 ± 0.9 wt.% of the BSG. The volatiles in current proximate analysis are related with the presence of hemicellulose, cellulose and lignin (Asad S N Mahmood *et al.*, 2013; Tanger *et al.*, 2013) which corresponds to more than half of the current composition, thus representing a significant fraction in BSG. The presence of the lignocellulosic component is also supported by the FTIR spectrum obtained (Figure 4-4), and details on lignocellulosic composition will be discussed further in section 4.2.3. In addition to this, another significant mass loss appears at the temperature of 900 ºC in which the atmospheric gas changed from nitrogen to oxygen after the devolutisation. Oxygen prompts combustion of carbon in the sample and allows the fixed carbon content to be determined; 20.15 ± 0.5 wt.%. Finally, the ash content is 5.71 ± 1.2 wt. % as determined by the differences of the other elements obtained from the TG curve.

According to Garcia *et al.,* (2013), as the future of biomass energy conversion appears to be optimistic, the proximate analysis is one of the most reliable characterisation methods to predict the behaviour of a biomass as a fuel. The following values are essential; moisture, volatile matter and fixed carbon content, as they affect both the combustion behaviour as well as the plant design. For example, high moisture values decrease the combustion yield, while high volatile matter/fixed carbon ratios are related to the fuel's reactivity. On the other hand, the ash content affects the combustion rate and influences corrosion and slag formation (Y.D Singh 2017).

Biomass feedstock is also described in terms of ultimate analysis based on its relative content of individual elements. This individual profile is a unique fundamental code that characterise and determines the properties, quality, potential applications and the environmental problems related to any fuel (Vassilev *et al.*, 2010). For example, C, H and O elements are related to the components of the cell wall (Tanger *et al.*, 2013), and these affect the fuel efficiency. The correlation between (H/C) and (O/C) element ratios has been simplified by the Van Krevelen diagram (McKendry, 2002b) as shown in Figure 7-10. According to the diagram, the lower the ratio, the higher the energy content of the biomass. A material with a relatively low O/C ratio has a greater energy density and higher HHV due to there being more chemical energy in C-C bonds than in C-O bonds (Y.D Singh 2017).

Meanwhile, the presence of minerals and elemental ions in the biomass are related to the ash content. Mussatto (2014) found that due to a higher mineral content in the BSG from Brazilian barley malt, the mass of ash was four times higher compared to BSG from Irish barley malt. The chemical composition of the ash can bring significant operational problems. Apart from lowering the heating value of the biomass and changing the distribution of the products, mineral and elemental ions will interfere with the operation of thermo-chemical equipment. This is especially true for combustion processes, where the ash can react to form a `slag'; a liquid phase formed at elevated temperatures, which can then reduce plant throughput and result in increased operation costs (McKendry, 2002a). Table 4-3 summarises the chemical composition of the BSG used in this work based on the individual elements studied.

Table 4-3: Chemical composition of BSG used for current work and comparison with other BSG from other studies, expressed in dry basis unit.

Individual element	BSG used in current work	(Yinxin, Jishi and Yi, 2015)	(Mussatto , 2014)	(Poerschmann *et al.*, 2014)	(Vanreppelen *et al.*, 2014)
[a]Carbon, hydrogen, oxygen and nitrogen (g/kg^{-1} dry basis)					
Carbon (C)	436.3 ±0.09	425 ± 2.5	NR	513	495 ± 14
Hydrogen (H)	63.7 ± 0.04	NR	NR	NR	68.7 ± 1.9
Nitrogen (N)	22.6 ± 0.04	36.8 ± 0.2	NR	NR	43.5 ± 1.5
Oxygen (O)[d]	382.5 ± 0.09	NR	NR	NR	361 ± 14
[b]Minerals and elemental ions (mg/kg^{-1} dry basis)					
Phosphorus (P)	3989 ± 0.03	960 ± 0.02	5186	5260	NR
Calcium (Ca)	4259 ± 0.00	480 ± 0.02	3515	5750	NR
Silicon (Si)	1977 ± 0.02	520 ± 0.02	10740	6480	NR
Sulphur (S)	1865 ± 0.00	NR	1980	3540	NR
Magnesium (Mg)	608 ± 0.01	620 ± 0.02	1958	1180	NR
Manganese (Mn)	104 ± 0.00	NR	51.4	69	NR
Iron (Fe)	341 ± 0.00	NR	193.4	165	NR
Zinc (Zn)	102 ± 0.00	NR	178.0	144	NR
Potassium (K)	233 ± 0.00	NR	258.1	650	NR
Chlorine (Cl)	108 ± 0.00	NR	NR		NR
Aluminium (Al)	NR	320 ± 0.01	36	<200	NR
Sodium (Na)	NR	NR	309.3	<300	NR
[c]Ash content (wt.% dry basis)	9.3 ± 2.05	16.8 ± 0.8	4.6	4.5	3.20 ± 0.08

[a]determined by elemental analysis
[b]determined by XRF
[c]determined by TGA
[d]determined by difference O % = 100% - C% - H% - N% - %ash
NR – not reported

Although it is well known that BSG is rich in sugars, proteins and minerals, the chemical composition of this material may suffer significant variations due to various factors. According to Mussatto (2014), the chemical composition of BSG varies depending on; barley variety, harvest time, malting and mashing conditions,

and type of adjuncts added during the brewing process. As can be seen from Table 4-3, the main elements in BSG are composed of carbon, hydrogen, nitrogen and oxygen. The overall ratio of these elements is significantly related to the biochemical components of BSG which are the protein and the fibres (cellulose, hemicellulose and lignin) (Mussatto and Roberto, 2005). The main elemental sequence of BSG obtained in this study is in agreement with other researchers' which is carbon > oxygen > hydrogen > nitrogen. Generally, carbon represents the major contribution to the overall heating process, and the carbon content of the fuel is estimated via the composition of lignin, hemicellulose and cellulose (Gollakota, Kishore and Gu, 2018).

BSG also contains a variety of minerals elements, including phosphorus, calcium, silicon, sulphur, magnesium, manganese, iron, zinc, potassium, chlorine, aluminium and sodium, at levels up to 10740 mg/kg of dry weight. Phosphorus and calcium are the minerals present in the highest amounts in the BSG used in this study, being 3989 mg/kg and 4259 mg/kg respectively. Similarly, Meneses *et al.*, (2013) reported that phosphorus represents up to 6000 mg/kg dry weight of the BSG and calcium is 3600 mg mg/kg. This is notably higher than other reported cereals such as rice, oat and wheat straw (Mussatto, 2014) in which the use of BSG has also been proposed in human nutrition (Mussatto, Dragone and Roberto, 2006; Waters *et al.*, 2012). However, BSG is too granular for direct addition to food. Therefore, BSG must first be converted to flour and should undergo several stages of pre-treatment. In other studies, silicon has been reported as the most abundant mineral in the BSG, being 10740 mg/kg or 6480 mg/kg and is followed by other minerals such as sulphur, magnesium, manganese, potassium and sodium, as shown in Table 4-3 by both authors Mussatto (2014) and Poerschmann *et al.*, (2014). Minerals present in the biomass are also responsible for the concentration of the ash content (Anukam *et al.*, 2017). They cause problems during thermo-chemical processes as the material will form a liquid slag during combustion and form solid deposits as it cools down. The elements Na, K, Mg, Ca as well as Cl, S and Si are the most problematic (Miles *et al.*, 1996), and the combination of alkali metals with silica can form alkali silicates (McKendry, 2002b).A low amount of sulphur will minimise SO_X pollution from gasification or combustion systems and avoids catalyst poisoning in fast pyrolysis

systems. A low level of nitrogen, which contributes to NO_X emissions, is good for similar reasons. High levels of nitrogen can be problematic for the quality of liquid fuel products from fast pyrolysis (Tanger *et al.*, 2013).

Results obtained from FTIR spectrum, proximate and ultimate analysis provide a tremendous amount of information about the BSG characteristics, both qualitatively as well as quantitatively. The ash content of the BSG from the proximate analysis, for example, is related to the mineral content, as detected from the ultimate analysis. The FTIR spectrum of BSG shows a characteristic of lignocellulosic biomass. Through the proximate analysis, the decomposition behaviour proves that the major components are the volatile matter which indicates the presence of lignocellulosic biomass in the BSG. Section 4.2.3 will focus on the lignocellulosic biomass content, including cellulose, hemicellulose and lignin.

4.2.3 BSG composition

The different chemical component in biomass influences the chemical reactivity differently. Lignocellulosic biomass contains various amounts of cellulose, hemicellulose, lignin and also a small amount of other extractives (McKendry, 2002a). Therefore, it is crucial to know the chemical composition of this complex biomass to enable the process of converting the biomass into the green fuels or valuable chemicals (Carrier, Loppinet-Serani and Denux, 2011). For example, the relative proportions of cellulose and lignin are one of the determining factors in identifying the suitability of biomass for subsequent processing as energy crops (McKendry, 2002a). In this section, the chemical compositions of BSG are discussed in detail and the extracted compositions are subjected to TGA, FTIR and elemental analysis as characterisation methods.

4.2.3.1 Extractive free (*EF*) BSG

Prior to determination of the BSG composition, it is necessary to conduct an experiment to remove any compounds which are not part of the biomass (extractive content). Extractives are a heterogeneous group of substances which can be extracted from biomass by means of polar or non-polar solvents (Telmo and Lousada, 2011).

Figure 4-6 shows photos of dry BSG before and after the extraction process which was conducted according to Section 4.1.4.1. It can be seen that for BSG before the extraction, the colour of the grain was darker compared to the *extractives-free BSG (EF-BSG)*. Clearly, there are some compounds which have been removed from the grain throughout the process suggesting that the use of ethanol as a solvent enables the removal of the extractive compounds from the BSG. According to J. Sluiter and Templeton (2008), there are three critical reasons for the extraction process:

i) The mouldy or aged samples may contain structural material that has been modified and now soluble in the solvent extractor.

ii) Extractable materials should be removed from the biomass to avoid an error in structural sugar values. Hydrophobic extractives can cause incomplete hydrolysis by inhibiting penetration of the sulphuric acid into the sample of biomass.

iii) Failure to remove extractable material may result in falsely high lignin values when the unhydrolysed carbohydrates are condensed with the acid-insoluble lignin.

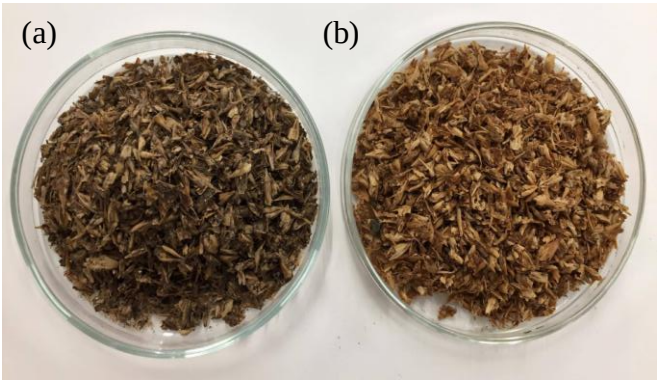

Figure 4-6: Photo of BSG (a) before extraction (b) after extraction (extractive- free BSG). Both samples underwent oven drying at 105°C for 24 hours.

The weight percentage (wt. %) of the extractive content of the BSG is shown in Figure 4-7. All three samples showed extractive contents in the BSG was around 9 to 10 wt. % of the dry basis with the mean value being 9.62 wt.% and 0.64 for the standard deviation. The value obtained is consistent with the findings by Silva *et al.*, (2004) which was 9.5 wt.% and Meneses *et al.*, (2013) who reported that the

extractive content in BSG was 10.73 wt.%. Although the extractive content of the BSG is a minor proportion, the need to remove those extractive components such as waxes, fats, resins, gums, sugars, starches, pitch, sterols, flavonoids, tannins, terpenes and many other minor building blocks (Carrier, Loppinet-Serani and Denux, 2011) is a necessary step before the determination of the main components in the biomass can be conducted.

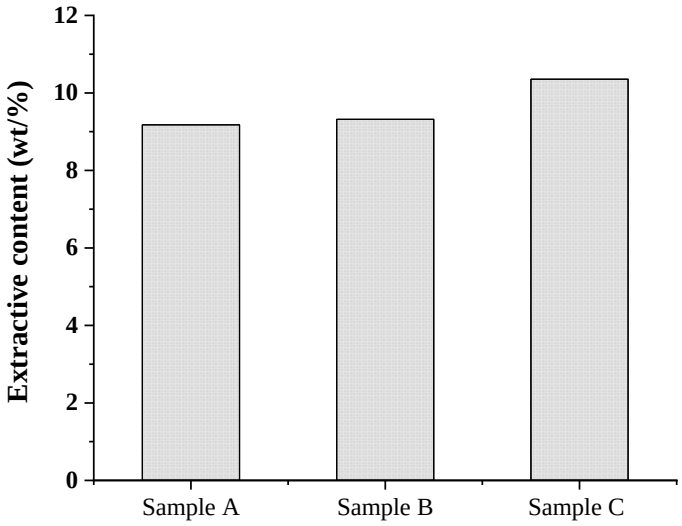

Figure 4-7: Weight percentage (wt. %) of extractive content in BSG obtained by Sohxlet extraction and using ethanol as solvent. Three replicate samples of BSG were used for extractive content data analysis.

TGA was used on the *EF-BSG*, and the focus in current section is the volatiles release region (temperature range of between 250-600 ºC). This analysis was conducted as an alternative method to determine the lignocellulosic content in the *EF-BSG* as the relative intensities of the peaks in this region can be related to the global quantity of hemicellulose, cellulose and lignin (Carrier, Loppinet-Serani and Denux, 2011). Figure 4-8 shows the TG and DTG curve of *EF-BSG* obtained from the TGA analysis. As can be seen from the TG curve (black line), the devolatilisation process starts at a temperature of 260 ºC and the maximum weight loss occurs in the range of 300 to 450 ºC, represented by the highest gradient of the curve. Another change in the slope can be seen at a temperature of 450 ºC which involves another weight loss in the range of 450 to 600 ºC. The volatiles region in the EF-BSG represents 59.14 ± 1.1 wt.%. This value is lower than the volatiles obtained from raw BSG, by 9.48 %. This difference may be due to the removal of extractive content from the BSG in the *EF-BSG*.

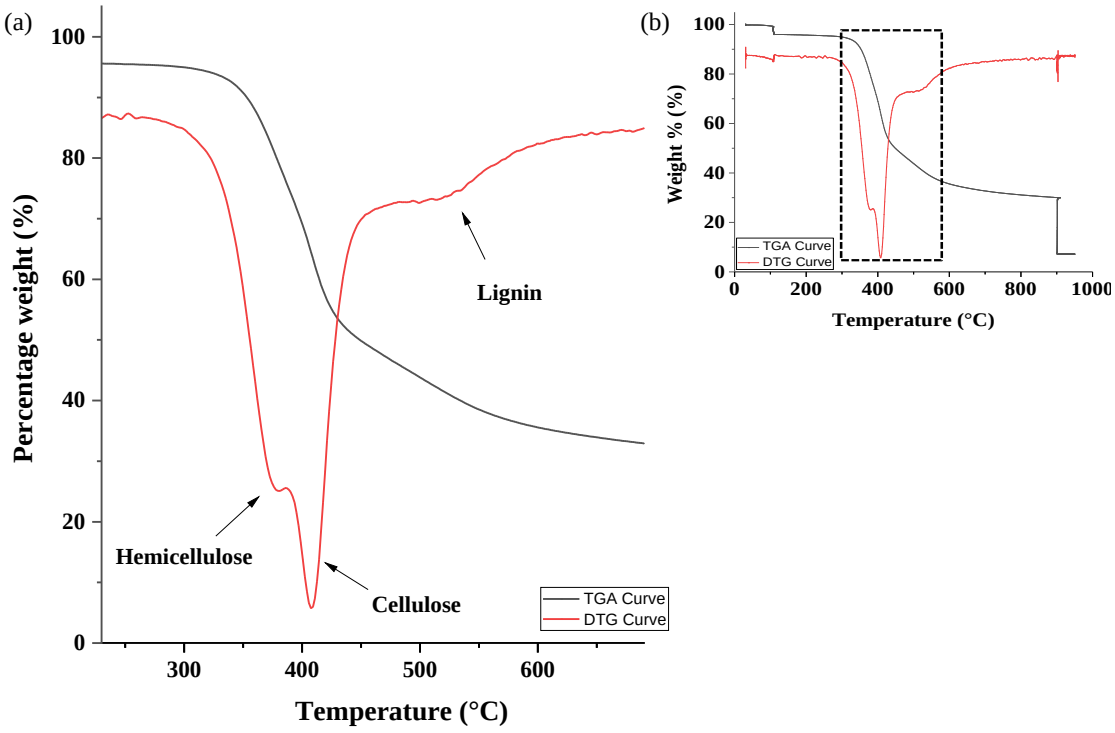

Figure 4-8: TGA and DTG curve of EF- BSG conducted using thermogravimetric analysis at a temperature range 30 °C to 950 °C; (a) volatiles release region represents the degradation of the lignocellulosic component, (b) full curve for proximate analysis.

The derivative weight loss (DTG) curve in the volatile region (red line) shows that the major decompositions occur in three main steps at 380 ºC, 405 ºC and 500 ºC. There are three main peaks; the largest peak occurs in the range of 300 ºC to 450 ºC and this is due to the degradation of the holocellulose content, which includes the hemicellulose and cellulose. For hemicellulose, the degradation takes place at a lower temperature (380 ºC) compared to the cellulose (405 ºC) due to the amorphous nature and branched structure of hemicellulose. The other peak appeared in the temperature range of 430 ºC to 600 ºC which corresponds to lignin which needs a higher temperature to degrade due to its polymeric complex structure. Lignin is abundant in aromatic functionality and the most complex polymer in lignocellulose (Alonso, Wettstein, and Dumesic, 2012).

In general, TGA analysis used in this study is able to determine the presence of cellulose, hemicelluloses and lignin in the *EF-BSG*. Further experimental work in extracting the component was conducted and the results are detailed in 4.2.3.2.

4.2.3.2 Extracted holocellulose and cellulose from *EF-BSG*

Holocellulose and cellulose were obtained from *EF-BSG* by using a two-stage extraction process. Details of each step were explained in section 4.1.4.2. Holocellulose obtained from the first step in the extraction process represented 69.76 ± 0.5 wt.% of the total weight of *EF-BSG*. After the second step, 36.79 ± 1.7 wt.% of cellulose was obtained, which meant that the hemicellulose content in *EF-BSG* was 31.74 ± 0.51 wt. %; assuming that the obtained holocellulose was in an ideal state.

From the extraction process conducted, cellulose represented the largest weight fraction in the *EF-BSG* and was the primary component of the BSG. In order to confirm the purity of the extracted cellulose obtained, structural and thermal characterisation of the extracted cellulose from *EF-BSG* were carried out using both FTIR and TGA. Commercial cellulose (microcrystalline powder) was obtained from Sigma-Aldrich UK Ltd and was used as reference material in this study. It is essential to validate the sample from the experimental work conducted with the commercial sample in order to provide the overall characteristic of the sample obtained.

Figure 4-9 shows the FTIR spectra for the extracted cellulose from the BSG in this work and the commercial cellulose in the range between 4000 and 400 cm^{-1}. From the FTIR spectrum shown, it can be seen that almost the same pattern of spectra was obtained for both celluloses, suggesting that similar functional groups were present in both samples. Detail about the characteristic/prominent peaks for both celluloses and their functional groups are provided in Table 4-4. The spectrum for the commercial cellulose has nine distinct peaks, while the extracted cellulose from the BSG showed an additional three peaks at the wavenumber of 1215, 1512 and 2853 cm^{-1}. The peak identified at 1215 cm^{-1} was associated with C-O stretching of phenolic hydroxyl groups (Boeriu *et al.*, 2004), 1512 cm^{-1} with symmetric CH_3 stretching of the methoxyl group/aromatic ring modes (Hu *et al.*, 2008) and 2853cm^{-1} was attributed to the C-H stretching in aromatic methoxy groups in side chains (Boeriu *et al.*, 2004). In this case, it be seen that the three additional peaks present in the extracted cellulose may be due to the trace lignin in the sample.

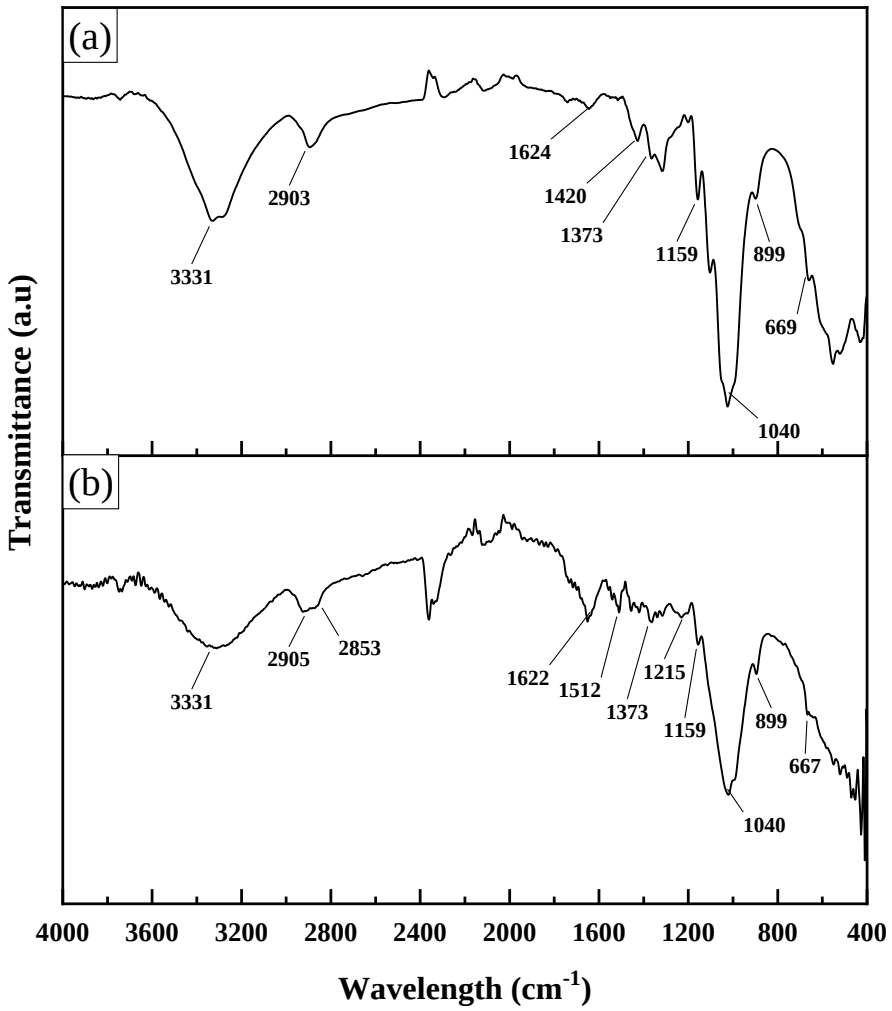

Figure 4-9: Comparison of FTIR spectra for (a) commercial cellulose vs (b) extracted cellulose from BSG.

Table 4-4: FTIR absorbance bands and functional groups present in the structure of extracted cellulose from BSG vs commercial cellulose.

Wavenumber (cm^{-1})		Functional group/ Band assignment
(a) Commercial cellulose	**(b) Extracted cellulose from BSG**	
669	667	C-OH out of plane bending
899	899	COC, CCO and CCH deformation and stretching
1040	1040	C-O
1159	1159	C-O-C asymmetric stretching
-	1269	G- ring
-	1215	C-O stretching (phenolic hydroxyl groups)
1315	-	CH_2 rocking vibration
1373	1373	In-the-plane CH bending
1420	-	CH_2 symmetric bending
-	1512	C-H deformation for an aromatic ring
1622	1624	OH bending of absorbed water
2903	2905	C-H stretching
-	2853	Tertiary CH group
3331	3331	OH- stretching

In order to confirm the purity of the cellulose obtained, the sample was also subjected to TGA. The thermal behaviour of the extracted cellulose and the commercial cellulose are shown in Figure 4-10. The TGA curve of the commercial cellulose shows only one slope in the region of volatile compounds (temperature range 350 to 450 ºC) which indicates pure cellulose without the traces of any additional elements in the sample. This slope resulted in about 88.25 wt.% loss from the total weight of the commercial cellulose while the other 5.14 wt.% was due to the moisture content and 6.61 wt. % was from fixed carbon content. Under the same conditions, the TGA and DTG curves of the extracted cellulose from the BSG were also plotted. Results obtained show one large smooth peak in the temperature range of 350 to 410 ºC, suggesting the presence of cellulose without any hemicelluloses

remains. This result also indicates that hemicellulose is fully hydrolysed from the holocellulose during the second stage of acid hydrolysis which then confirms that there was an efficient extraction process. However, from the curve, there is a presence of a small peak in the temperature region of 450 to 600 ºC. The mass loss in this region was due to decomposition of trace lignin and was 7.37 wt.%. The volatiles present in the extracted cellulose comprised 72.62 %, and the moisture content was 6.27 wt. %. Compared to the commercial cellulose, the fixed carbon in the extracted cellulose is higher, making up 21.13 wt. %. It is worth noting that both celluloses are "ash-free" compounds as no ash was detected in the samples.

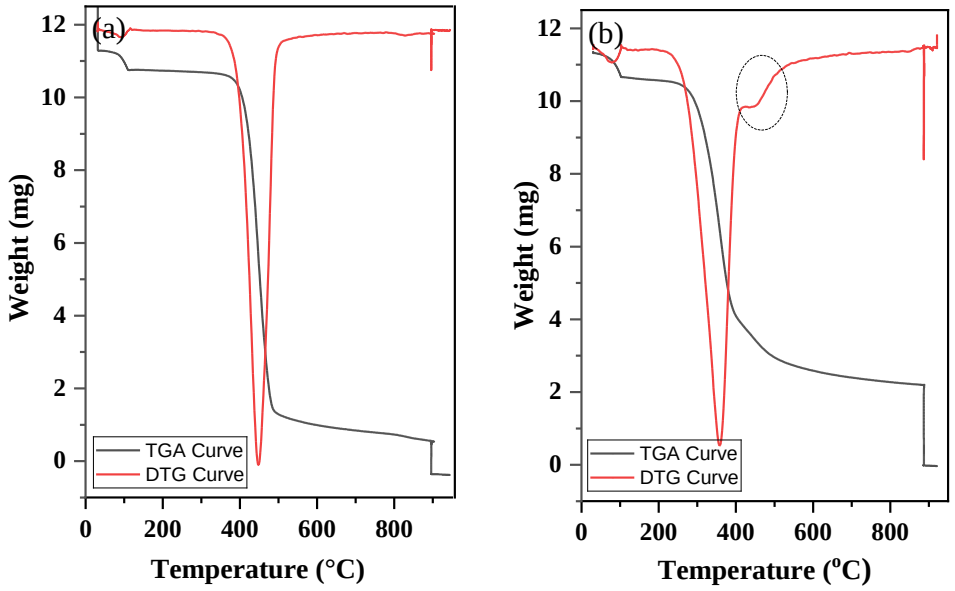

Figure 4-10: Comparison of TGA/DTG curve of (a) commercial cellulose vs (b) extracted cellulose from BSG

Result obtained from both characterisation techniques show similar pattern in commercial and the extracted cellulose obtained from this work. The work conducted in extracting the cellulose from BSG is a success as the results obtained show a some what similar trend in chemical structure (FTIR) and thermal properties (TGA) as the commercial cellulose. The traces present in the extracted sample are also identified and quantified by both methods. These results indicate that the cellulose component has been successfully extracted from the *EF-BSG* sample.

4.2.3.3 Extracted lignin from BSG

Lignin was extracted from the *EF-BSG* according to the method in section 4.1.4.3, and the amount of the lignin present in the sample was 28.85 ± 0.3 wt.% . Lignin represents one of the three major components of lignocellulosic biomass, however, this compound has received little attention relative to cellulose with regards to its valorisation (Zakzeski *et al.*, 2010). In this section, the characteristics of lignin were studied using two characterisation methods: FTIR and TGA analysis. The properties of the extracted lignin were also compared with commercial lignin. The reference lignin used in this work was the Kraft lignin type with low sulfonate content, purchased from Sigma-Aldrich UK Ltd.

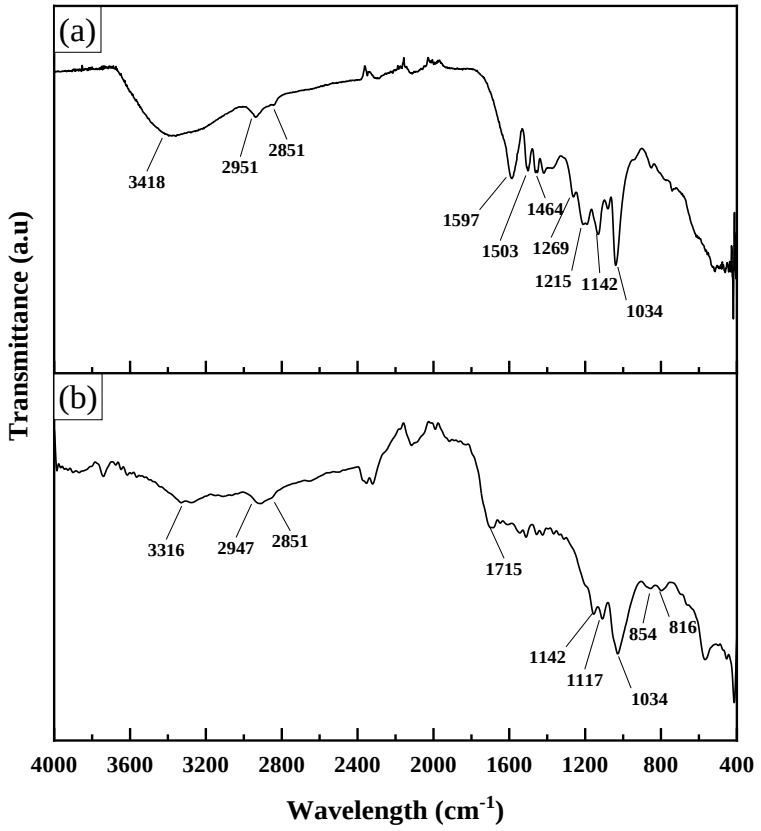

Figure 4-11: Comparison of FTIR spectra of (a) commercial lignin vs. (b) extracted lignin from BSG

Figure 4-11 shows the FTIR spectrum obtained for both lignin samples in the range of 4000 to 400 cm^{-1}. The FTIR spectra reflect the chemical structure as well as the purity of the lignin. The commercial lignin shows a broad band at 3418 cm^{-1} which is attributed to the hydroxyl groups in phenolic and aliphatic structures while

this band is less intense in the extracted lignin. Both lignin have bands centred around 2951 and 2851 cm^{-1}, predominantly arising from CH stretching in the aromatic methoxyl groups and in both methyl and methylene groups of side chains. The aromatic skeleton vibrates at 1597, 1512 and 1464 cm^{-1} and the C–H deformation combined with aromatic ring vibration at 1462 cm^{-1} is common for all lignins although the intensity of the band may differ (Boeriu *et al.*, 2004). The difference in the spectrum obtained in the extracted lignin is that the sample shows vibrations characteristic of the guaiacyl unit (CH in-plane deformation; 854 and 817 cm^{-1}, C–H out-of-plane vibrations in position 2, 5 and 6 of guaiacyl units). However, this is absent in the commercial lignin. The spectrum of the extracted lignin was not distorted by traces of any other element suggesting that pure lignin was obtained during the extraction process. The detail on functional groups and the corresponding band assignments for both lignins is tabulated in Table 4-5.

*Table 4-5: Chemical characteristic of commercial lignin and extracted lignin from BSG waste determine from FTI*R *analysis*

Wavenumber (cm^{-1})		**Functional group/ Band assignment**
(a) Commercial lignin	**(b) Extracted lignin from BSG**	
-	816	C-H out of the plane
-	854	In-the-plane C-H deformation
1034	1034	C-O deformation (methoxy group)
1142	1142	C=O stretching
1215	-	C-O stretching (phenolic hydroxyl groups)
1269	-	C-O stretching
1464	-	C-H deformation
1512	-	Aromatic ring vibration
1597	-	Aromatic ring stretching band
-	1715	Unconjugated carbonyls
2851	2851	Tertiary CH group
2951	2947	C-H stretching
3418	3316	OH- stretching

Thermogravimetric analysis (TGA) was conducted in this study to evaluate the pyrolytic behaviour of the lignin. The TGA/DTG curve of extracted lignin from BSG vs. commercial lignin is shown in Figure 4-12. In general, lignin is known to decompose slowly over a broad temperature range (Carrier, Loppinet-Serani, and Denux, 2011), resulting in the distorted broad peak appearance of the DTG curve. The degradation process of the lignin involves several stages, starting with the fragmentation of inter-unit linkages inside the lignin. This is then followed by the release of monomers and the derivatives of the phenol into the vapor phase. Moreover, at temperatures higher than 500 ºC, the decomposition of the aromatic rings occurs (Watkins *et al.*, 2015). From the DTG curved, it can be seen that the commercial lignin decomposes at a much lower temperature compared to the extracted lignin from BSG. This suggests that the extracted lignin contains a higher number of aromatic rings, which causes the degradation to occur at a much higher temperature.

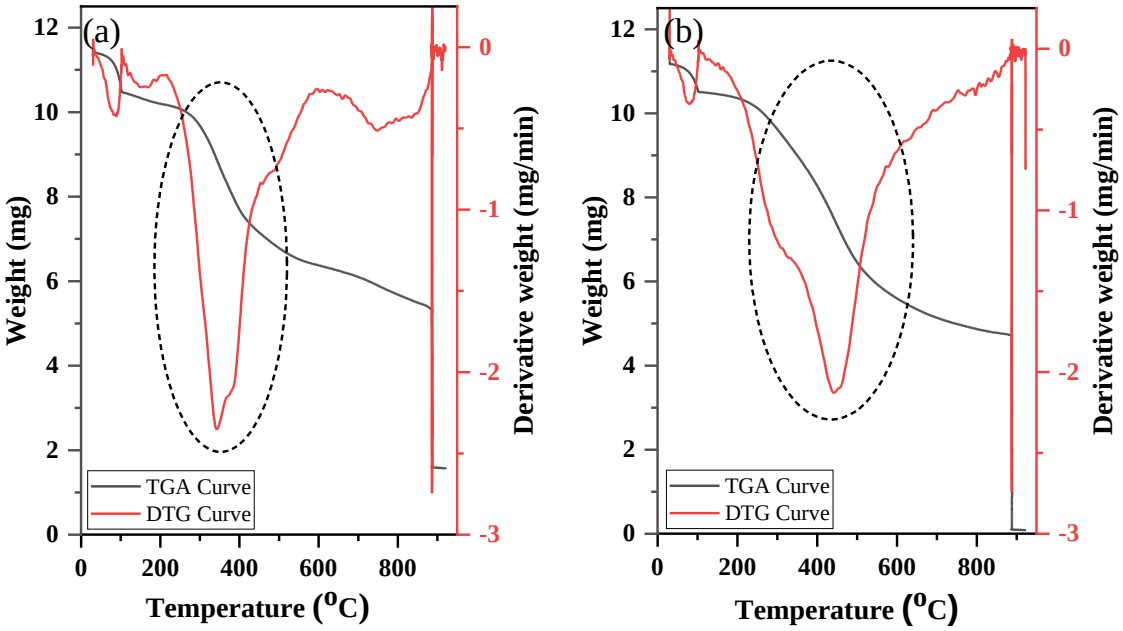

Figure 4-12: Comparison of TGA/DTG curve of (a) commercial lignin vs (b) extracted lignin from BSG conducted in the temperature range of 30 ºC to 950 ºC.

Overall, this proximate analysis contributes to the understanding of the decomposition of the lignin, and due to the significant amount of lignin present in current BSG, its successful utilisation could be considerably interesting for the valorisation of this agro-industrial by-product.

4.2.3.4 BSG as lignocellulosic biomass

Numerous fractionation methods exist for separation of the macromolecules contained in biomass: lignin, holocellulose and cellulose. Throughout this section, the method used to determine the content of BSG is shown to be acceptable and is proven by the characterisation techniques conducted. The major components in the BSG waste were extracted, quantified and characterised. Three major components of BSG from this study were cellulose, hemicellulose and lignin and their percentage weights (wt. %) are tabulated as shown in

Table 4-6 together with the values reported by another researcher. The compositions obtained in the current work are similar to the values reported by other researches. This confirms that BSG is lignocellulose biomass which has potential as a source of energy (Pathak, Chaudhari and Fulekar, 2013).

Lignocellulosic biomass has gained interest and gives a significant impact not just as biomass feedstock for the second generation of biofuel, but also able to produce more sustainable and environmentally friendly material (Isikgor and Becer, 2015). Thus, the interest in utilizing BSG is not just for increasing the value of industrial waste but also as a raw material for energy production and fine materials.

Table 4-6: Hemicellulose, cellulose and lignin content of extractives-free BSG obtained for current work and comparison to other BSG

Component (wt.% dry basis)	**BSG[a]**	**BSG[c]**	**BSG[d]**	**BSG[e]**
Hemicellulose	31.74 ± 0.5[b]	21.58	51.55	28.57
Cellulose	36.79 ± 1.7	30.39	29.13	16.89
Lignin	26.85 ± 0.3	21.73	37.54	27.96

[a]BSG used in current experimental work and report

[b]by the difference of extracted holocellulose and cellulose

[c] adapted from Meneses *et al.*, (2013)

[d] adapted from Mahmood *et al.*, (2013)

[e] adapted from Mussatto(2014)

4.3 Conclusion

The characterisation results shown in this chapter contribute significantly to the understanding of the components present in this agro-industrial waste. BSG has been shown to be a lignocellulosic rich material. The lignocellulosic material is an interesting raw material which offers tremendous potential for future utilization. The overall component of raw BSG based on current characterisation conducted in this work is summarising in Figure 4-13.

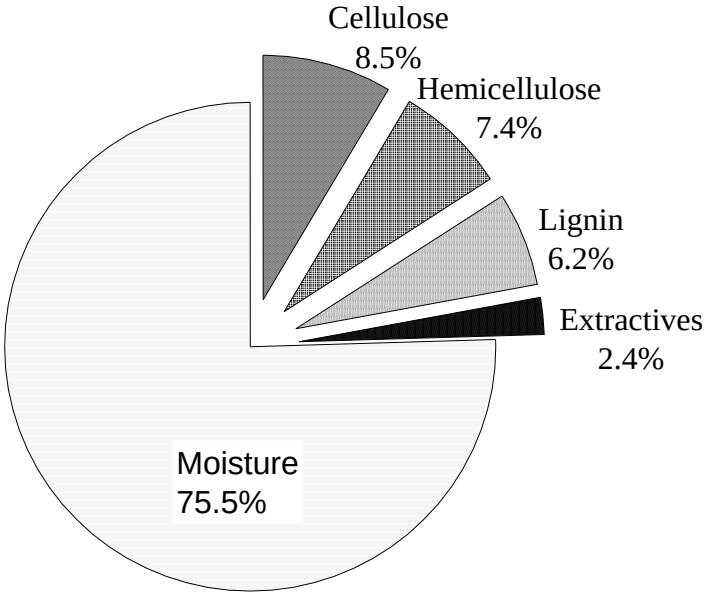

Figure 4-13: The overall component of raw BSG based on characterisation technique conducted in current work.

The primary factor that must be considered when trying to increase the value of BSG is the moisture content. Moisture content in wet BSG represents about three-quarters of this raw waste. Due to this, any application using BSG as a feed source needs to consider the best way to handle the moisture content. In view of changing the way in which BSG waste is utilised, a research roadmap for handling its moisture content is vital.

The literature suggests that numerous attempts have been made to recycle the constituents of spent grain from the brewing process, such as in feeding and food ingredients (Waters *et al.*, 2012; Fărcaş *et al.*, 2014), energy production (Russ, Mörtel and Meyer-Pittroff, 2005; White, Yohannan and Walker, 2008; Weger *et al.*, 2014) and chemical processes (Sežun *et al.*, 2011; Asad S.N. Mahmood *et al.*, 2013;

Malomo, 2013). However, in spite of all the possible applications described, BSG use is still limited; mainly it is used as animal feed or ends up in landfill. For this reason, the development of new techniques to optimize this agro-industrial by-product is of great interest since BSG is produced in large quantities throughout the year.

.

CHAPTER 5

PRELIMINARY STUDY ON HYDROTHERMAL LIQUEFACTION (HTL) REACTION

Chapter 5: Preliminary study on HTL

5.0 Introduction

In chapter 4, it was shown that brewers spent grain (BSG) is lignocellulosic biomass with high moisture content. The moisture can represent up to 75 wt. % of the total weight of the BSG. Wet biomass that contains > 50wt.% water is generally considered as an unattractive feedstock due to increased transport costs, energy consumption, and also environmental considerations related to unpleasant odours and large numbers of pathogens (Pavlovič, Knez and Škerget, 2013). For this reason, the best way to utilise this waste is by treatment with a hydrothermal liquefaction (HTL) reaction. HTL is the thermo-chemical conversion of biomass into liquid fuels by processing in a hot, pressurised aqueous environment for sufficient time to break down the solid biopolymeric structure to mainly liquid components (Gollakota, Kishore and Gu, 2018). HTL uses subcritical water as the reaction medium and, as such, this process can be used for high moisture containing biomass without the need for a drying process (Elliott *et al.*, 2014).

This chapter presents investigations into HTL using two biomass models. A preliminary study is conducted in which these model systems are used in HTL; a mixture of cellulose and lignin was used in multi-component system to mimic the real biomass. The main objective of the current chapter is to understand the reaction pathway and behaviour of these major components during the HTL reaction. The study will focus on the effect of reaction temperature and reaction time on the liquid product obtained. The findings in this chapter will create a better understanding of the use of the HTL reaction and its eventual application to with real biomass systems.

5.1 Materials and methods

Details on materials used were listed in section 5.1.1. The experimental work involves the HTL reaction set-up and product analysis was elaborate in detail in section 5.1.2 and 5.1.3.

5.1.1 Materials

The cellulose model used is microcrystalline cellulose (Avicel® PH-101, Sigma Aldrich), while Kraft lignin (low sulfonate content lignin, Sigma Aldrich) was used as for lignin. Other materials used in the current work are compressed helium gas (BOC, 99.99%) and distilled water (produced in an Elga reservoir of 75 L).

5.1.2 Method

The experimental set-up employed has generally been explained in Section 3.2. In the current section, the biomass used is microcrystalline cellulose and Kraft lignin. 0.1 g model biomass with 10 mL of distilled water was loaded into the autoclave. The air trap in the reactor was purged, and 30 barg of helium gas was used to pressurise the reactor. The desired temperature was set, and the mixer was set to stir at 500 rpm. After the reaction was complete, the mixer was stopped, and the reaction was quenched by placing the reactor in an ice bath. When the temperature reached approximately to 25 ºC, the pressure was released and the reaction products were recovered. The overall process taken in current work is simplified in Figure 5-1.

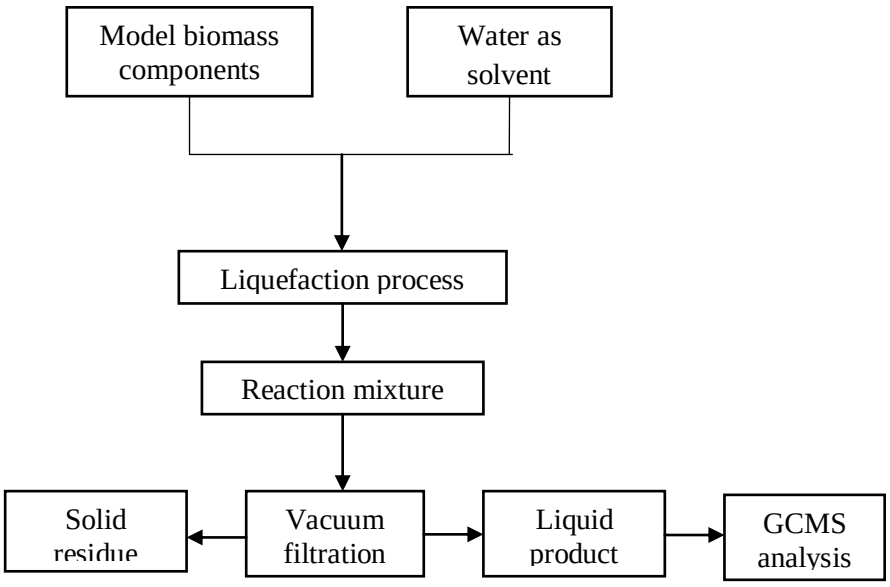

Figure 5-1: An overall flow chart for HTL reaction for model biomass conducted in current chapter.

5.1.3 Product analysis

In the model HTL reaction, the solid-liquid mixture was separated from the autoclave by filtration through Whatman No.1 filter paper under vacuum. The water soluble fraction was the liquid product and was analysed for identification while the solid residue was discarded.

5.1.3.1 Liquid product

The liquid products were analysed using GCMS with a HP-INNO-wax column. Conditions used in the column are described in Table 3-1. The injection temperature port was set at 250 ºC. The temperature used was to ensure that the whole sample was vaporised entirely before it entered the column.

For better separation of the product, a column temperature program was developed and details are tabulated in Table 5-1. The interface temperature between the GC column and the MS was set at 5 ºC higher than the highest temperature used in the GC column program. This temperature was set to avoid condensation of the products in the MS. The ion source temperature was 200 °C, and the m/z ratios between 33 and 500 were used. The injection was done using split mode, with a split ratio of 20 and was conducted using automatic sampler injection. This GCMS method was used in all the liquid product analysis conducted in the current work.

Table 5-1: The column oven temperature programme used for GCMS analysis of the liquid sample.

Temperature rate (°C/min)	Final temperature (°C)	Hold time (min)
-	50	2.00
10	90	0.00
4	120	0.00
8	230	10.00

5.1.3.2 Product identification

The liquid product was identified using a GCMS and the MS was operated using GCMS Solutions software version 4.44. This included the NIST MS Search

version 2.0 library with mass spectra of several compounds, thereby allowing the identification of the reaction products. The products were labelled based on their mass spectra and the peak areas were quantified. The confirmation on the target product was determined based on the concurrence of retention times between the calibration standards and the experimental data, which were confirmed by MS spectrum.

5.2 Result and discussion

The discussion will focused on two different model biomass systems; single and binary (mixture of cellulose and lignin) based on their liquid product composition. The comparison was made between these two systems and effect of reaction temperature and time in HTL of biomass model compound were also presented.

5.2.1 Single model system

Effect of HTL reaction temperature on lignin and cellulose was conducted in single model system. The results obtained were elaborate in details in this section.

5.2.1.1 HTL of cellulose

Cellulose was chosen as the model material in the current work as it represents the major component of the lignocellulosic biomass of interest, BSG. Cellulose is often used as a model compound and offers a good starting point for the more complex biomass materials used in various other studies (Kumar and Gupta, 2008; Hegner *et al.*, 2010; Liu *et al.*, 2012). Cellulose is composed of glucose units connected by β- 1,4- glucosidic bonds and is linked via strong inter-molecular and intra-molecular hydrogen bonding (Pasangulapati *et al.*, 2012). This structure is responsible for cellulose resistance towards depolymerisation under mild conditions in conventional solvents (Tekin, Karagöz and Bektaş, 2014).

In the current work, HTL of cellulose was conducted at different reaction temperatures Figure 5-2 shows an example GC chromatogram for the liquid product obtained. The results show that cellulose decomposes into several water-soluble products with furfural, levulinic acid (LA) and hydroxymethylfurfural (HMF) as the

main liquid phase products. It was reported that the primary step for cellulose decomposition in HTL is hydrolysis, which then produces oligosaccharides and monosaccharides (Yu, Lou and Wu, 2008; Yin and Tan, 2012) . Figure 5-3 show a simplified schematic of the hydrolysis process for the cellulose polymer in HTL. Water at elevated temperatures and pressure can both break up the hydrogen-bound crystalline structure and hydrolyse the β-1,4-glucosidic bonds, resulting in the production of glucose monomers (A. A. Peterson *et al.*, 2008). However, sugars, e.g., glucose, may be easily decomposed to form stable products, such as hydroxymethylfurfural (HMF), during HTL (Yu, Lou and Wu, 2008).

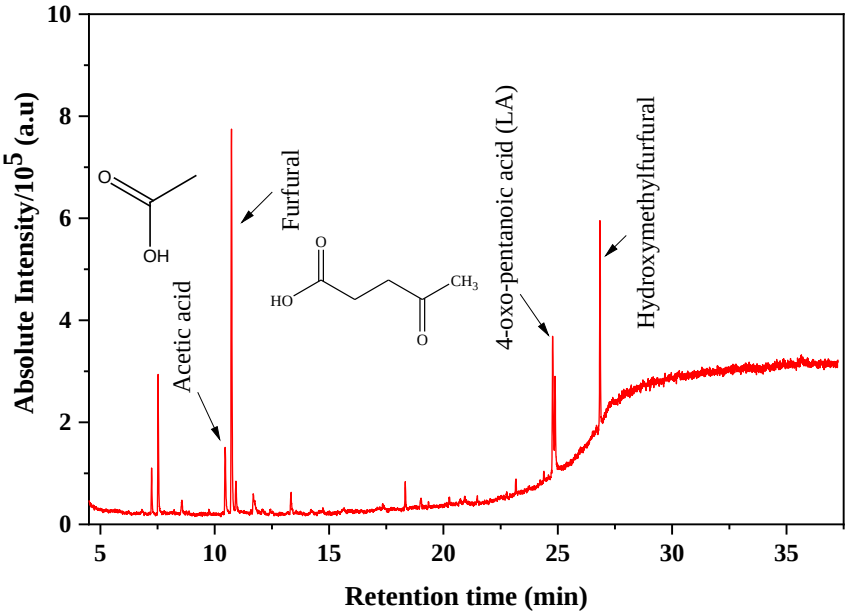

Figure 5-2: GCMS chromatogram for liquid products of the HTL of cellulose. Reaction conditions: microcrystalline cellulose = 0.1 g, distilled water = 10 mL, P_{He}= 80 barg, reaction temperature= 250 ºC and reaction time=30min.

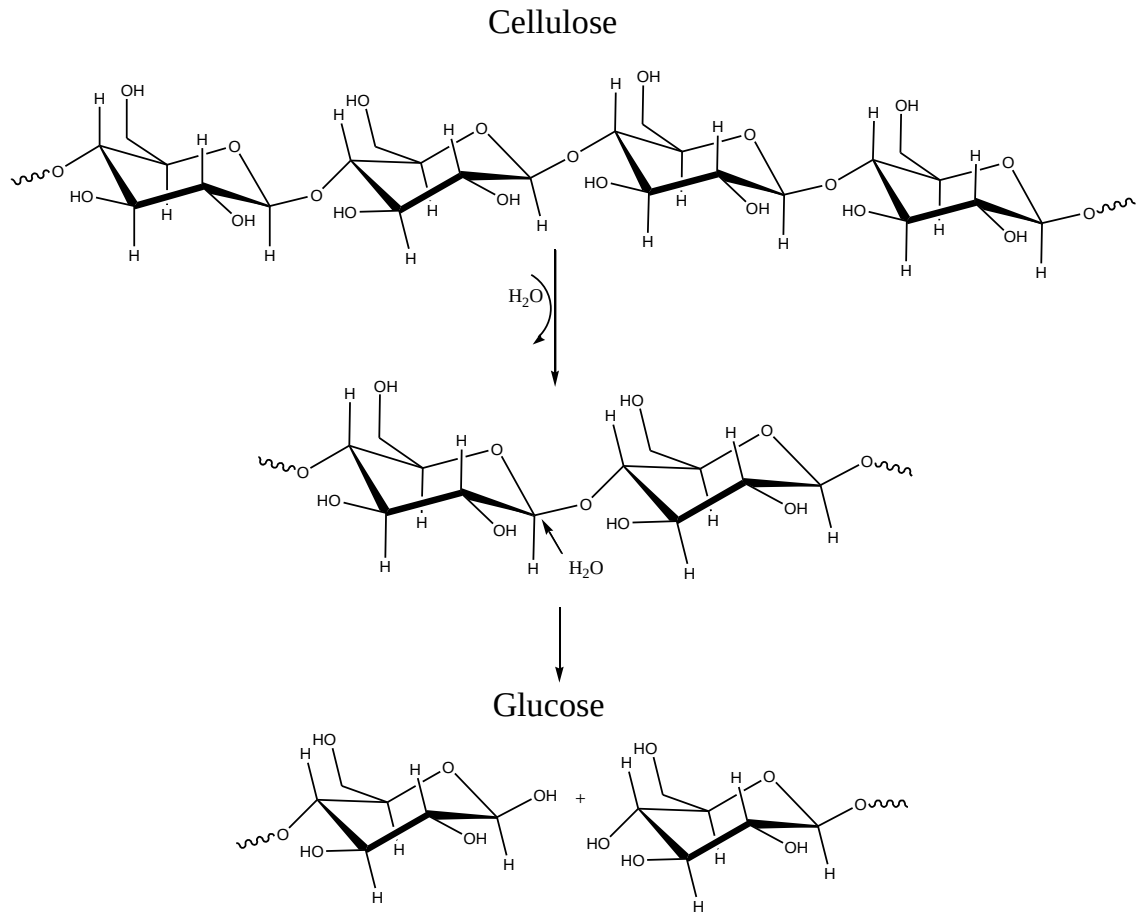

Figure 5-3: The hydrolysis of cellulose is a process to break the β-1,4-glycosidic bonds of the polymer which is the essential step for the conversion of cellulose to produce glucose as a monomer unit (Huang and Fu, 2013).

The formation of HMF, furfural and LA in the liquid product has been shown as a reaction scheme in Figure 5-4. Yu, Lou and Wu, (2008) reported that the primary reaction of glucose was found to be as follows (1) glucose isomerisation into fructose via keto-enol tautomerization, (2) glucose dehydration to 1,6-anhydroglucose, (3) glucose decomposition into aldehydevia keto-enol tautomerization and finally (4) dehydration of the tautomerisation intermediate and fructose to produce 5-HMF. Glucose and mannose can also undergo dehydration to form HMF (Weingarten, Conner and Huber, 2012). Subsequently, HMF can rehydrate to produce levulinic acid and formic acid. HMF can also decompose to produce furfural via loss of formaldehyde. Formic acid is also a by-product of the hydrolytic fission of furfural.

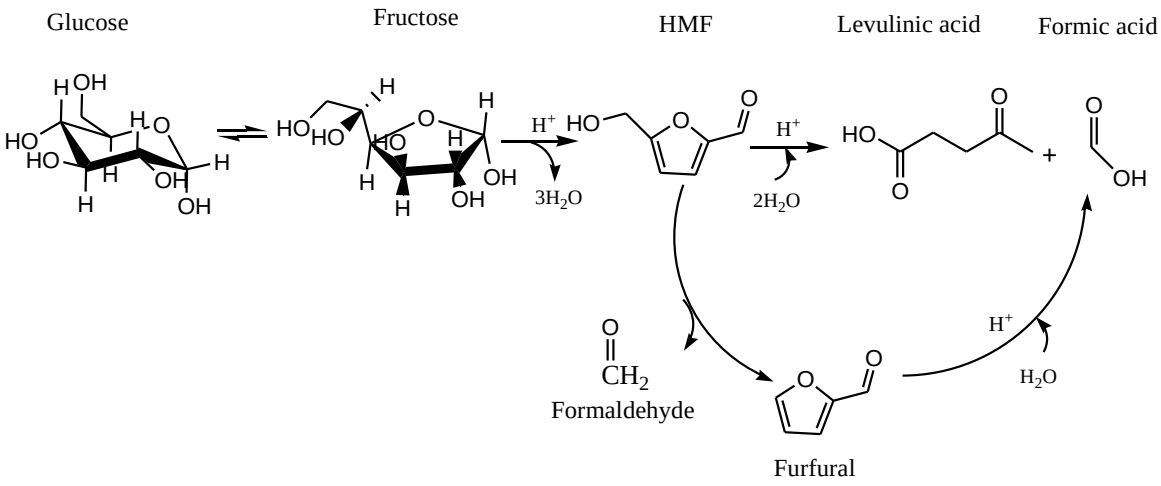

Figure 5-4: Proposed reaction scheme for aqueous phase degradation of glucose in HTL of cellulose to HMF, levulinic acid and furfural adapted from Yu, Lou and Wu, (2008) and Weingarten, Conner and Huber (2012).

HTL uses subcritical water as a solvent and the properties of water are strongly influenced by temperature and pressure (Pavlovič, Knez and Škerget, 2013). The nature of the biomass degradation and conversion in the HTL reaction hence depends on changes in temperature and pressure. In this work, hydrothermal decomposition of cellulose was carried out in a batch reactor at temperatures ranging from 200 °C to 300 °C for a reaction time of 30 min. Due to difference temperature was set, the pressure during the reaction may vary. Details on the reaction pressure and the amount of liquid product obtained are tabulated in Table 5-2. As can be seen, higher reaction temperatures lead to higher reaction pressure. The maximum liquid product, 8.8 g was obtained at a temperature of 250 °C.

Table 5-2: Recorded reaction pressure during the HTL of cellulose at different temperatures and the amount of liquid product obtained. Reaction conditions: microcrystalline cellulose = 0.1 g, distilled water = 10 mL, initial He pressure at 20 °C = 30 barg, reaction time = 30 min.

Reaction temperature	Reaction pressure	Liquid product (g)
200 °C	≈ 74 barg	8.5
250 °C	≈ 80 barg	8.8
275 °C	≈ 84 barg	8.4
300 °C	≈ 89 barg	8.4

Figure 5-5 shows the concentration for HMF, furfural and LA in the liquid product obtained at the different reaction temperatures. The furfural concentration increases by 40% at 250 °C (2.8 g/L) compared to at a temperature of 200 °C (1.9 g/L). However, at temperatures of 275 °C and 300 °C, the furfural concentration drops to 2.3 g/L and 2.4 g/L, respectively. The levulinic acid concentration increases from 0.3 g/L at 200 °C to 0.5 g/L at 250 ºC and eventually reaches a plateau at higher temperatures. Meanwhile, the HMF concentration is highest at 200 ºC (1.2 g/L) and then decreases by 35% (0.8 g/L) at 250 ºC. As the temperature increases further to 275 ºC and 300 ºC, no HMF was detected in the liquid product.

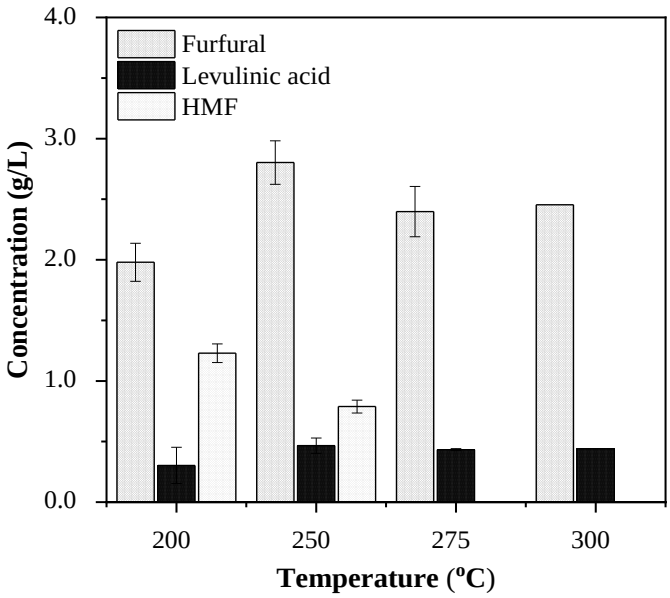

Figure 5-5: Effect of reaction temperature on HTL of cellulose. Reaction conditions: microcrystalline cellulose=0.1g, distilled water = 10 mL, initial He pressure at 20 °C = 30 barg, reaction time = 30 min.

During HTL, HMF is produced from cellulose via an acidic reaction pathway due to the self-disassociation of water to H^+ and OH^-. The pKa of water is greatly influenced by temperature and at 200 ºC, the pH of water is nearly 5 (Yin, Pan and Tan, 2011), which explains the high concentration of HMF obtained in the current work. However, when increasing the temperature from 200 ºC to 250 ºC, there was a significant decrease in the HMF concentration, with the highest concentration in furfural and levulinic acid recorded. This can be related to the glucose degradation pathway in Figure 5-4, as HMF may undergo a secondary reaction and produce furfural and levulinic acid. Asghari and Yoshida, (2006) studied acidic conversion of

fructose to HMF at temperatures between 200 to 320 ºC and also reported that more levulinic acids were produced as the HMF yield decreased with increasing temperature. Furthermore, at 250 ºC the maximum amount of liquid product was obtained, possibly due to the highest amount of water-soluble product being produced from cellulose around this temperature (Yu, Liu and Wu, 2012).

5.2.1.2 HTL of lignin

Lignin can be derived from biomass through a specific form of pre-treatment, for example; sulfite pulping treatment will produce lignosulfonate, while treatment of wood or bagasse with various organic solvents will form organosolv type (Zakzeski *et al.*, 2010). The model lignin used in the current work is Kraft lignin, alkali. The structure of this compound is shown in Figure 5-6.

Lignin is more thermally stable than other biomasses. According to Karagoz *et al.*, (2005) the order of hydrothermal conversion for biomass and biomass componentsis as follows: cellulose > sawdust > rice husk > lignin. HTL of model lignin was conducted to provide an insight into the degradation and reaction of the lignin polymer structure as a whole. Figure 5-7 shows example GCMS identification for the liquid product of HTL lignin at 250 ºC, 80 barg and a reaction time of 30 minutes. The identities of these compounds were determined through a match of mass spectra in the GCMS computer library. Guaiacol, 4-methyl-guaiacol, 4-ethyl-guaiacol and phenol are detected as the decomposition products for HTL of lignin, which are produced from coniferyl alcohol and p-coumaryl alcohol (Y.-P. Zhao *et al.*, 2013). According to the proposed mechanism in Figure 5-8, HTL could cleave the ether bond and aliphatic C-C bond in lignin, yielding the product obtained.

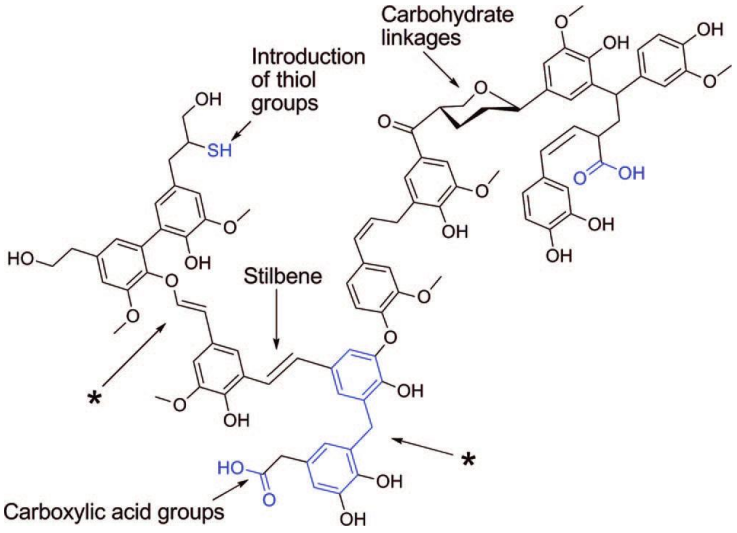

*Figure 5-6: Structural features of Kraft pine lignin. * indicates that no evidence for the presence of either diphenylmethane or vinyl aryl ether linkages in Kraft lignin. (Figure and justification were adapted from Zakzeski et al., (2010)).*

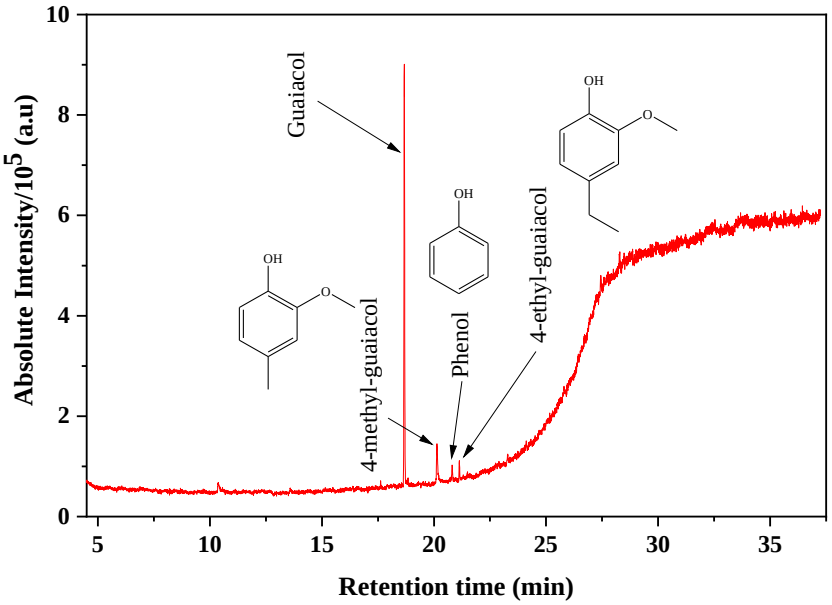

Figure 5-7: GCMS chromatogram for liquid product obtained in HTL of lignin. Reaction conditions: Kraft lignin = 0.1 g, distilled water= 10 mL, P_{He}= 80 barg, reaction temperature=250 ºC and reaction time= 30 min.

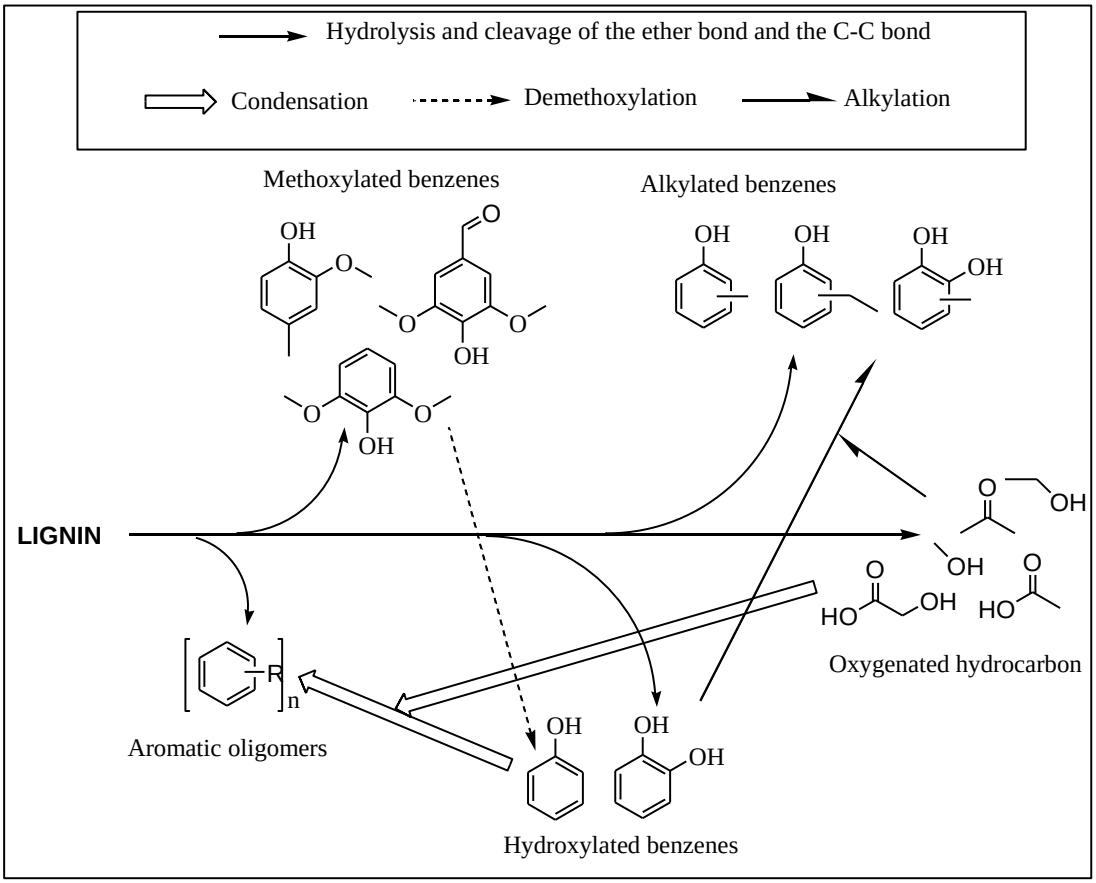

Figure 5-8: Proposed mechanism for the hydrothermal reaction of lignin adapted from Wahyudiono, Sasaki and Goto, (2008), Bargbier et al., (2012) and Kang et al., (2013).

Unlike cellulose, which has a single repeating linkage of β-1,4 glucosidic bonds, lignin contains very complex linkages among its aromatic centres, including C–O–C bonds (β-O-4/4′, α-O-4/4′, α/γ-O-γ, 4-O-5/5′, etc.) and C–C bonds (5–5/5′, β-β, β-1, β-5, etc.) which make lignin a highly stable material. During HTL, lignin breakdown into monomer units and phenolic compounds indicates that the lignin fragmentation reaction does not play a major role in the decomposition of the lignin structure. Due to this, researchers are more interested in using supercritical conditions (Wahyudiono, Sasaki and Goto, 2008; Yong and Yukihiko, 2013), organic co-solvent systems (Saisu *et al.*, 2003; Kang *et al.*, 2013), monomer lignin units (Wahyudiono *et al.*, 2007; Besse, Schuurman and Guilhaume, 2015) and other demanding conditions in investigating the lignin degradation because of the recalcitrate properties of this polymer.

In the current work, HTL of lignin was conducted at three different temperatures and the results are shown inFigure 5-9. At a temperature of 200 ºC, only guaiacol is present as water soluble product with a concentration of 30 mg/L. As the temperature is increased to 250 ºC, depolymerisation of lignin produces 4-ethyl guaiacol (7 mg/L) and phenol (8 mg/L) together with guaiacol (0.2 g/L). Further increases in temperature to 300 ºC resulting in the concentration of phenolics increasing to 0.4 g/L, 17 mg/L and 30 mg/L for guaiacol, 4-ethylguaicol and phenol, respectively. This study indicates that the depolymerisation (endothermic) of lignin through a hydrolysis reaction can be promoted at a higher temperature to overcome the activation energy barrier.

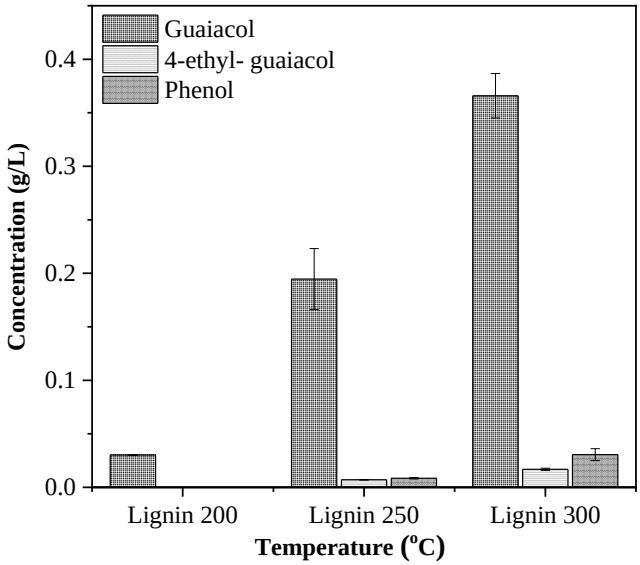

Figure 5-9: Effect of reaction temperature in HTL of lignin. Reaction conditions: Kraft lignin = 0.1 g, distilled water = 10mL, initial He pressure at 20 °C = 30 barg, reaction time = 30 min.

5.2.2 Binary model system

In order to understand HTL of biomass in more detail, a binary model biomass system was used. The binary model is a mixture of both cellulose and lignin in and mimics the composition of real biomass more closely. Figure 5-10 shows an example of GCMS for the liquid product of HTL of the binary model biomass system at 250 ºC, 80 barg and at a reaction time of 30 minutes. As can be seen from the figure, the liquid obtained is a complex mixture of chemical products. Compared with its separate constituent components (cellulose and lignin) from the earlier single

model systems, the distribution of the liquid product was different for the binary model; most of the compounds present in the liquid phase are ketones, aldehydes, organic acids and phenolics with 1-hydroxy-propanone and 3-methyl-1,2-cyclopentanedione being the major products. These compounds, having greater variance in their structure, must involve extensive and complex mechanistic pathways to enable their production (Demirbaş, 2000).

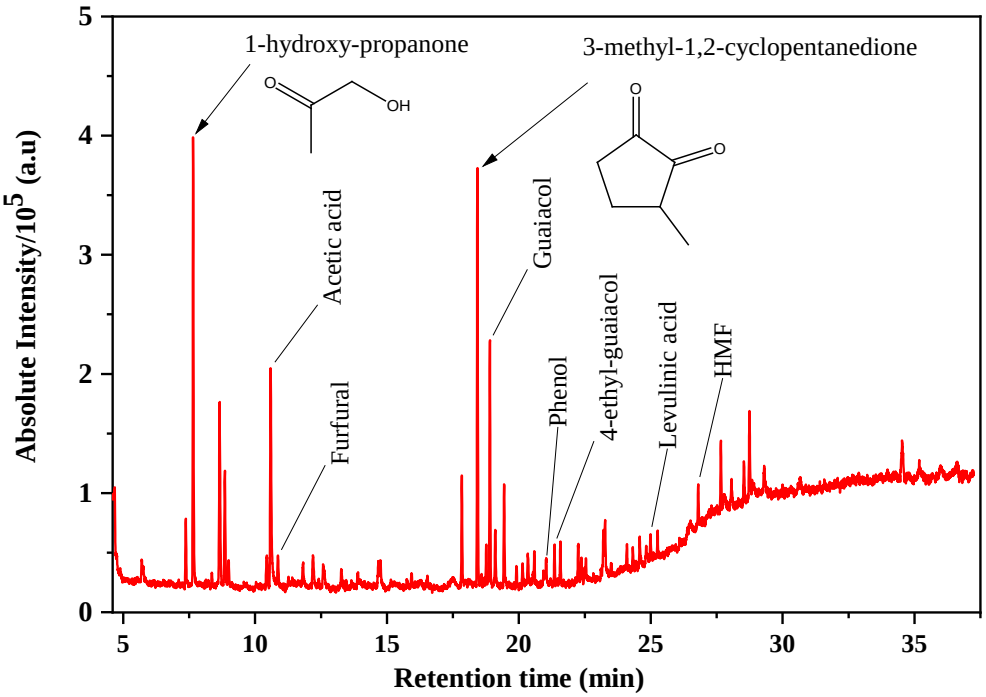

Figure 5-10: GCMS chromatogram for liquid product obtained in HTL binary model biomass system. Reaction conditions: Microcrystalline cellulose = 0.1 g, Kraft lignin = 0.1 g, distilled water= 1 0mL, P_{He}= 80 barg, reaction temperature = 250 ^{o}C and reaction time = 30min.

Due to the complexity of the product obtained, the profile of individual components may give a better understanding of the degradation of the biomass in both of the model systems; single and binary. For the current work, two components were used as being representative of the product stream; guaiacol (Figure 5-11) and acetic acid (Figure 5-12).

Guaiacol is the major product in lignin HTL (Figure 5-9) and as shown in Figure 5-11, guaiacol concentrations proportionally increase as the temperature increases in the single system. In the binary system, although the same initial amount of lignin was used, different trends and product concentrations were obtained. These data show that the guaiacol behaves differently in the single and binary model systems. One of the possible reasons for the lower concentration of guaiacol in the binary system might result from the degradation of cellulose to carboxylic acid in an alkaline medium (Yin, Mehrotra and Tan, 2011) which may change the overall pH in the reaction medium and inhibit lignin degradation.

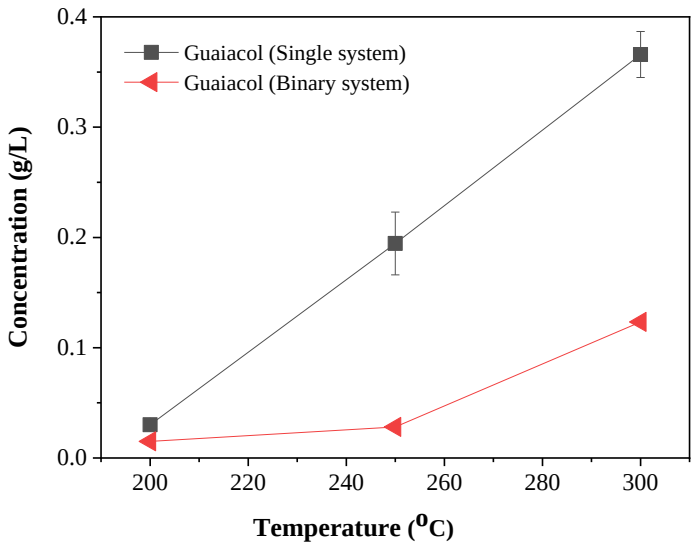

Figure 5-11: Comparison of guaiacol concentrations produced in single and binary HTL model biomass systems. Reaction conditions: Microcrystalline cellulose = 0.1 g, Kraft lignin = 0.1 g, distilled water = 10 mL, initial He pressure at 20 °C = 30 barg and reaction time=30min.

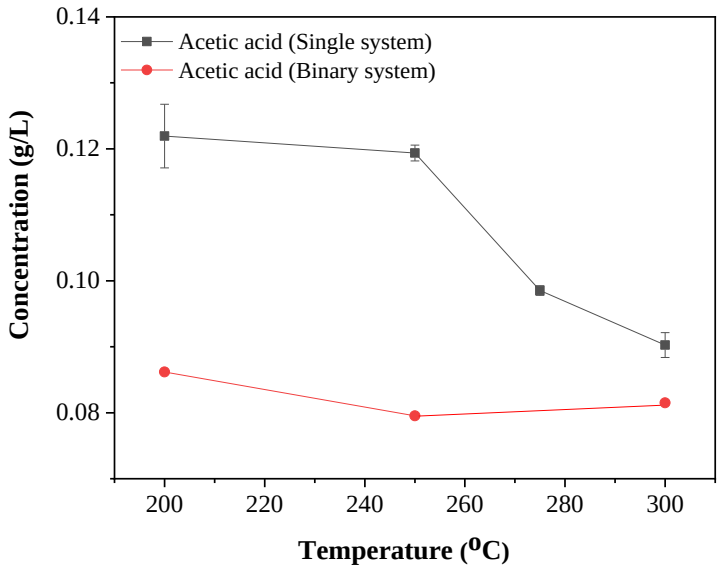

Figure 5-12: Comparison of acetic acid concentration produced in single (cellulose) and binary HTL model biomass systems. Reaction conditions: microcrystalline cellulose = 0.1 g, Kraft lignin = 0.1 g, distilled water = 10 mL, initial He supply = 30 barg and reaction time=30min.

It has previously been that there are two possible formation mechanisms for the acidic derivatives during liquefaction of biomass: i) cellulose is hydrolysed to produce furan derivatives and the further decomposition of these products leads to the formation of acetic fragments which a source for the acidic compounds; ii) small functional groups cracked from lignin monomers could also be the sources of acidic compounds (Karagöz *et al.*, 2004; Y.-P. Zhao *et al.*, 2013).

Figure 5-12 shows the comparison on acetic acid concentration produce in HTL of cellulose and HTL of binary model biomass system. In single system, acetic acid concentration decrease by 2 % at 250 °C (119 mg/L) compare to temperature 200 ºC (122 mg/L) and further increase in reaction temperature to 275 ºC the concentration drop by 17% to 98 mg/L. At temperature 300 °C, lowest concentration was recorded for acetic acid in single system at 90 mg/L. Meanwhile, for binary system, increase temperature from 250 °C to 300 °C acetic acid concentration increased by 3%, to 82 mg/L from 79 mg/L. The possible explanation for these phenomena is that acetic acid production in the single system might only depend on the breakdown of glucose monomer which may fully decompose as temperature increase. Meanwhile, for a binary system, this compound may result from both

cellulose degradation and lignin monomer breakdown to phenolic; cellulose may decompose at high temperature, but the phenolic products will increase as temperature increase resulting in high acetic acid formation.

Both representative components; (i.e.guaiacol and acetic acid) show that the individual chemical component behaves differently as in single and binary system. Those results demonstrate that the presence of other polymers in the system might affect the HTL system in different way. These findings provide insight in understanding the HTL of real biomass; a complex polymer mixture.

5.2.2.1 Effect of reaction time

The effect of the reaction time in HTL of the binary model biomass system was investigated at 250 ºC for various reaction times (15 to 120 min). Components present in the liquid product were divided based on the results of the preliminary study using the single model system (5.2.1.1 and 5.2.1.2) and the results obtained are shown in Figure 5-13.

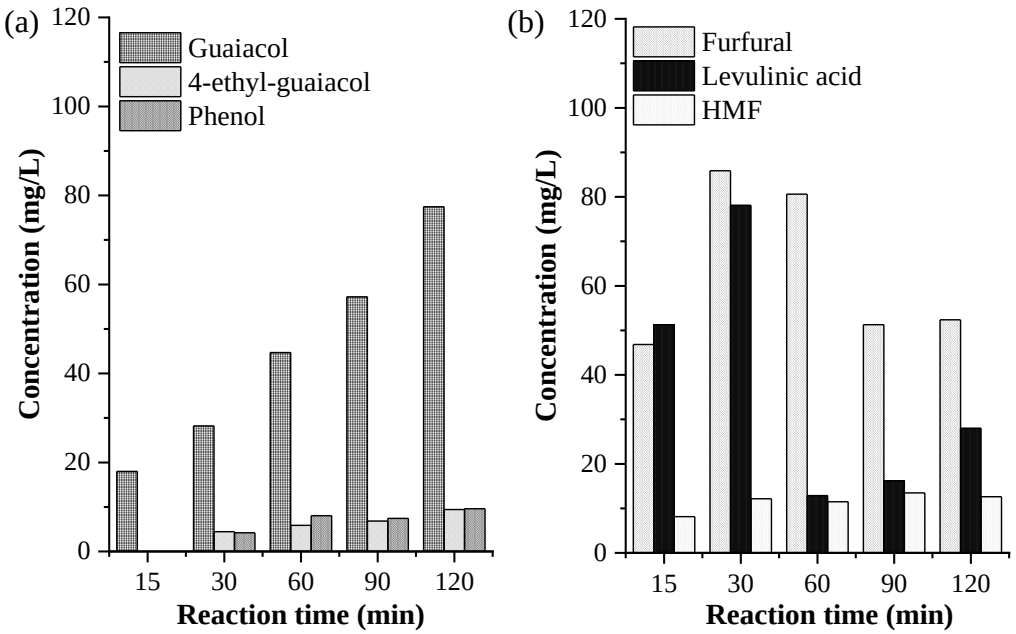

Figure 5-13: Effect of reaction time in binary model biomass system on (a) components from lignin degradation (b) components from cellulose degradation. Reaction conditions: microcrystalline cellulose = 0.1 g, Kraft lignin = 0.1 g, distilled water = 10 mL, initial He supply = 30 barg and reaction temperature = 250 ºC.

Figure 5-13 (a) shows the concentration for guaiacol, 4-ethylguaiacol and phenol obtained in the binary model liquid product over time. At 15 min reaction time, only guaiacol is present as a lignin fragmentation product but when the reaction time increases from 30 min to 120 min, all three phenolics show an increase in their concentration with time. A similar trend was obtained by Wahyudiono, Sasaki and Goto (2008); the authors studied the lignin decomposition at times ranging from 0 to 250 min and reported that yields of phenol, *m,p*-cresol and *o*-cresol increased gradually with the reaction time. However, Pińkowska, Wolak and Złocińska, (2012) reported that for alkali lignin hydrothermal decomposition, the yields of phenol and creosol isomers did not proportionally change with time, which was probably due to gasification and/or repolymerisation.

Figure 5-13 (b) shows the concentration of furfural, levulinic acid and HMF over the reaction time as a result of the HTL of the binary model biomass. These three components are the major compounds detected in cellulose degradation in the single system, so it is interesting to study details of these components. The results show that the reaction time affects the individual components differently. For furfural, the maximum concentration is obtained at 30 min reaction time (86 mg/L) and decreases substantially with further increases in time. For HMF, the concentration increased by 50 % to 12 mg/L after changing the reaction time from 15 min to 30 min and reached a plateau after that time. For levulinic acid, a high concentration was obtained at a reaction time of 15 min (50 mg/L) whilst the optimum concentration was obtained at 30 min (78 mg/L). Furthering increases to the reaction time after this point saw the concentration of the levulinic acid drastically decrease. However, at longer times still, the levulinic acid concentration starts to increase again. Overall, a reaction time of 30 min appears to be optimum for production of furfural, levulinic acid and HMF in the binary model system.

Relating to the mechanism for glucose degradation in Figure 5-4, HMF will undergo a secondary reaction to produce furfural and levulinic acid in the aqueous solution. However, in the current work, the addition of alkali lignin into the binary system may change the reaction pathway for the glucose. Figure 5-14 show a simplified schematic of the acidic and alkali pathways of the hydrothermal

conversion of cellulose. In alkaline solution, carboxylic acids were first formed from cellulose via the alkaline pathway and then neutralised/acidified by the alkaline solutions (Yin, Mehrotra and Tan, 2011); this may explain the high concentration of levulinic acid present at early reaction times and why the concentration starts to drop after 60 min in the current system. As the time was increased, carboxylic acid was obtained and the lignin started to degrade to produce phenolics which may reduce the pH of the reaction medium. After the pH of the reaction media was reduced, the acidic pathway became active, and the main pathway gradually became HMF, which further produces levulinic acid and furfural.

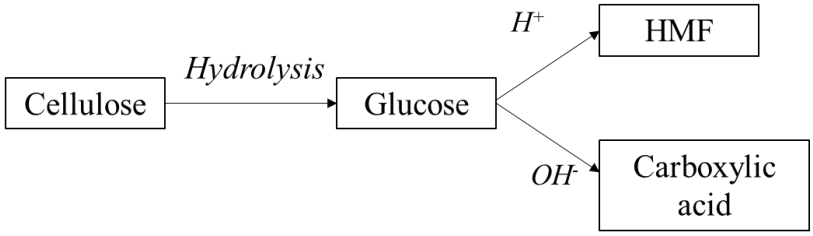

Figure 5-14: Simplified acidic and alkali pathway of hydrothermal conversion of cellulose (Yin, Mehrotra and Tan, 2011)

5.3 Conclusion

The aim of the current preliminary study was to use model biomasses, cellulose and lignin, in the HTL reaction to understand the reaction pathway and behaviour of these major components during the HTL reaction. The results showed that the use of water in the HTL system is able to break down the cellulose and lignin into various chemicals. The result obtained when using the single system showed that breakdown of cellulose leads to the production of platform chemicals such as a levulinic acid (LA), HMF and furfural while lignin degradation contributes to the phenolic compounds present in the liquid product. Temperature plays a vital role for both model compounds; high temperature was favourable for phenolic products while cellulose decomposes at a lower temperature compared to lignin.

The binary model system was used to mimic real biomass and it shows that by having a complex polymer in the system, a complex mixture of chemical products is obtained. Due to the greater variance in the product obtained, the HTL binary model reaction system must involve extensive and complex mechanistic pathways. An example has been given to show that each compound may be involved in different reaction pathways compared to the single model reaction.

CHAPTER 6

A CASE STUDY: HYDROTHERMAL LIQUEFACTION (HTL) OF BREWER'S SPENT GRAIN (BSG)

Chapter 6: HTL of BSG

6.0 Introduction

In Chapter 5, cellulose and lignin were used as model system to mimic lignocellulosic biomass and applied in HTL. It was shown that HTL converted cellulose into three product major product; namely furfural, levulinic acid (LA) and hydromethylfurfural (HMF). Thermal degradation of lignin in hot compressed water is believed to proceed via cleavage of the ether and methylene bridge connecting the structural units, thereby producing phenolic compounds in the liquefied product. By combining both model compounds, the product distribution showed a different pattern from the single component systems as a result of the chemical properties of both polymers. The potential of HTL to break down the lignocellulosic compounds was therefore demonstrated.

The liquefaction of model biomass compounds can inform the selection of experimental parameters and provide the necessary theoretical basis for liquefaction of biomass. However, the composition of real biomass is more complex than a binary mixture of lignin and cellulose and its mechanism of transformation is not yet clear (Gao *et al.*, 2011). In this chapter, HTL was conducted using raw BSG investigating the product distribution and compared with the biomass model system. The conversion, water-soluble oil (WSO) product and total product quantity were also reported. Two different aspects have been investigated:

i) Liquid product distribution

ii) Effect of reaction time on BSG HTL

To the author's best knowledge, this reaction system which involves raw BSG as real biomass in direct HTL process is reported here for the first time.

6.1 Experimental

Details on materials used in current work were listed in section 6.1.1. The experimental procedure involves in BSG HTL; i.e. reaction set-up and separation process were explained in detail in section 6.1.2.

6.1.1 Materials

The materials used in current work were compressed raw BSG, helium gas (BOC, 99.99%) and distilled water (produced in an Elga reservoir of 75 L).

6.1.2 Experimental procedure

Reaction studies employed the set-up described in Section 3.2 using initial parameters derived from the result presented in Chapter 5. The experiment was carried out using raw BSG without any pre-treatment and the overall process for HTL is summarised in Figure 6-1.

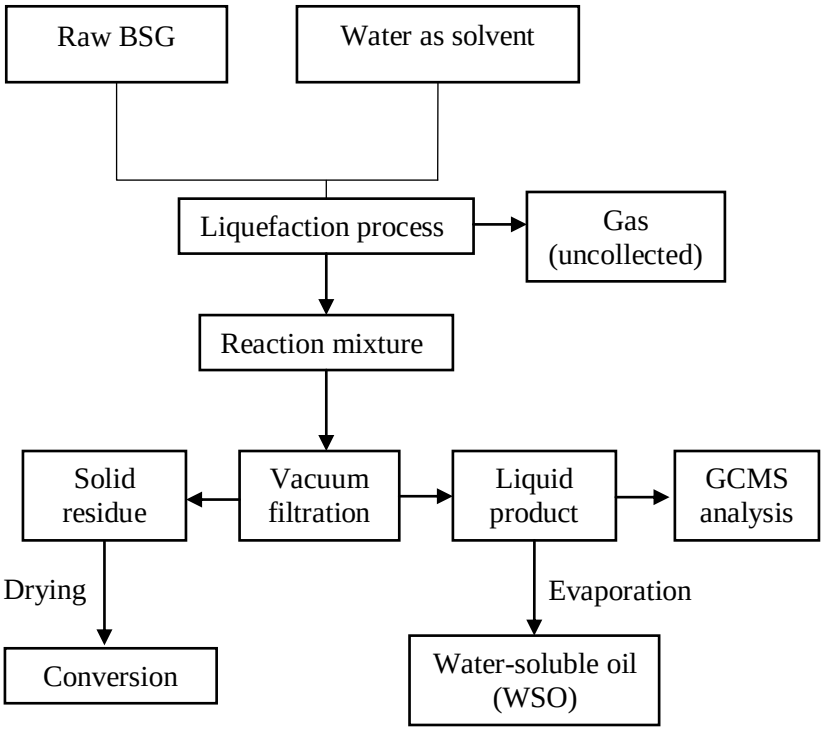

Figure 6-1: An overall flow chart for the HTL process of real biomass, BSG

The reactor was loaded with 5 g of raw BSG which represents approximately 1.25 g of BSG as a dry basis. The overall component based on 5 g raw BSG summarise in Figure 6-2. The BSG to solvent ratio was set at 1: 10 weight basis and the in all the experiment conducted, distilled water been used as a solvent. Helium gas was set at 30 barg for the initial pressure supply. The reaction was conducted at a specific temperature and time range, while the mixer speed was set at 500 rpm. After the reaction was complete, the solid-liquid product was separated through vacuum filtration. Figure 6-3 depicts the overall process for BSG liquefaction reaction and product separation.

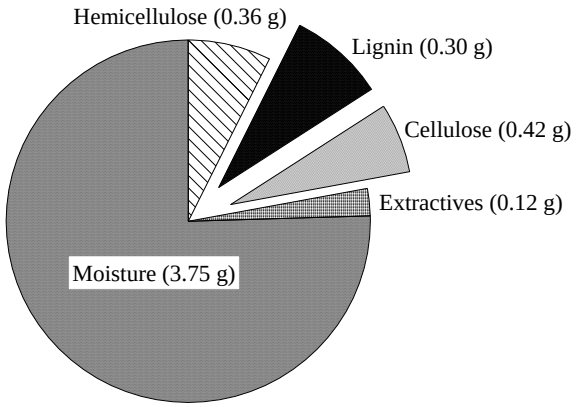

Figure 6-2: The overall composition for5 g raw BSG used in current work based on characterisation conducted in Chapter 4.

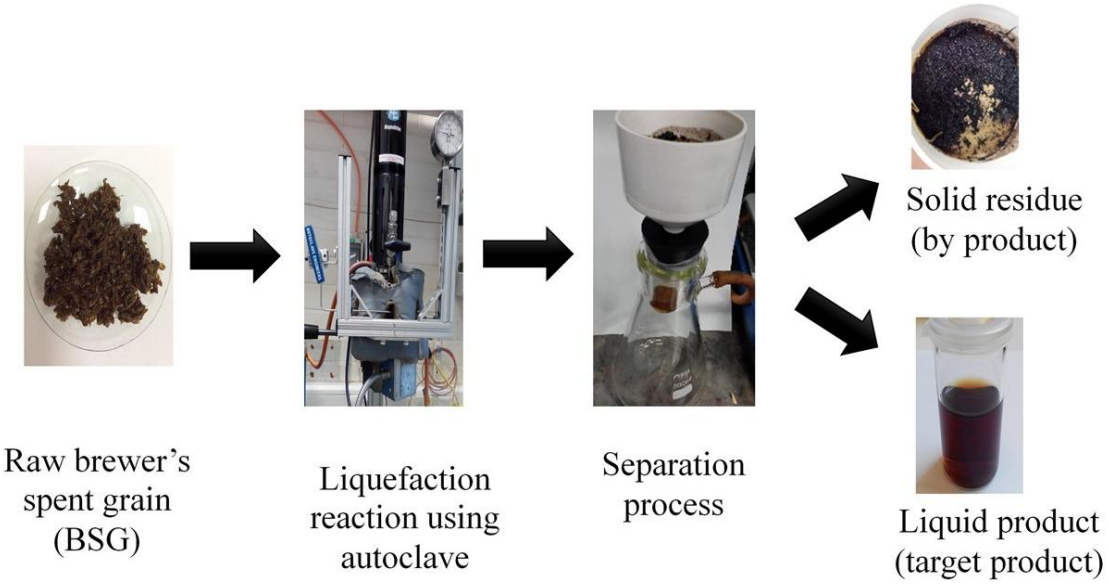

Figure 6-3: Reaction and separation procedure for BSG liquefaction process.

6.2 Product analysis

After the separation process, water-soluble fraction was taken as a liquid product and the solid residue was used to determine the residue and conversion yield. Details on liquid product analysis were explained in Section 6.2.1 while, the solid residue recovery process were elaborated in Section 6.2.2.

6.2.1 Liquid products

The liquid product obtained after the separation stage was used for product identification using GCMS without further modification. This liquid product is typically malodorous and dark in colour (Figure 6-4). The second filtration using microsyringe filter was conducted towards the liquid product before the sample was injected to GCMS. This step is to remove the remaining solid particles in the liquid product and to make sure that only liquid sample was injected in GCMS. The presence of the solid particle in the injected sample can cause damage to the GC column. The column used for the current analysis is HP-INNO-wax, and the details on the procedure taken are discussed in Section 5.1.3.1.

The recovered liquid product after the GCMS analysis underwent evaporation to obtain the bio-oil, in current work defined as water-soluble oil (WSO). The water was evaporated by heating in the oil bath or by using direct heating on the hot plate at temperature of 100 ºC. With the intention of calculating the WSO yield, the weight of the empty flask or beaker was recorded prior to the process and the liquid product. The weight difference of the flask before and after the process was used to determine the amount of the WSO obtained. Figure 6-4 shows the liquid product and the WSO obtained after the evaporation process. It should be noted that the WSO obtained after the evaporation process was not recovered as the bio-oil is highly viscous and strongly adheres to the wall of the container (Figure 6-4). This however is not the limitation in the research as:

i) The amount of the WSO obtained has already been measured using the weight difference of the flask before and after the evaporation process; and

ii) The composition of the WSO has already been determined using the liquid product before the evaporation process was conducted

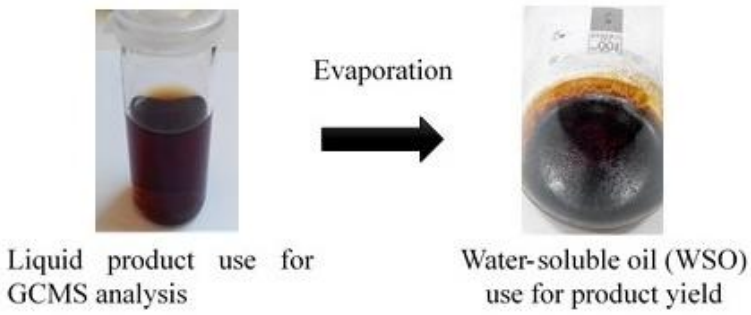

Figure 6-4: Evaporation of the water solvent in the liquid product was conducted at temperature 100 ºC. The liquid remains after the evaporation process was used to obtain the water-soluble oil (WSO) for product yield.

The WSO yield was defined as the weight percentage of the WSO per weight of dry BSG input as follow:

$$WSO\ yield\ (wt.\%) = \frac{weig\,ht\ of\ WSO\ (g)}{weig\,ht\ of\ dry\ BSG\ input\ (g)}\ X\ 100\% \qquad \textit{Equation 6-1}$$

6.2.2 Solid residue and biochar yield

The solid residue was separated from the product mixture by using vacuum filtration. Prior to the process, the reactor has also been washed with 15 mL of distilled water to ensure that the entire solid residue in the reactor is fully recovered. Next, the solid residue together with the filter paper was place in an oven and dried at 105 ºC for 12 h. The dried BSG residue and the pre-weighed filter paper then were weighted in order to determine the product yield. Figure 6-5 shows the BSG residue before and after the drying process.

Figure 6-5: The drying process was conducted towards solid residue recovered after the liquefaction by undergone oven dry heating at 105 ºC for 12 hours. The exact amount of dried BSG after the process was used for residue and conversion yield.

The BSG conversion for the current HTL process was determined based on the solid residue remaining after the liquefaction reaction, which were defined as the weight percentage per dry BSG input as follow:

$$Solid\ yield\ (wt.\%) = \frac{weig\,ht\ of\ solid\ \ residue\ \ (g)}{weig\,ht\ of\ \ dry\ \ BSG\ input\ \ (g)}\ x\ 100\% \qquad \text{Equation 6-2}$$

$$BSG\ conversion\ \ (wt.\%) = \ 100 - solid\ yield\ (\%) \qquad \textit{Equation 6-3}$$

6.3 Results and discussion

Result and discussion section will focus on two main findings: i) liquid product distribution obtained from BSG HTL (0.1) and ii) effect of reaction temperature on BSG HTL (6.3.2).

6.3.1 Liquid product distribution

The composition of the liquid product was analysed using a GCMS as described in Section 6.2.1. Figure 6-6 shows an example of the total ion chromatograms obtained. As can be seen from the chromatogram, the liquid products is a complex mixture with more than 100 compounds detected. When mass spectra were compared to the NIST MS Search version 2.0 library, 38 compounds (peak area > 0.5%) with varying molecular weight were identified and the results are presented inTable 6-1.Due to the complexity of liquid products, it is difficult to perfectly separate every peak. Thus, the only compound with peak area higher than 0.5% of the total area are reported. It should be noted that the qualitative analysis was based

on the library identification and manual inspection of individual mass spectra, however retention times have only been corroborated using individual compound where specifically stated.

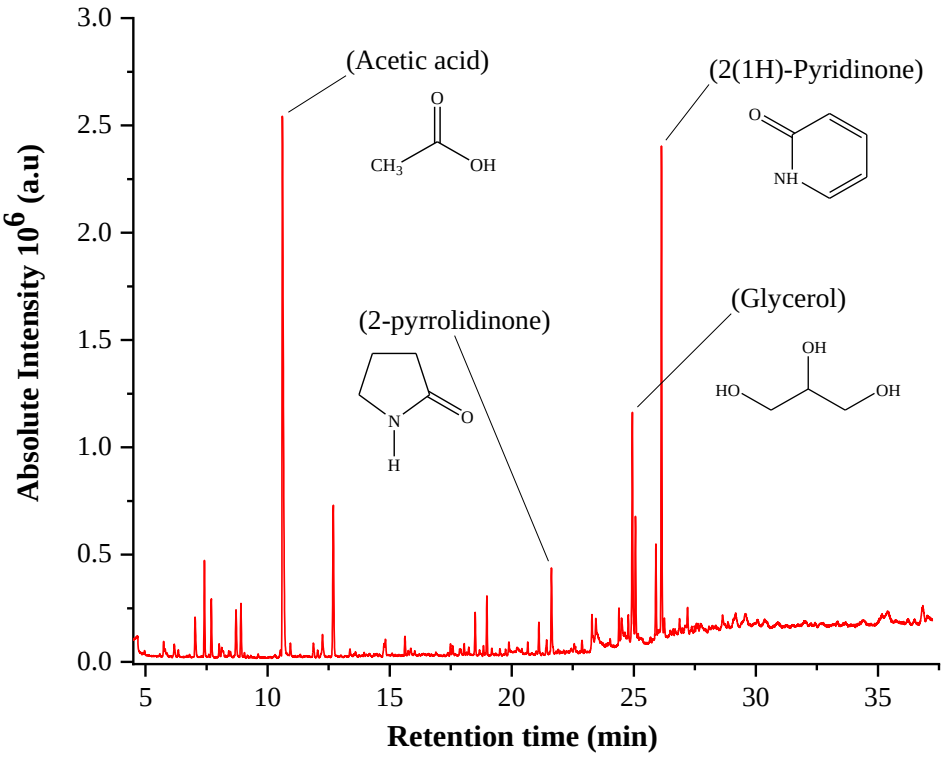

Figure 6-6: Total ion chromatogram of liquid phase product of HTL reaction from BSG. Reaction conditions: raw BSG = 5 g, distilled water= 10 mL, Initial He pressure at 20 °C = 30 barg, reaction temperature= 300 ºC and reaction time = 30 min.

The liquid products obtained in current work are composed of ketones, aldehydes, alcohols, organic acids phenolic compounds and nitrogen-containing heterocyclic compounds. As can be seen from Figure 6-6**,** acetic acid contributes to ~25 % of the total area, followed by 2-pyridinone at ~15 % and glycerol with ~9 %. These three major compounds represent approximately 50% of the total products in the liquid phase obtained by BSG HTL. Note that quantitative calibration has not been conducted and these do not correspond directly to concentration.

Table 6-1: Major chemical composition in liquid product obtained in HTL of BSG. Reaction conditions: raw BSG = 5 g, distilled water= 10 mL, P_{He} = 30 barg, reaction temperature = 300 ºC and reaction time = 30 min.

No	Ret.Time (min)	Compound name	Formula	MW	% Area
1	5.74	Cyclopentanone	C_5H_8O	84	0.9
2	6.18	Pyrazine	$C_4H_4N_2$	80	0.5
3	7.03	Pyrazine, methyl-	$C_5H_6N_2$	94	1.4
4	7.41	Acetoin	$C_4H_8O_2$	88	2.6
5	7.69	2-Propanone, 1-hydroxy-	$C_3H_6O_2$	74	1.7
6	8.01	Pyrazine, 2,5-dimethyl-	$C_6H_8N_2$	108	0.5
7	8.12	Pyrazine, 2,6-dimethyl-	$C_6H_8N_2$	108	0.6
8	8.70	2-Cyclopenten-1-one	C_5H_6O	82	1.6
9	8.91	2-Cyclopenten-1-one, 2-methyl-	C_5H_8O	96	1.7
10	10.60	Acetic acid	$C_2H_2O_2$	60	24.9
11	11.87	Ethanone, 1-(2-furanyl)-	$C_6H_6O_2$	110	0.6
12	12.24	2-Cyclopenten-1-one, 3-methyl-	C_6H_8O	96	1.1
13	12.80	2,3-Butanediol	$C_4H_{10}O_2$	90	5.8
14	14.77	3,4-Dihydroxy-5-methyl-dihydrofuran-2-one	$C_5H_8O_4$	132	0.5
15	14.82	Butyrolactone	$C_4H_6O_2$	86	0.5
16	15.62	Pentanoic acid, 3-methyl-	$C_5H_{10}O_2$	102	0.7
17	18.50	1,2-Cyclopentanedione, 3-methyl-	$C_6H_8O_2$	112	1.3
18	18.98	Phenol, 2-methoxy-	$C_7H_8O_2$	124	1.6
19	19.88	Hydroperoxide, 1-ethylbutyl	$C_6H_{14}O_2$	118	0.6
20	21.11	Phenol	C_4H_6O	94	0.8
21	21.43	Phenol, 4-ethyl-2-methoxy-	$C_9H_{12}O_2$	152	0.6
22	21.62	2-Pyrrolidinone	C_4H_7NO	93	3.1
23	22.87	2-Piperidinone	C_5H_9NO	99	0.5
24	23.28	Furan, tetrahydro-2-methyl-	$C_5H_{10}O$	86	1.9
25	23.44	Propylene Glycol	$C_3H_6O_3$	91	1.3
26	24.39	Phenol, 2,6-dimethoxy-	$C_8H_{10}O_3$	154	1.1
27	24.49	4-(Dimethylamino)pyrimidine	$C_6H_9N_3$	123	1.0
28	24.77	3-Pyridinol, 2-methyl-	C_6H_7NO	109	0.8
29	24.94	Glycerol	$C_3H_8O_3$	92	7.8
30	25.06	Pentanoic acid, 4-oxo-	$C_5H_8O_3$	116	3.5
31	25.90	3-Pyridinol, 2-methyl-	C_6H_7NO	109	2.8
32	26.13	2(1H)-Pyridinone	C_5H_5NO	95	14.6
33	26.25	3-Octyn-2-one	$C_8H_{12}O$	124	0.6
34	26.87	2-Ethoxyethyl 3-methylbutanoate	$C_9H_{18}O_4$	190	0.7
35	27.20	(2H)Pyrrole-2-carbonitrile, 5-amino-3,4-dihydro-	$C_5H_7N_3$	109	1.1
36	28.63	12-Crown-4	$C_8H_{16}O_4$	176	0.8
37	29.17	4-Methyl-2-hexanol	$C_7H_{14}O$	116	1.7
		Total area (%)	**92.9**		

Various nitrogen-containing compounds were found in the liquids products including 2-pyridinone (14.6 %), 2- pyrrolidinone (3.1 %), pyrazine derivatives (3.0 %), etc. in total these represent 26 % of the total product area obtained. These compounds mainly arise from the decomposition of proteins and it was reported that besides fibres, protein is one of the main constituents in the BSG (19-30 % w/w) (Lynch, Steffen and Arendt, 2016). Additionally, the degradation rate of the amino acid at hydrothermal conditions is relatively rapid compared to other biomass monomers (Toor, Rosendahl and Rudolf, 2011). During hydrolysis of biomass, amino acid and sugars are simultaneously formed from protein and cellulose, respectively. These compounds can react together through the Maillard reaction leading to the formation of nitrogen-containing cyclic organic compounds such as pyridines and pyrazine (Peterson, Lachance and Tester, 2010; Toor, Rosendahl and Rudolf, 2011). The Maillard reaction is the reaction of the amine group present in the protein with the carbonyl group present in carbohydrates. This reaction is not a single reaction pathway, but is an interconnected reaction network (Peterson, Lachance and Tester, 2010).

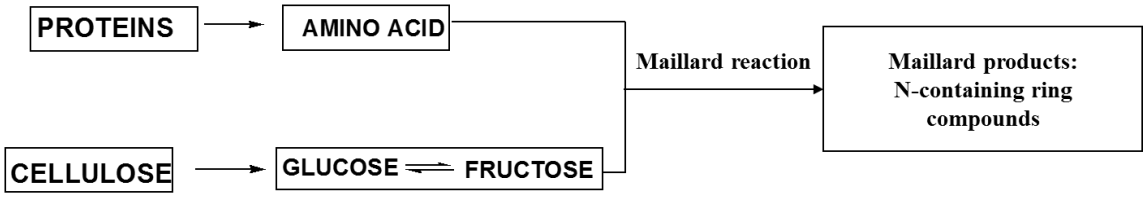

Figure 6-7: Maillard reaction pathway adapted from Toor, Rosendahl and Rudolf, (2011).

A significant fraction of alcohols (21.7 %) were also detected in the liquid products which denoted by a mixture of furan, polyols and phenolic compounds, with the highest fraction was obtained by glycerol at 7.8 %. Glycerol can be considered as a platform chemical (Werpy and Petersen, 2004) which has a multitude of uses in the pharmaceutical, cosmetic, and food industries (Quispe, Coronado and Carvalho Jr., 2013; Tan, Abdul Aziz and Aroua, 2013). Glycerol is a typical product generated from the hydrolysis of triglycerides in the biomass. According to del Río, Prinsen and Gutiérrez (2013), triglycerides were identified in high amounts among the lipids in the BSG, accounting for 67% of all identified compounds by area. Thus, significant amount of glycerol present in the liquid product is due to triglycerides

content in the BSG. The hydrolysis of triglycerides produces a mixture of glycerol and fatty acids, shown schematically in Figure 6-8 (Mika, Edit and Horvath, 2015). During HTL, glycerol is not converted to any oily phase but rather turns to a water-soluble compound (Lehr *et al.*, 2007).

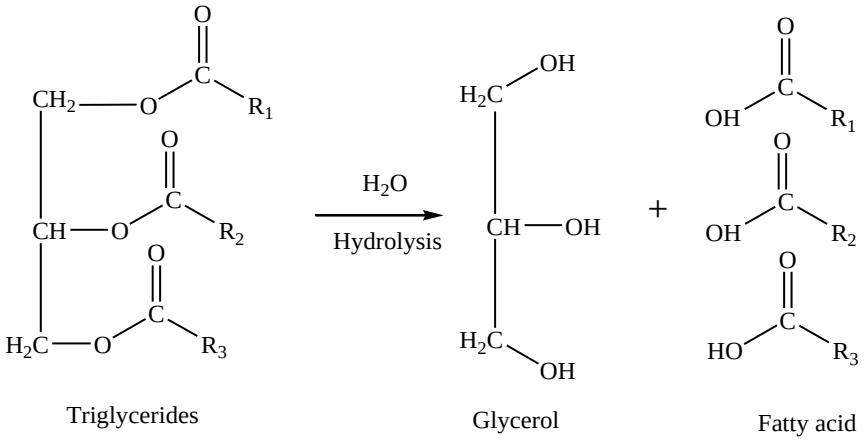

Figure 6-8: Hydrolysis of triglycerides will produce one molecule of glycerol together with three molecules of fatty acid.

Organic acids are the principal component in liquid products which represent 29.2 % of the total area; acetic acid (24.9 %), levulinic acid (3.5 %) and 3- methyl-pentanoic acid (0.76 %). The high content of organic acid in HTL of BSG may result from the high amount of cellulose and lignin in BSG. Decomposition of furan from cellulose and breakdown of small functional group from lignin monomer may leads to formation of acetic fragments; a source for the acidic compounds (e.g: acetic acid) (Karagöz *et al.*, 2004). Levulinic acid is one of the main product from dehydration and rehydration of glucose monomer from cellulose (Pileidis and Titirici, 2016).

Lignin present in BSG was liquefied into phenolic compounds such as 2-methoxyphenol(1.61%), 4-ethyl-2-methoxyphenol (0.59%), and phenol (0.8%). Compared to HTL of model lignin in both single and binary system (Chapter 5), BSG HTL shown an additional lignin liquid products, 2,6-dimethoxy- phenol (1.06%). This which produce from the decomposition of sinaplyl alcohol (Kleinert and Bargth, 2008). Ketones detected comprise both aliphatic and cyclic compound such as acetoin (2.58 %), 2-methyl-2-cyclopentenone (1.71%), 1-hydroxy-2-propanone (1.66 %) and2-cyclopentenone (1.64%). Chen *et al.*, (2014) reported that

ketones were primarily derived from monosaccharides generated from the decomposition of holocellulose, however they may transform to alcohols and acids since they are relatively unstable under hydrothermal condition.

As to the product obtained is a complex mixture, it is challenging to measure each compound quantitatively. In an effort to evaluate the HTL of BSG in current work, the quantitative analysis was conducted to acetic acid, furfural, guaiacol and 4-ethylguaiacol; products obtained in the preliminary study in Chapter 5. The binary model biomass system, which is used to mimic the real biomass system, was also used to compare with the BSG HTL. In addition, the conversion, WSO yield and total liquid product obtained on BSG HTL were also reported.

6.3.2 Effect of the reaction time of BSG HTL

In Chapter 5, preliminary studies on binary model biomass systems have shown that the reaction time influences the degradation on cellulose and lignin in a different way; longer times are favourable for phenolics products while cellulose degradation products more selective at lower reaction times. In the current section, the effect of reaction time on BSG HTL was studied in the range of 15 min to 120 min. The conversion, WSO yield and liquid product obtained at different reaction time are shown in Figure 6-9**.**

Those data show shows that upon increasing the reaction time from 15 min to 30 min, there is a significant increase in both conversion and WSO yield of the BSG HTL reaction. The conversion increased from 58 % to 73 %, while WSO yield reached 22 % at 30 min compared to 12% at 15 min. As the reaction time was extended, the conversion decrease to 69 %, 62% and 59 % for 60 min, 90 min and 120 min, respectively which related in increase in biochar yield. A similar trend was obtained for the WSO yield; maximum yield was obtained at 30 min, however, increasing time beyond this point causes a reduction in WSO production. For liquid products, the maximum mass was obtained at 30 min (9.7 g) and slightly decreased as the time was extended to 60 min (8.8 g) and underwent sudden decrease to 7.2 g at 120 min. Result show that the amount of liquid product is proportional with WSO yield obtained in the system.

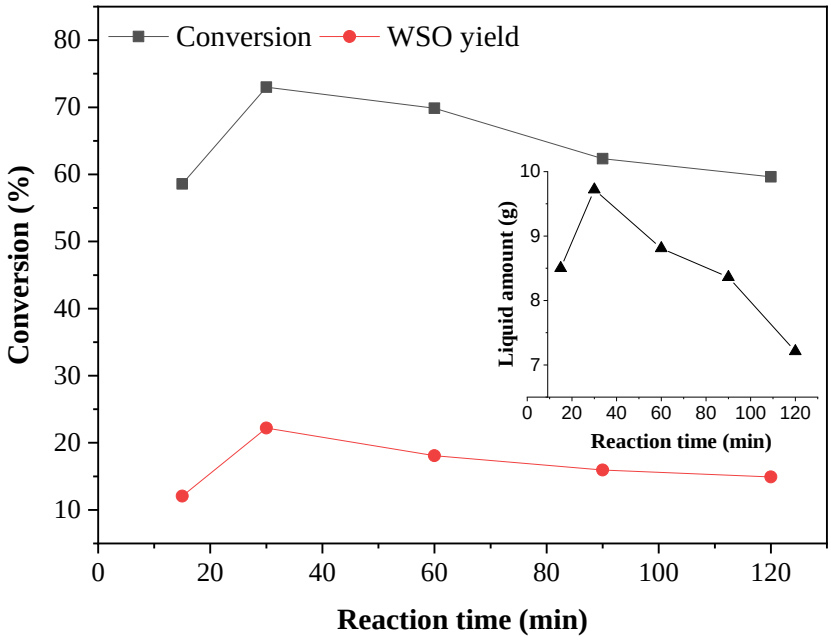

Figure 6-9: The conversion, WSO yield and liquid amount obtained from BSG HTLat different reaction time. Reaction condition: reaction temperature = 250ºC, initial He pressure at 20ºC = 30 barg, 5 g of BSG, 8.75 mL of water.

Karagöz *et al.*, (2005), studied the decomposition of biomass waste (sawdust) under HTL condition. They found that at 280 ºC for 15 min, some compounds such as vanillin, phenol, 2,4-dihydroxybenzaldehydewere obtained but, these compounds were not observed at the longer reaction time (60 min). They also conclude that the decrease in bio-oil yield as the reaction time increase was due to a secondary decomposition reaction of the bio-oil composition over time. For a better understanding of the result obtained, the data on liquid product composition are consulted and are compared with the model system. It should be noted that the concentration of compounds in both systems may differ due to a different amount of biomass been used. The aim of the current discussion is to quantitatively compare the product distribution over time and not the product yield.

One of the significant products obtained from BSG HTL is acetic acid (25 %). Figure 6-10 shows acetic acid concentration over time in two HTL systems; BSG and the binary model system. As can be seen from data obtained, the concentration of acetic acid in BSG increased as the time increased from 15 min to 30 min at 2.3 g/L and slightly decrease after that time. A sudden drop was recorded at 120 min reaction from 2.2 g/L (90 min) to 1.6 g/L. Meanwhile, for the binary

model system, the maximum concentration is obtained at 120 min (0.2 g/L) and the concentration is relatively increased over time, with a small dip at 90 min (0.12 g/L). Acetic acid formation may correlate directly with other species present, e.g.: decomposition of hemicelluloses and cellulose (Liu *et al.*, 2013) and functional groups cracked from lignin monomers could be the sources for acidic compounds(Y. P. Zhao *et al.*, 2013).

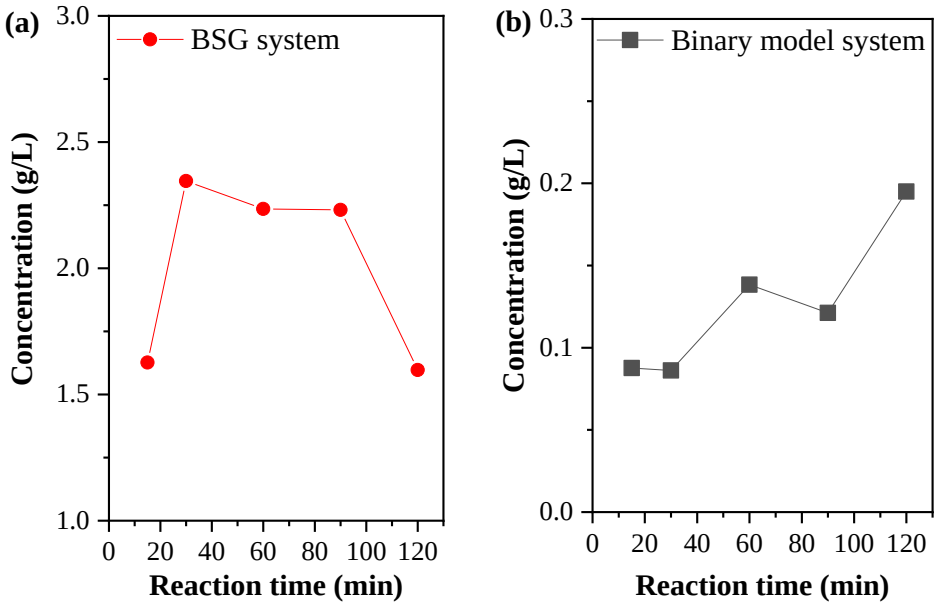

Figure 6-10: Acetic acid concentration at different reaction time obtained in HTL (a) BSG system and (b) model biomass system. Reaction condition: reaction temperature = 250 ºC, initial He pressure at 20 °C= 30 barg, real system = 5 g of BSG, model system = 0.2 g model biomass.

Figure 6-11 shows the concentration as s function of reaction time for two phenolic compounds obtained from the lignin monomer; guaiacol and 4-ethylguaiacol. For the binary model system, the result show that concentration for both phenolics increase over time, with maximum concentration obtained at the maximum reaction time studied; 120 min. The concentrations obtained are 77 mg/L and 15 mg/L, for guaiacol and 4-ethyl-guaiacol respectively. However, in the BSG system, the results show that increasing reaction time may help the formation of phenolics up to a point, but that the concentration reduces at longer reaction times. Guaiacol shows the highest concentration at 90 min reaction time (168 mg/L), while for 4-ethylguaiacol, the optimum concentration is 50 mg/L at 60 min. The result

obtained from BSG HTL did not support the model biomass decomposition system directly as both phenolics produce maximum concentration at different reaction time. This may due to the different concentration of lignin present in both system; BSG contain 0.02 g/mL while the model system was set at 0.01 g/mL of lignin. Due to this, the current comparison may just was made based on first part of lignin curve in the model system which resulted in different pattern obtained. In spite of that, there is a correlation between acetic acid and phenolics obtained from lignin monomer shown by both HTL system; higher degradation of lignin monomer to phenolics, high concentration acetic acid obtained and vice versa.

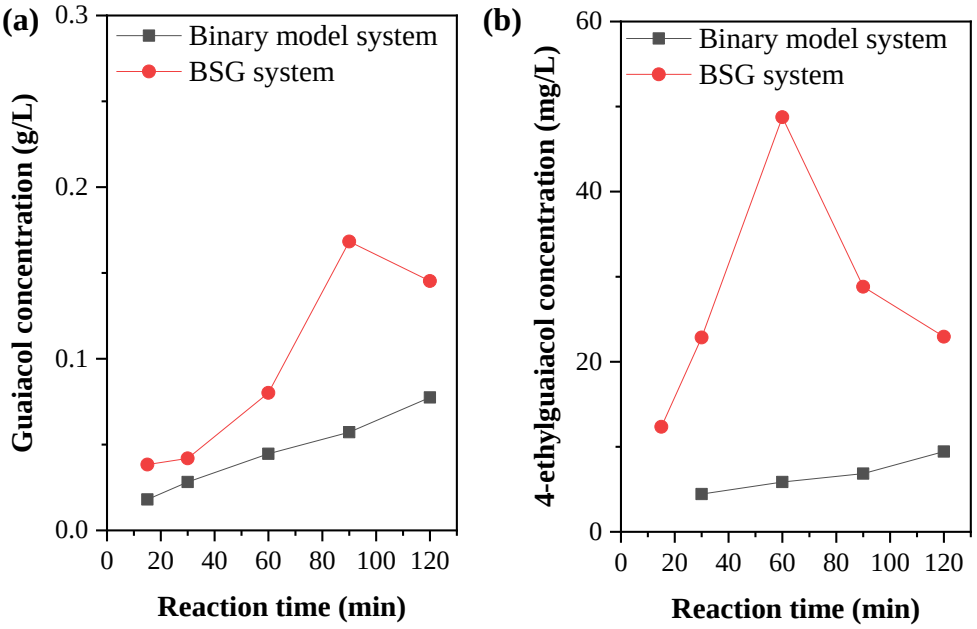

Figure 6-11: (a) Guaiacol and (b) 4-ethylguaiacol concentration in HTL over reaction time. Reaction condition: Reaction temperature = 250 ºC, initial He pressure at 20 ºC = 30 barg, real system = 5 g of BSG, model system = 0.2 g model biomass.

Furfural is the main product obtained from HTL of cellulose in the single model system (Figure 5-2) and during HTL of binary model biomass system, furfural has shown the highest concentration compared to levulinic acid and HMF (Figure 5-11). In current work, the concentration of furfural in BSG HTL was plotted over time and results obtained were shown in Figure 6-12. Result shows that at 30 min, the highest amount of furfural was recorded at 0.65 g/L and as reaction time was prolonged, furfural concentration drop by 84 % (0.12 g/L) at 120 min. Compare to

the binary model system, there is a sharp drop in the furfural concentration after 30 min (indicate by arrow) obtained by BSG system. This result may suggest that the hemicellulose in BSG was fully decomposed after 30 min in HTL which resulted in a lower concentration of furfural were obtained; furfural is generally derived from C_5 sugars, mainly xylose and arabinose, that are contained in the hemicellulose (Lange *et al.*, 2012). This result in agreement with Liu *et al.*, (2013) which had shown that sugars in biomass had dropped remarkably to zero with the prolongation of retention time from 20 to 40 min at 260 ºC during HTL reaction of cypress.

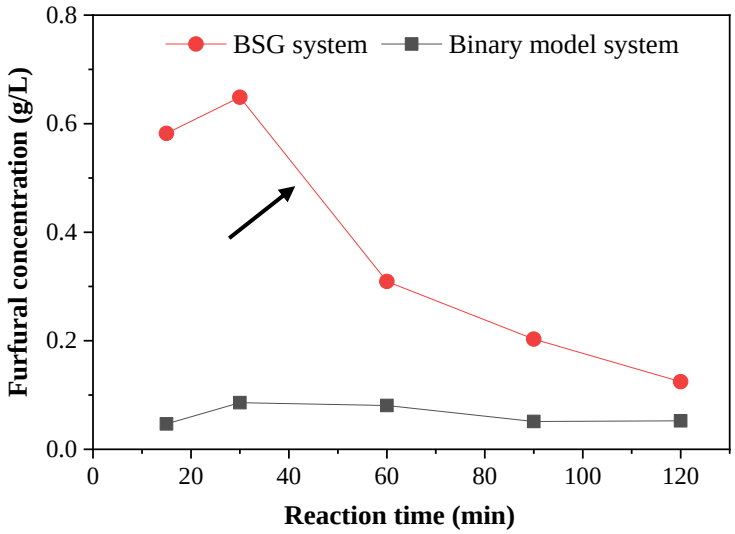

Figure 6-12: Comparison on furfural concentration over reaction time between BSG system and binary model system. Reaction condition: reaction temperature = 250 ºC, initial He pressure at 20 ºC = 30 barg, real system = 5 g of BSG, model system = 0.2 g model biomass.

In general, result obtained in BSG HTL show that as the reaction time prolonged to 120 min, the concentration in all studied component decreased significantly. These findings may relate in overall process in HTL system; longer reaction time decrease conversion, liquid amount and WSO yield (Figure 6-9). During HTL, increase in reaction time may increase the competition of two reactions; hydrolysis and polymerisation. And, it is accepted that at longer reaction time, the polymerisation reaction are dominant (Liu *et al.*, 2013) which lead to lower the conversion, liquid amount and WSO yield.

6.4 Conclusion

In summary, the product distribution obtained from real biomass is significantly different when compared to the model biomass (Chapter 5). The presence of other components in BSG such as protein and triglycerides leads to the production or various products which were not detected in the pure cellulose and lignin model system.

At this point, comparison made based on liquid products; acetic acid, guaiacol, 4-ethyl-guaiacol and furfural show the behaviour of this particular component in model system does not represent the actual biomass system; BSG. The presence of other complex polymers in BSG in addition to cellulose and lignin, may direct those compound to a more complex reaction pathway. Besides, the fraction of cellulose and lignin in real biomass should be identified for the better comparison towards the model system. The discussion may limited to just particular components in BSG HTL but, it somehow may related the overall product obtained in the system; conversion and WSO yield.

In conclusion, while hydrothermal technologies have been shown to handle a range of feedstock compositions, in actuality, the processes are susceptible to the individual makeup of the feedstocks and must be tailored to the chemistry taking place as a result of the feedstock composition and processing condition.

CHAPTER 7

LIQUEFACTION OF BREWER'S SPENT GRAIN (BSG): EFFECT OF SOLVENT

Chapter 7: Liquefaction of BSG: Effect of solvent

7.0 Introduction

Throughout Chapter 5 and 6, it was shown that the use of water in HTL processes was able to break down lignocellulosic material into various value-added chemicals. Breakdown of cellulose lead to the production of platform chemicals such as levulinic acid, furfural and HMF, while lignin degradation contributes to the phenolic compounds presents in the liquid obtained. Chapter 6 summarised that the use of BSG as real biomass in liquefaction directed the product distribution into a different pattern from the model component due to the chemical complexity of biomass polymers.

The main difference between liquefaction technology and other thermochemical conversion processes (combustion, pyrolysis and gasification) is that water or other suitable solvents must be adopted as the reaction medium (Huang and Yuan, 2015). The liquefaction of biomass with an appropriate solvent is a process that can produce fuel additives and other valuable chemicals, simultaneously (Liu and Zhang, 2008). In a biomass liquefaction process, the presence of the solvent promotes such reactions as solvolysis, hydration, and pyrolysis, which helps achieve better fragmentation of biomass and enhancing dissolution of reaction intermediates. Given this, the effect of different solvent towards BSG liquefaction process was investigated. In this chapter, the reaction process focusing on direct liquefaction of BSG in different solvents and their effect on the product distribution and the biochar obtained is reported.

7.1 Material and experimental procedure

Details on materials used in current work are listed in Section 7.1.1. The experimental procedure involved in studying the effect of solvent in direct BSG liquefaction; i.e. the reaction set-up, is explained in Section 7.1.2.

7.1.1 Material

Effect of solvent on liquefaction was carried out using wet BSG as the case study. The materials used in current work were compressed helium gas (BOC, 99.99%), distilled water (produced in an Elga reservoir of 75 L), methanol (Sigma – Aldrich, ≥ 98%), ethanol (Sigma – Aldrich, ≥ 99%) and 2-propanol (Sigma – Aldrich, ≥ 99%).

7.1.2 Experimental procedure

In this chapter, the experiment performed according to set up represented in Figure 3.1 and follows the procedure used for liquefaction of real biomass in Section 6.1. Compared to the previous chapter, the findings in current work will focus on the effect of different solvents on both the liquid product and solid residue obtained after the reaction. Figure 7-1 depicts the overall process used in current work.

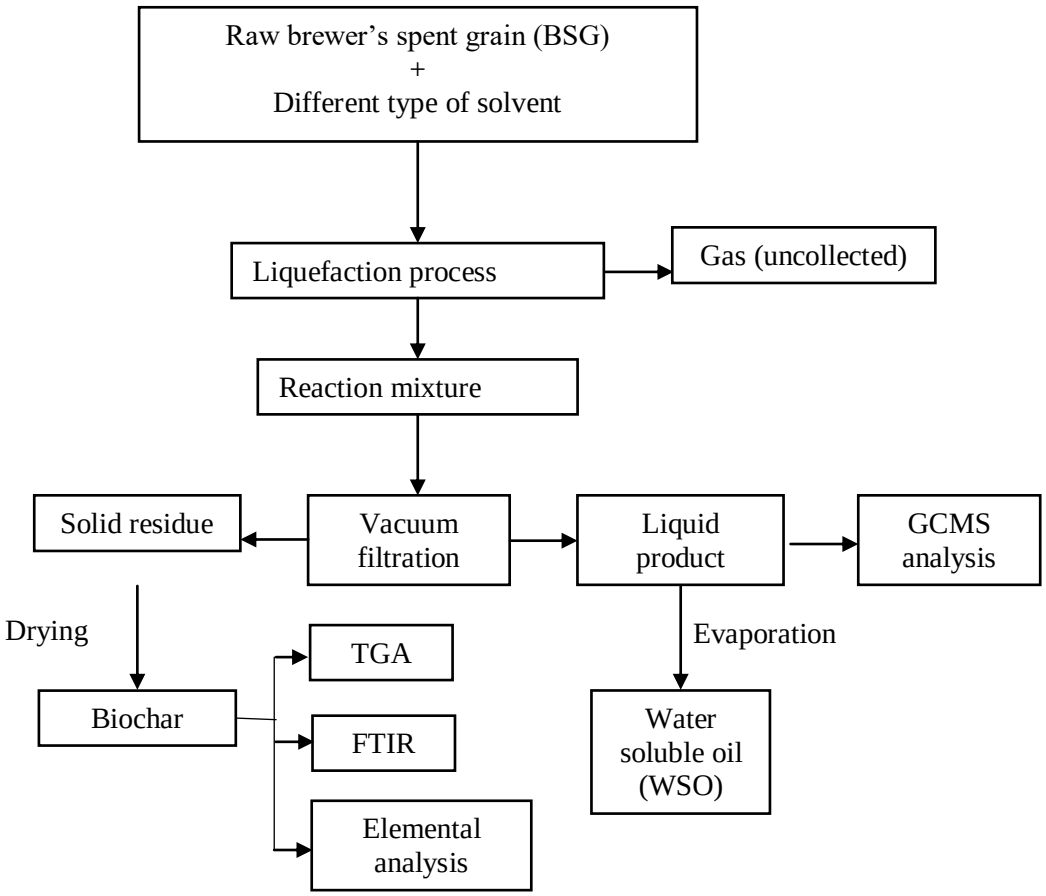

Figure 7-1: An overall flow chart for the effect of the different solvent system on BSG liquefaction process.

The liquefaction process was studied using four different solvents, namely water, methanol (MeOH), ethanol (EtOH) and 2-propanol (2-PrOH) under identical experimental conditions. For parameter control, the results obtained from Chapter 6 were consulted. The reaction was conducted at temperature 250 ºC for 30 minutes reaction time, and the mixer speed was set at 500 rpm. Firstly, the reactor was loaded with approximately 5 g of raw BSG and the BSG: solvent ratio was set at 1:10 wt. % for both distilled water and the alcoholic solvents. Before the reaction takes place, the air trapped in the reactor was purged out, and the reactor was loaded with 35 barg of helium prior to the reaction. After 30 minutes reaction time, the reaction, and the mixture of the solid-liquid product was separate using vacuum filtration. The soluble fraction was taken as liquid product while the insoluble solid residue was pointed as biochar.

7.2 Analysis of the product obtain

In the current chapter, the characterisation on liquid product and solid residues obtained after BSG liquefaction is presented. Details on liquid product analysis are given in Section 7.2.1, while the solid residue was used to determine the biochar and conversion yield as described in Section 7.2.2.

7.2.1 Liquid product and bio-oil yield

The liquid product obtained after the separation was injected to GCMS for product identification. The column used is HP-INNO-wax, and the details on the procedure taken are elaborated in Section 6.2.1. After the analysis, the solvent was removed from the liquid product to obtain the WSO, the yield of which was calculated using Equation 6.1.

7.2.2 Solid residue and biochar yield

The solid remained after the separation was used to determine the biochar yield and conversion for the reaction. The procedure taken to recover the solid product and the drying process were explained in Section 6.2.2. The determination on biochar yield and conversion were calculated using Equation 6.2 and Equation 6.3, respectively. The biochars obtained underwent several characterisation methods

to investigate their physical and chemical properties for the potential to be used as the solid fuel. The range of characterisation techniques included TGA, elemental analysis and FTIR spectroscopy.

7.3 Results and discussion

The discussion of results focuses on two main findings in the current chapter: i) effect of solvent in conversion, WSO yield and product distribution (7.3.1) and ii) effect of solvent on BSG biochar. Details on both findings and explanation on the result obtained will be discussed in detail.

7.3.1 Alcoholic solvents in direct liquefaction of BSG

Although water is the most commonly used medium for liquefaction reaction, using water as a solvent has the following drawbacks:

i) The critical value for water (374^{o}C, 22.1 MPa) means that the subcritical water liquefaction process requires challenging operative conditions (C.Ji 2017, Yuan 2007)

ii) Bio- oil obtained from aqueous HTL contains a high amount of oxygen and nitrogen, and thus limits its application for transport fuel (C. Ji,2017)

To ease this severe requirement of reaction condition and enhance the quality of bio-oil, addition of various organic solvent with lower critical value and dielectric constant to subcritical water have been adopted for liquefaction including alcohol (MeOH, EtOH, butanol and phenol) (Huang and Yuan, 2015), glycerol (Hassan and Shukry, 2008), acetone and 1,4- dioxane (C. Ji 2017). It has been shown that a mixture of organic solvent-water has a synergistic effect on the liquefaction of biomass. Compared to water as a sole solvent, the mixed solvent will decrease the critical temperature and pressure of reaction system leading to higher conversion and alsoimproves the quality of bio-oil products (Y.-P. Zhao *et al.*, 2013; Lai *et al.*, 2018). Additionally, the mixed alcohol-water solvents have also previously been investigated in a range of processes (Li *et al.*, 2014; McGregor *et al.*, 2015; Bye *et al.*, 2017). These solvent systems have been shown to behave as a non-ideal mixture

and are not simply an additive mixture of the properties of the individual component. This has been ascribed to changes in the mesoscale structuring of the solvents induced by hydrogen bonding between water and alcohol molecules.

In the current work, MeOH, EtOH and 2-PrOH were used as solvents in direct liquefaction of BSG. Raw BSG has a high moisture content (~ 75 wt. %), and with the use of alcohol as a solvent, the liquefaction can be considered to take place in an alcohol-mixed-water solvent system. It is worth to underline that the pressure during the reaction was different and varies depending on the solvent system used. Details on the amount of solvent, reaction pressure and liquid product are summarised in Table 7-1. Meanwhile, Figure 7-2 shows a comparison of conversion and WSO yield on BSG liquefaction under the different alcohol-mixed-water solvent system.

Table 7-1: Summary of solvent density (at 20 °C), solvent amount and recorded reaction pressure during liquefaction reaction of BSG. Reaction conditions: BSG:solvent wt% ratio = 1:10, initial He pressure at 20 °C= 30 barg, reaction temperature=250 ^{o}C and reaction time = 30 min.

Solvent system	The density of solvent (g/mL)	Amount of solvent (mL)	Reaction pressure (barg)	Liquid product (g)
HTL (Water)	0.99	8.75	~ 80	9.1 ± 0.3
MeOH	0.79	11.0	~ 86	8.1
EtOH	0.79	11.0	~ 82	9.3
2-PrOH	0.80	11.0	~ 80	10

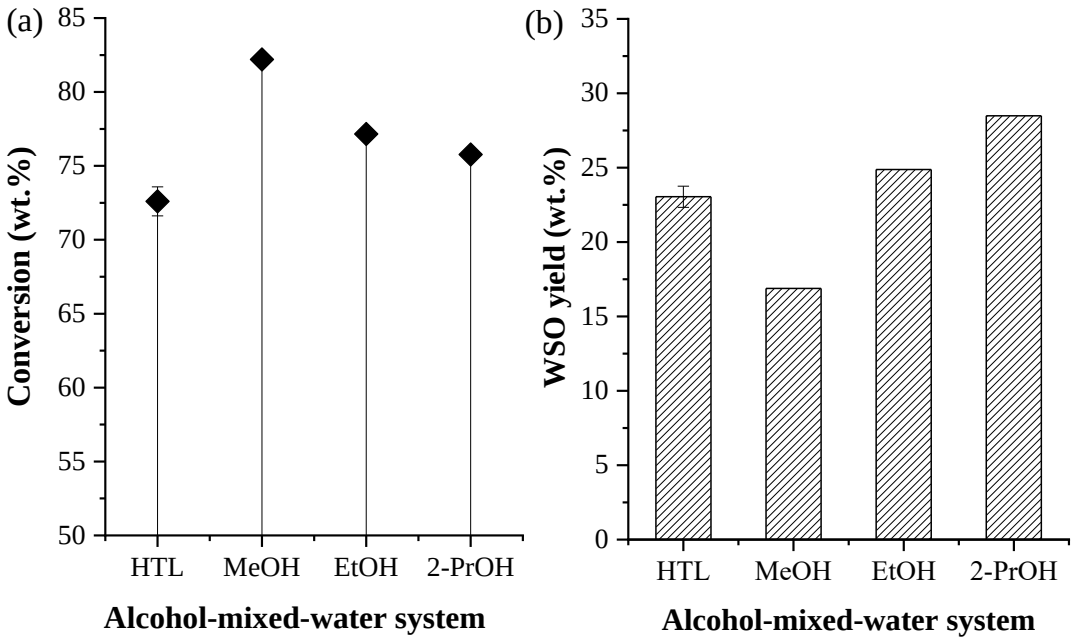

Figure 7-2: Comparison on(a) conversion and (b) WSO yield on direct liquefaction of BSG under different solvent namely water (HTL), MeOH, EtOH and 2-PrOH. Reaction conditions: BSG:solvent wt% ratio = 1:10, initial He pressure at 20 °C= 30 barg, reaction temperature = 250 ^{o}C and reaction time = 30 min.

As can be seen from Figure 7-2 (a), with the addition of organic solvent in direct liquefaction reaction, the conversion increased significantly with regard to pure water; MeOH provide the highest conversion at 82%, followed by 77%, 75% and 72% for EtOH, 2-PrOH and water (HTL) as solvent, respectively. The high conversion of alcohol-mixed-water system compare to HTL may relate to lower dielectric constant of the solvent. Figure 7-3 shows the dielectric constant value for the alcohol-water-mixed solvent used in current work. The plot indicates that the dielectric constant of water gradually decreases with the addition of the alcoholic solvent in the water system. Lower dielectric constant increase the affinity between the solvent and the organic material (Huang and Yuan, 2015), in our case BSG. This is resulting in an increase in the conversion of BSG liquefaction system.

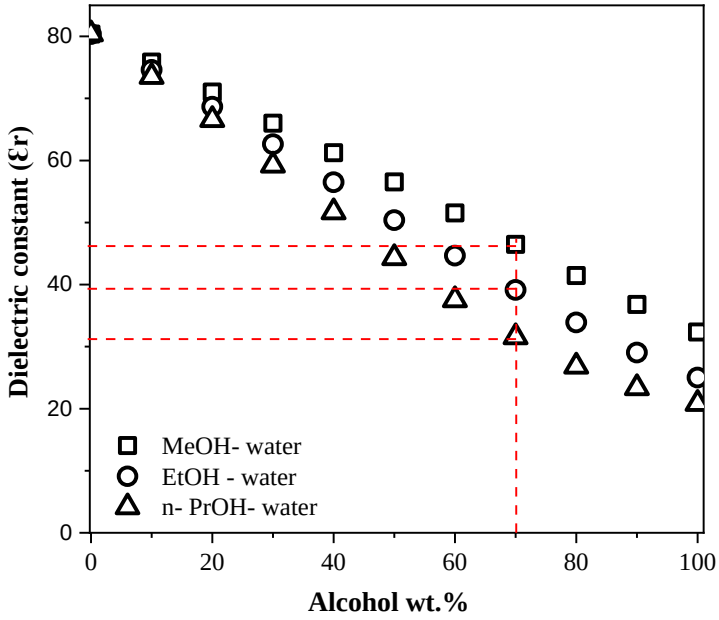

Figure 7-3: The dependence of dielectric constant at 25°C of different alcohols-water-mixed solvent; (a) MeOH (b) EtOH (c) 2-PrOH (Åkerlöf, 1932).

Although MeOH-water system has higher dielectric constant than EtOH and 2-PrOH (indicate by the red line), the literature reports that the molecule size of a solvent has an important effect solvation capacity in liquefaction (Castellví Bargnés *et al.*, 2017). Smaller molecules are generally better solvents as they provide a larger entropic driving force to dissolution. Furthermore, they can diffuse more easily through polymeric structures of biomass which explain the high conversion obtained by MeOH-water system (simplest alcohol molecule) compare to EtOH and 2-PrOH.

Figure 7-2 (b), shows that the WSO yield was highest in case of liquefaction with 2-PrOH, at 29% and decreasing to 25% for EtOH, 23% for water and with MeOH producing the lowest yield at 16%. The WSO yield is proportionally related with the amount of liquid product obtained as shown in Table 7-1. MeOH-water has the lowest liquid product at 8.1 g compared with other solvent system, although this system provides the best conversion in liquefaction. This result might due to the lowest boiling point of MeOH compared to other alcohol which causes the liquid product to vaporise and favourable the formation of a gas product; as indicated by highest pressure recorded in MeOH-water system (~ 86 barg). As the result of both factors, lower dielectric constant and higher boiling point than other alcohols, the 2-PrOH-water system provides the optimum condition in current liquefaction system.

This system produces the highest liquid product; 10 g and WSO yield at 29 % were recorded. Based onWSO yield obtained, the solvent efficiency in the BSG liquefaction can be sequenced as follows: 2-PrOH+ water > EtOH + water > water > MeOH + water. It is notable that WSO yields in water do not follow the same trend with the boiling point as the alcohols. This may be related to the enhanced mesoscale structure provided by the strong hydrogen-bond network in the aqueous system.

Details of this study will further be confirmed by liquid product analysis which determines the WSO composition. Figure 7-4 compiles the GCMS chromatogram of liquid products under the different solvent system. As can see in the figure, there was a notable difference in term of peak distribution, peak intensity and major peaks between all the spectra. It was clear from the figure that the MeOH-water shows the relatively a broader distribution of product with no particular products dominating the chromatogram. In contrast, 2-PrOH-water chromatogram shows a wider differential in peak intensity between the largest and the smallest peaks. The highest intensity of individual peaks is due to the maximum yield of WSO yield obtained. From the Figure 7-4, it also can be seen that a greater number of peaks appeared in chromatogram from alcohol-water solvent compare to water system suggesting that wider product distribution in the liquid product obtained (Liu and Zhang, 2008).

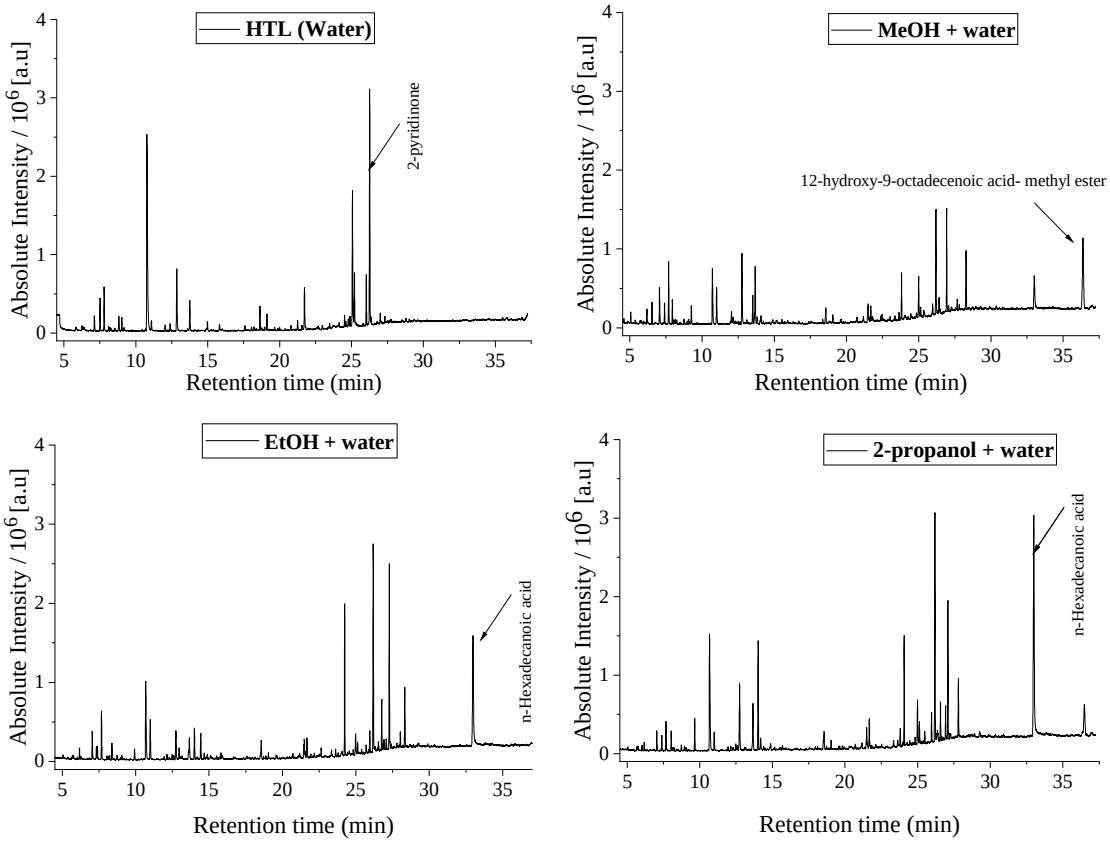

Figure 7-4: GCMS chromatogram on liquid product distribution for BSG liquefaction under different solvent. Reaction conditions: BSG: solvent wt% ratio=1:10, Initial He pressure at 20 °C = 30 barg, reaction temperature=250 ^{o}C and reaction time = 30min.

The chromatogram peaks were identified, and the area under the graph was measured for product identification and qualitative analysis. Details on the identified compounds based on retention time, chemical name and their percentage area were tabulated in Table 7-1. It is important to note that the values illustrated in the table do not represent the actual concentration but indicate the product composition associated with each solvent based on library identification and manual inspection of individual mass spectra. Due to the complexity of the liquid product, it is difficult to perfectly separate every peak. Thus, only those compounds with peak area (%) higher than 1% are shown on the table.

Table 7-2: Major chemical components in liquid product for BSG liquefaction under different alcohols-water-mixed solvent; water (HTL), MeOH, EtOH and 2-PrOH analysed by GCMS.

No.	RT (min)	Name	Peak (area %)			
			Water	MeOH	EtOH	2-PrOH
1	6.53	2-(methoxymethyl) furan	-	1.26	-	-
2	7.12	Methyl pyrazine	1.25	2.70	1.86	1.00
3	7.51	Acetoin	2.28	1.31	-	-
4	7.80	1-hydroxy- 2-propanone	2.84	4.26	3.09	1.44
5	8.43	Ethyl ester-2-hydroxy- propanoic acid	-	1.51	1.07	-
6	8.82	2-cyclopentenone	1.36	-	-	-
7	9.03	2-methyl-2-cyclopentenone,	1.06	-	-	-
8	9.26	Acetic acid, hydroxy-, methyl ester	-	1.40	-	-
9	9.65	Propane, 1-(1-methylethoxy)-	-	-	-	1.55
10	10.77	Acetic acid	24.33	5.27	7.16	8.59
12	11.00	1-heptyn-6-one	-	-	-	1.05
13	11.09	Furfural	-	2.93	2.94	-
14	12.85	2,3-Butanediol, [R-(R*,R*)]-	6.08	6.41	2.19	4.33
15	12.96	2-Hydroxy-3-methylsuccinic acid			1.03	
16	13.51	Methyl ester 4-oxo- pentanoic acid	-	2.31	-	-
17	13.76	2,3-Butanediol, [R-(R*,R*)]-	2.46	5.03	1.83	3.07
18	14.02	Hexadecane	-	-	-	6.09
19	14.09	10-methyl- eicosane		-	2.26	
20	14.51	Ethyl ester, 4-oxo- pentanoic acid	-	-	1.72	-
22	14.98	Butyrolactone	1.12	-	-	-
25	18.63	3-methyl-1,2-cyclopentanedione	1.68	1.04	1.36	1.42
26	19.12	2-methoxy-phenol	1.09	-	-	-
27	21.55	4-ethyl-2-methoxy phenol	-	-	1.01	1.16
28	21.73	2-pyrrolidinone	3.75	1.19	1.31	1.66
29	22.69	Butane-2-one, 3-methyl-3-(2-oxopropylamino)-	-	-	1.40	-
30	23.81	Methyl ester hexadecanoic acid	-	2.74	-	-
31	24.07	Isopropyl palmitate	-	-	-	4.54
32	24.33	Ethyl ester hexadecanoic acid	-	-	8.23	-
33	25.07	Glycerol	11.06	3.14	1.77	2.18
34	25.20	4-oxo- pentanoic acid	3.71	-	-	1.01
35	26.03	6-methyl-3-pyridinol	3.67	-	1.46	1.41
36	26.26	2- pyridinone	17.56	7.75	14.54	11.91
37	26.57	9-Hexadecenoic acid	-	-	-	1.64
39	26.84	9-octadecenoic acid ethyl ester	-	-	2.91	-
40	26.94	Methyl ester-8,11- octadecadienoic acid	-	6.17	-	1.52
41	27.08	Isopropyl linoleate	-	-	-	6.05
42	27.36	Ethyl ester-9,12-octadecadienoic acid	-	-	10.87	-
43	27.80	Pidolic acid	-	-	4.48	2.86
44	28.28	Methyl ester-5-oxo-L-prolin	-	4.86	-	-
45	33.01	Octaethylene glycol monododecyl ether	-	4.89	-	-
47	33.14	n-Hexadecanoic acid	-	-	15.21	21.21
48	36.37	Methyl ester-12-hydroxy-9-octadecenoic acid	-	12.06	-	-
53	36.48	Triethylene glycol monododecyl ether	-	-	-	2.65
Total area (%)			84.18	78.21	90.41	88.34

-: Not detected or peak area less than 1% of the total area

There are significant differences in composition and relative content between the liquid products obtained in water and that from alcoholic- water solvents.For pure water HTL, three significant peaks appeared at 10.8, 25.1 and 26.3 min identified as acetic acid, glycerol and 2-pyridinone and these three compounds accounted for about 52.9 % of total peak area. MeOH-water system had relatively smaller peaks with 12- hydroxy-9-octadecenoic acid- methyl ester identified as the primary compounds at 36.4 min (12.1% of total peak area). Meanwhile, the EtOH and 2-PrOH mixed water systems, produced the same major product, n-hexadecanoic acid, at 33.1 min. The relative area for the n-hexadecanoic acid present is 15.2% and 21.2% for EtOH and 2- PrOH, respectively. It can be seen the major product (indicate by the arrow in Figure 7-4), and product composition was significantly affected by the solvent system.

Organic acids dominated the chromatogram in 2-PrOH-water (31.4%) and pure water HTL (28.0%), mainly consisting of n-hexadecanoic acid, acetic acid and LA. Meanwhile, MeOH and EtOH mixed water system directed the reaction towards esterification producing high numbers and amount of ester compound. Ester compounds obtained in MeOH-water are 35.9 %, and EtOH-water contributed to 28.2 %. The high content of esters could make the liquid more similar to bio-diesel which indicates the high quality of the product obtained by this solvent system (Fa-Ying Lai, 2018).

In Chapter 6, results show that the liquid component produces from the major component of lignocellulosic biomass (cellulose and lignin) represent the majority of the overall product obtained in the system. WSO yield obtained in current work as follow: 2-PrOH+ water > EtOH + water > water > MeOH + water. Quantitative analysis was conducted to analyst furfural, LA, guaiacol and 4-ethylguaiacol concentration obtained in a current solvent system and results summarised in Figure 7-5. As shown in the figure, the concentration on each component does not relate in the overall WSO yield obtained in the current system. For example; although 2-PrOH produce highest WSO yield, the concentration of furfural (0.6 g/L), LA (0.2 g/L), 4- ethylguaiacol (50 mg/L) and guaiacol (25 mg/L) are lower when compare to other solvent systems.

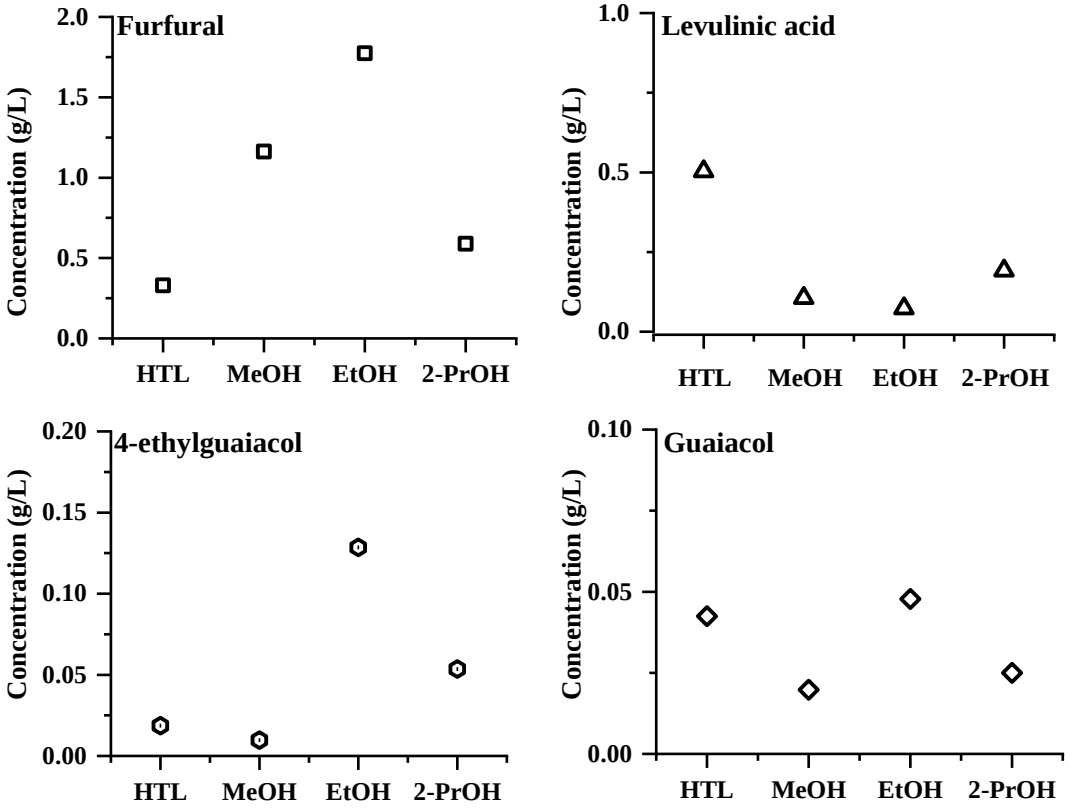

Figure 7-5: Quantitative analysis on liquid product for BSG liquefaction under different alcoholic-mixed solvent systems.. Reaction conditions: BSG: solvent wt% ratio=1:10, Initial He pressure at 20 °C = 30 barg, reaction temperature = 250 ºC and reaction time = 30min.

These current findings show that the nature of the liquefaction solvent has a significant influence on the composition and abundance of liquid product (Liu and Zhang, 2008; Y. P. Zhao *et al.*, 2013; Singh *et al.*, 2015). Apparently, the uses of water or organic solvents as liquefaction solvent have their advantages and disadvantages. In consideration of this fact, the chosen of solvents in liquefaction was depend on the final product of interest and also cost-effective of the process.

7.3.2 Effect of liquefaction solvent on bio-char of BSG

Solvent does not only affect the composition and liquid products, but it also has a remarkable effect on the biochar in the liquefaction reaction. Biochar yield as the function of the different type of solvent is shown in Figure 7-6. Among studied solvent system, the lowest yield of biochar present in MeOH-water (17.8%) followed EtOH- water (22.8%), 2-PrOH-water (24.2%) and pure water HTL produce highest

biochar yield at 28.0%. In order to determine the properties and potential of this biochar as the solid fuel, various characterisation methods have been conducted.

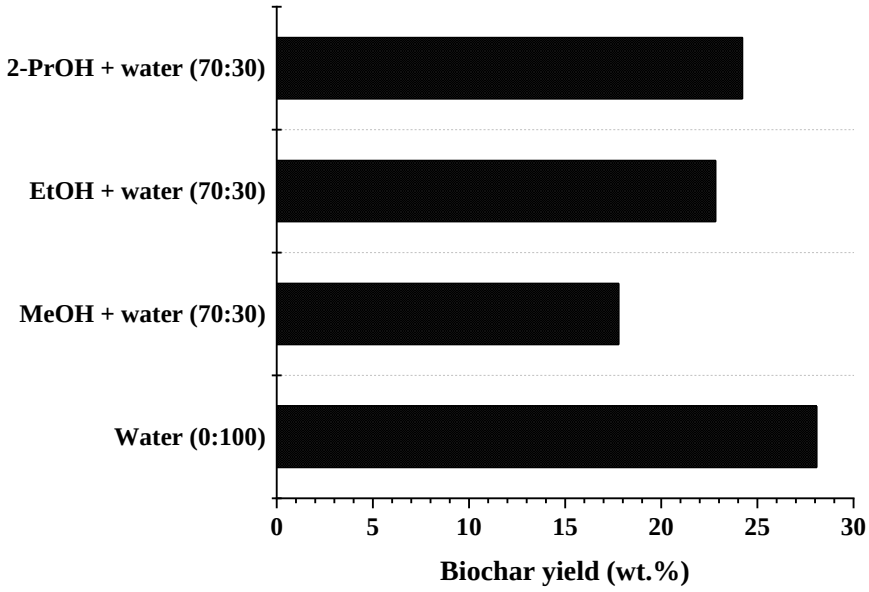

Figure 7-6: Amount of solid residue/ biochar obtained under different liquefaction solvent (alcohol: water, wt.%). Reaction conditions: BSG: solvent wt. % ratio=1:10, Initial He pressure at 20 °C = 30 barg, reaction temperature=250 ºC and reaction time = 30min.

Figure 7-8 shows FTIR spectra of BSG biomass and the biochars, in the range of 400 to 4000 cm^{-1}. BSG biomass is mainly constituted of cellulose, hemicellulose and lignin as has been explained in detail in Chapter 4 on BSG characterisation. From the FT-IR spectra, the strong band at 1030 cm^{-1} can be attributed to the β-glycosidic bond vibration in cellulose. The absorption at 572 cm^{-1} represents lignin, and the absorption at 1638 cm^{-1}can be attributed to unconjugated C=O bonds of xylan in hemicellulose (Yip *et al.*, 2009). In all biochar samples, all of these peaks (572cm^{-1}, 1030 cm^{-1} and 1638 cm^{-1}) diminish as compared to the original biomass spectra, implying that the reaction decomposes the cellulose, hemicellulose and lignin in BSG biomass. Peaks were also plotted at 1030 cm^{-1} which represent the wavelength for cellulose/ carbohydrate band and was shown in Figure 7-8. It can be seen that the peak almost disappeared in biochar using water as solvent liquefaction. Meanwhile, this peak was still can be observed in other biochar (MeOH, EtOH and 2-PrOH liquefaction systems), indicate that some cellulose fragments or intermediate structures remain in the resulting biochar. This result shows that water can break down most of the cellulose component in BSG compared to other alcoholic solvents.

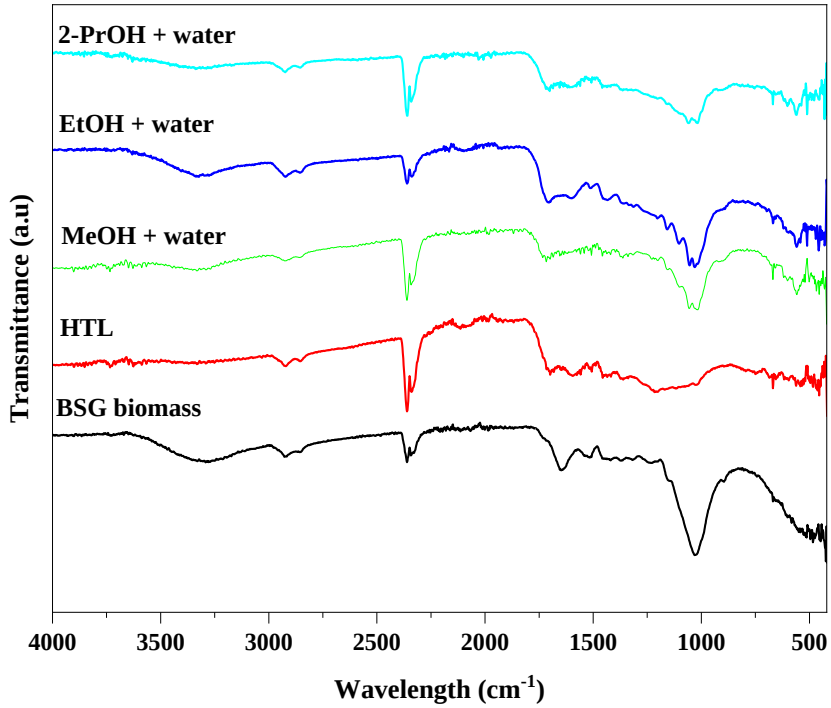

Figure 7-7: FTIR spectrum of BSG biomass and bio-char under different liquefaction solvent. Reaction conditions: BSG: solvent wt. % ratio=1:10, P_{He}= 30 barg, reaction temperature=250 ºC and reaction time = 30min.

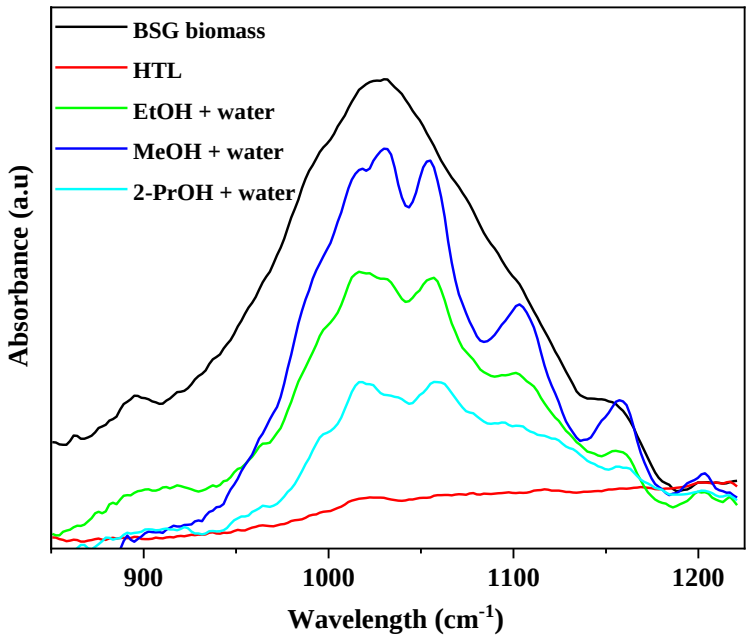

Figure 7-8: Peak for BSG biomass and bio-char at carbohydrate peak (1030 cm^{-1}) under different liquefaction solvent. Reaction conditions: BSG: solvent wt. % ratio=1:10, P_{He} = 30 barg, reaction temperature = 250 $^{\circ}C$ and reaction time = 30min.

Proximate analysis of BSG biochar under different liquefaction solvents was summarised in Figure 7-9. Result shows that the value for moisture, volatiles, fixed carbon and ash was significantly affected by the solvent system. It was worth noting that the volatile content of biochar from water liquefaction system is the lowest compared to other organic solvents. Support by FTIR spectrum, lower volatile matter in the biochar is due to the ability of water to break down most of the cellulose compound in the BSG. Another observation is biochar produced by water liquefaction gives the lowest yield of ash content and the highest yield of fixed carbon compared to other solvents. For potential used as solid fuel, it is noteworthy that high volatiles content can reduce combustion efficiency and increased the pollutant emission when biomass is directly combusted (Khan *et al.*, 2009). Concurrently, high moisture values will decrease the combustion yield, andthe fixed carbon ratios are related to the reactivity of the fuel. On the other hand, ash deeply influences the transport, handling and management costs of the process. It is also influential in corrosion and slag formation (Garcia *et al.*, 2013). Compared to other biochars obtained in the current work, biochar produced by pure water HTL system shows the best characteristic to be applied as solid biofuel.

Table 7-3 summarises the elemental and atomic molar ratio of BSG biomass and all the biochars. It is noteworthy that the values of H/C and O/C ratios of the biochar obtained from the water liquefaction system were the lowest in the present study. Generally, a fuel with low H/C and O/C ratios is favourable because of the reduced energy loss, smoke and water vapour during the combustion process. The molar ratio of the H/C and O/C was calculated and been plot in the van Krevelen diagram, as illustrated in Figure 7-10. The biochar quality fell in the boundary region of coal and lignite/ brown coal. This result indicates that biochar obtained in the present study can be used directly for coal-fuelled boilers without significant modifications. It is therefore interestingly to note that water liquefaction system may provide promising products not just through liquid obtained, but the solid residues can directly be used as solid fuel.

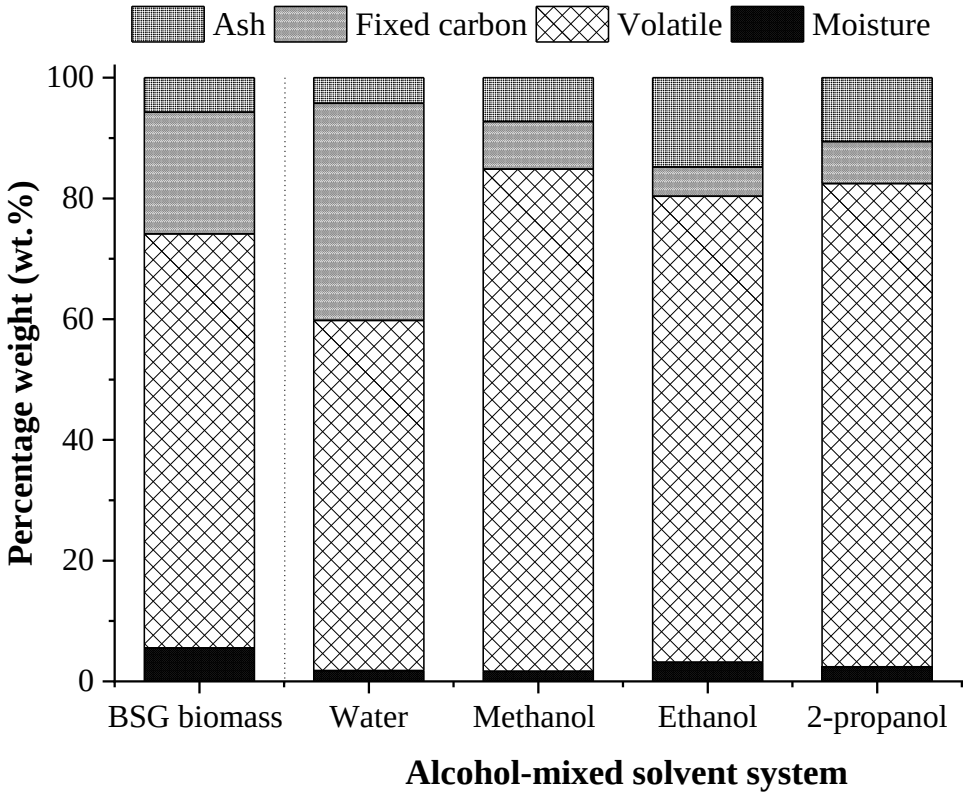

Figure 7-9: Proximate analysis of BSG biomass and BSG bio-char under different liquefaction solvents. Reaction conditions: BSG: solvent wt.% ratio=1:10, Initial He pressure at 20 °C = 30 barg, reaction temperature = 250 °C and reaction time = 30min.

Table 7-3: Ultimate analysis and the atomic molar ratio of BSG biochars produce under different liquefaction solvent.

Individual element and the molar ratio	**Biochar produce in a different solvent system**			
	HTL (water)	MeOH-water mixed	EtOH-water mixed	2-PrOH-water mixed
Ultimate analysis (wt. %)[a]				
Carbon (C)	63.1 ± 1.6	54.8 ± 0.8	48.8 ± 0.5	55.1 ± 0.3
Hydrogen (H)	5.2 ± 0.1	5.3 ± 0.3	4.43 ± 0.3	4.2 ± 0.2
Nitrogen (N)	3.5 ± 0.5	3.8 ± 0.5	3.31 ± 0.1	4.3 ± 0.6
Oxygen (O)[b]	23.9 ± 2.0	28.8 ± 0.1	28.6 ± 0.1	25.9 ± 0.7
H/C and O/C ratio (molar ratio)				
H/C ratio	0.99	1.17	1.09	0.91
O/C ratio	0.29	0.38	0.44	0.35

[a]: reported in mean ± SD value

[b]: were calculated by diff of C, H, N and ash

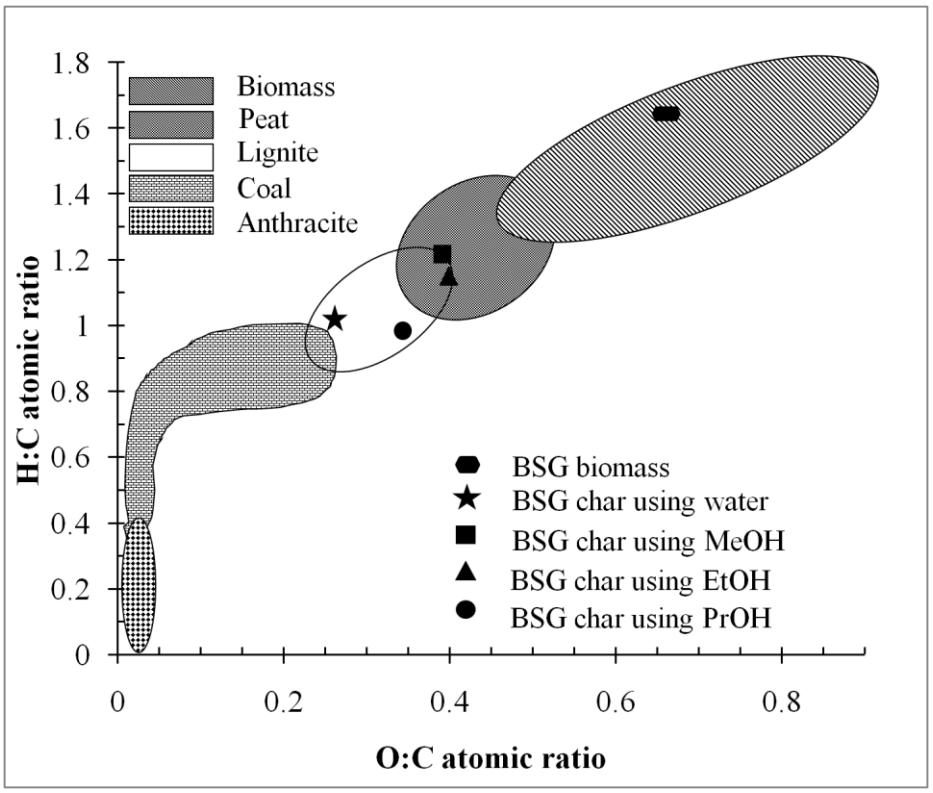

Figure 7-10: Van Krevelen diagram adapted from McKendry (2002) and plotted point for the biochar obtained in current work under different solvent system.

7.4 Conclusion

This chapter explored the influence of different liquefaction solvent using raw BSG as the biomass sources. MeOH, EtOH and 2-PrOH have been evaluated as solvents for liquefaction reaction using raw BSG. It was demonstrated that MeOH enhanced the liquefaction conversion to 79.8 %, while EtOH and 2-PrOH increased the production of bio-oil yield at 25 % and 29 %, respectively compared to pure water HTL (23 %). The liquid product distribution was significantly tailored with the use of the different solvent, which MeOH and EtOH produce esters as their major component. Meanwhile, 2-PrOH and water may be beneficial for the production of the organic acid. Current findings also demonstrated that alcoholic solvents might result in the formation of products with long retention times and, hence, with heavy carbon content compared to water.

In order for the potential biochar for biofuel benefit to be fully realised, the proximate and ultimate analysis has been conducted. Among all the solvents, the biochar produced by pure water HTL system shows the best quality as the solid fuel obtained through this study. The biochar quality fell in the boundary region of coal and lignite/ brown coal which can be used directly for coal-fuelled boilers without significant modifications.

Overall, the most significant conclusion to emerge from this study is that solvents are the key parameters that affect liquid product/ bio-oil and biochar obtained in the liquefaction process.

CHAPTER 8

CONCLUSION AND RECOMMENDATION FOR FUTURE WORK

Chapter 8: Conclusion and recommendation for future work

8.1 Conclusion

The aim of this thesis to contribute a better understanding on the HTL process for lignocellulosic material by using both systems; model biomass and BSG as real biomass. This chapter summarises the significant conclusions of the experimental work conducted in each chapter for current work. Based on the result obtained on characterisation and reaction studies, the following points have been concluded;

i) A case study: BSG characterisation

Throughout this chapter, the major components of BSG waste were extracted, quantified and characterised. The characterisation results have shown that BSG is a lignocellulosic rich material with high moisture content; 75.5 wt.% moisture, 8.5 wt.% cellulose, 7.4 wt.% hemicellulose, 6.5 wt.% lignin and 2.4 wt.% extractives content. The properties of extracted cellulose and lignin were compare with commercial samples via several characterisation techniques; FTIR spectroscopy, TGA and elemental analysis. The overall composition of raw BSG used in current work has also been compared with the values reported by other researchers showing a high level of similarity. This chapter contributes a significant understanding of components present in this agro-industrial waste and thereby indicating possible routes for their utilisation.

ii) Preliminary study on HTL

The aim for the current preliminary study is to use model biomass; cellulose and lignin in HTL to understand the reaction pathway and behaviour of this major lignocellulosic component during HTL based on their liquid product. The experiment was conducted in a single component system and binary system to mimic real biomass. The results show that

the used of water in HTL system able to break down the cellulose and lignin into various chemical. Temperature plays a vital role for both model compounds; high temperature was favourable for phenolics products while cellulose decomposes at a lower temperature as compared to lignin. The most favourable temperature for HTL was at 250 ºC.

iii) A case study: HTL of BSG

The liquid product obtained from HTL of BSG consist of a complex mixture of mainly carbon, oxygen, hydrogen and nitrogen which includes a multitude of carboxylic acids, aldehydes, alcohols, ketones, phenols and also pyrazines. The product distribution obtained from real biomass is significantly different when compared to the model biomass; the composition of real biomass is more complicated than a binary mixture of lignin and cellulose. These data strongly suggest that caution should be taken when evaluating results obtained from research on the model system as real biomass behave very differently. BSG HTL was studied in the range of 15 min to 120 min reaction time, and the data show that upon increasing the reaction time from 15 min to 30 min, there is a significant increase in both conversion (73%) and WSO yield (22%) in the BSG HTL reaction. However, increasing time beyond this point causes a reduction in conversion and WSO production. Results also show that the amount of liquid product is proportional with WSO yield obtained in the system.

iv) Direct liquefaction of BSG: Effect of solvent

In a biomass liquefaction process, the presence of solvent promotes such reactions as solvolysis, hydration, and pyrolysis, which helps achieve better fragmentation of biomass and enhances dissolution of reaction intermediates. In this chapter, the reaction process focusing on direct liquefaction of BSG in different solvents and their effect on the product distribution and the biochar obtained was investigated. The

results show that with the addition of an organic solvent in direct liquefaction reaction, the conversion increased significantly; MeOH-water system provides the highest conversion at 82 %, followed by 77 %, 75 % and 72 % for EtOH- water, 2-PrOH-water and water as the solvent, respectively. It was found that the 2-PrOH-water system provides the most favourable conditions of those studied with the highest liquid product (10 g) and WSO yield (29 %) recorded. Based onWSO yield obtained, the solvent efficiency in the BSG liquefaction can be sequenced as follows: 2- PrOH- water > EtOH-water > water >MeOH-water. Further investigation on BSG biochar as potential solid fuel also conducted by undergone several characterisation techniques; FTIR spectroscopy, proximate and ultimate analysis. Based on Van Krevelen plots, biochar obtained in the present study can be used directly for coal-fuelled boilers without the need for any modifications.

The overall data presented in this current work demonstrates that HTL process are possible to use as an excellent conversion method for BSG to produce a useful chemicals and valuable product. This process is meant to provide a conversion for BSG waste which consists very high moisture content without drying and by maintaining a liquid water processing medium as a green solvent.

8.2 Recommendation for future work

Results obtained in current work demonstrated the potential of direct liquefaction in converting BSG as lignocellulosic biomass into useful chemicals. However, further research is required to overcome the limitation in currents findings. The following recommendation can be made to improve and continue the work reported in here:

i) Further improved in separation and determination of the liquefaction products is one of the main task, which should be considered in the future work. Current method taken for analysing just the aqueous and solid products seems need to be improved. For example, all the product obtain throughout the liquefaction reaction should be taken into

consideration and should be analyse (gas phase, liquid phase and solid phase). These results may crucial to be determine qualitative and quantitativelyfor better understanding into this liquefaction processes.

ii) In Chapter 7, it was shown that the addition of alcohol solvent enhanced the production of liquid product and WSO yield in liquefaction. Further research in solvent selection; i.e. type of solvent, varying the mol ratio between water and solvent may be beneficial in optimising this process.

iii) In the present work, the liquefaction reactions are conducted in non-catalytic system. Water at subcritical condition is believe to act as both; acidic and basic catalyst through self-dissociation at elevated temperature. However, the used proper catalyst can improve the liquefaction efficiency by suppressing char and tar formation (Toor, Rosendahl and Rudolf, 2011; Stocker, 2013) andalso improve liquid products quality (Huesemann et al., 2010). On top of that, by using heterogeneous catalysts in the processes, it probably be an added value to HTL. Duan& Savage, 2011, in their research found that the bio-crude produced from liquefaction with Pd/C, Pt/ C, Ru/C, and $CoMo/Al_2O_3$ flowed easily and were much less viscous than the bio-crudes from uncatalysed or zeolite-catalysed liquefaction. Besides, they also find that the different catalysts had different effects on the gas yields and composition, which are Ni and Ru were the most effective materials for increasing H_2 yields and highest production of CH_4.

iv) In regards to catalytic liquefaction, the liquefaction product and potential catalyst should undergo characterisation in order to understand the chemical and physical characteristic of the catalyst. These characterisation methods will help in designing the desired catalyst with high activity and selectivity. A combination of an active catalyst and optimum reaction conditions must be developed and confirmed by this characterization stages. The range of characterisation

techniques used will provide different information on properties of catalyst:

- ✓ SEM-EDX and TEM: useful to understand the morphology and elemental dispersion on the surface of the prepared catalyst. Besides, EDX will provide the elemental composition on the surface of the catalyst.
- ✓ Nitrogen Adsorption (NA) and BET: the available method to determine the wide range of pore size and pore volume distribution of porous material catalyst which might effect in catalytic selectivity in liquefaction process.
- ✓ XRD: used to measure the structure of the catalyst and their degree of crystallinity

v) Once the catalyst and the optimization of reaction conditions are developed, this reaction can be apply to the other lignocellulosic biomass and their product distribution should be recorded and compared. This stage will contribute to a significant finding in this research which involves the versatility of the liquefaction reaction conditions towards other lignocellulosic biomass. Examples for other biomass waste are pine needle, corn cob and potato peeling.

vi) Another interesting factor in biomass conversion is the applicability and effectiveness of high-pressure CO_2 and CO_2–H_2O technology for biomass pretreatment. This system offer a potential as an alternative to conventional methods such as acid-catalysed and water-only reactions and it has been reviewed by (Relvas et al., 2015). They found that with presence of CO_2 in hydrothermal processes, it does allow *in situ* formation of acidic environment, which promotes acid-catalyzed hydrolysis of biomass-derived and without the typical disadvantages of acid-catalyzed reactions. In this respect, (Van Walsum et al, 2007) also observed that the addition of CO_2 to water-only reactions allowed to hydrolyse pure xylan to produce xylose oligomers at lower temperatures and at shorter holding times in comparison to those obtained with autohydrolysis (water-only) technology.

REFERENCES

Achinas, S. and Euverink, G. J. W. (2016) 'Consolidated briefing of biochemical ethanol production from lignocellulosic biomass', *Electronic Journal of Biotechnology*. Elsevier B.V., 23, pp. 44–53. doi: 10.1016/j.ejbt.2016.07.006.

Ail, S. S. and Dasappa, S. (2016) 'Biomass to liquid transportation fuel via Fischer Tropsch synthesis – Technology review and current scenario', *Renewable and Sustainable Energy Reviews*, 58, pp. 267–286. doi: 10.1016/j.rser.2015.12.143.

Åkerlöf, G. (1932) 'Dielectric constants of some organic solvent-water mixtures at various temperatures', *Journal of the American Chemical Society*, 54(11), pp. 4125–4139. doi: 10.1021/ja01350a001.

Akia, M., Yazdani, F. and Motaee, E. (2014) 'A review on conversion of biomass to biofuel by nanocatalysts', *Biofuel Research …*, 1, pp. 16–25. Available at: http://www.biofueljournal.com/article_4747_0.html.

Aliyu, S. and Bala, M. (2013) 'Brewer's spent grain: A review of its potentials and applications', *African Journal of Biotechnology*, 10(3), pp. 324–331. doi: 10.4314/ajb.v10i3.

Alonso, D. M., Bond, J. Q. and Dumesic, J. A. (2010) 'Catalytic conversion of biomass to biofuels', *Green Chemistry*, 12(9), pp. 1493–1513. doi: 10.1039/c004654j.

Alonso, D. M., Wettstein, S. G. and Dumesic, J. a (2012) 'Bimetallic catalysts for upgrading of biomass to fuels and chemicals.', *Chemical Society reviews*, 41(24), pp. 8075–98. doi: 10.1039/c2cs35188a.

Álvarez-Murillo, A. *et al.* (2016) 'Generation of biofuel from hydrothermal carbonization of cellulose. Kinetics modelling', *Energy*, 94, pp. 600–608. doi: 10.1016/j.energy.2015.11.024.

Anselmo Filho, P. and Badr, O. (2004) 'Biomass resources for energy in North-Eastern Brazil', *Applied Energy*, 77(1), pp. 51–67. doi: 10.1016/S0306-2619(03)00095-3.

Anukam, A. I. *et al.* (2017) 'Studies on Characterization of Corn Cob for Application in a Gasification Process for Energy Production', *Journal of Chemistry*, 2017. doi: 10.1155/2017/6478389.

Araújo, K. *et al.* (2017) 'Global Biofuels at the Crossroads: An Overview of Technical, Policy, and Investment Complexities in the Sustainability of Biofuel Development', *Agriculture*, 7(4), p. 32. doi: 10.3390/agriculture7040032.

Arni, S. Al (2018) ‘Comparison of slow and fast pyrolysis for converting biomass into fuel’, 124, pp. 197–201.

Asghari, F. S. and Yoshida, H. (2006) ‘Acid-catalyzed production of 5-hydroxymethyl furfural from D-fructose in subcritical water’, *Industrial and Engineering Chemistry Research*, 45(7), pp. 2163–2173. doi: 10.1021/ie051088y.

Atabani, A. E. *et al.* (2012) ‘A comprehensive review on biodiesel as an alternative energy resource and its characteristics’, *Renewable and Sustainable Energy Reviews*. Elsevier Ltd, 16(4), pp. 2070–2093. doi: 10.1016/j.rser.2012.01.003.

Babu, B. V (2008) ‘Biomass pyrolysis : a state-of- the-art review’, 031, pp. 393–414. doi: 10.1002/bbb.

Bajpai, P. (2015) ‘Management of pulp and paper mill waste’, *Management of Pulp and Paper Mill Waste*, pp. 1–197. doi: 10.1007/978-3-319-11788-1.

Barakat, A., de Vries, H. and Rouau, X. (2013) ‘Dry fractionation process as an important step in current and future lignocellulose biorefineries: A review’, *Bioresource Technology*. Elsevier Ltd, 134, pp. 362–373. doi: 10.1016/j.biortech.2013.01.169.

Barbier, J. *et al.* (2012) ‘Hydrothermal conversion of lignin compounds. A detailed study of fragmentation and condensation reaction pathways’, *Biomass and Bioenergy*, 46, pp. 479–491. doi: 10.1016/j.biombioe.2012.07.011.

Besse, X., Schuurman, Y. and Guilhaume, N. (2015) ‘Hydrothermal conversion of lignin model compound eugenol’, *Catalysis Today*, 258, pp. 270–275. doi: 10.1016/j.cattod.2014.12.010.

Bhatnagar, A. and Sillanpää, M. (2010) ‘Utilization of agro-industrial and municipal waste materials as potential adsorbents for water treatment-A review’, *Chemical Engineering Journal*, 157(2-3), pp. 277–296. doi: 10.1016/j.cej.2010.01.007.

Boeriu, C. G. *et al.* (2004) ‘Characterisation of structure-dependent functional properties of lignin with infrared spectroscopy’, *Industrial Crops and Products*, 20(2), pp. 205–218. doi: 10.1016/j.indcrop.2004.04.022.

Borugadda, V. B. and Goud, V. V. (2012) ‘Biodiesel production from renewable feedstocks: Status and opportunities’, *Renewable and Sustainable Energy Reviews*, 16(7), pp. 4763–4784. doi: 10.1016/j.rser.2012.04.010.

BP (2014) *BP Energy Outlook 2035*.

Brennan, L. and Owende, P. (2010) ‘Biofuels from microalgae-A review of technologies for production, processing, and extractions of biofuels and co-products’, *Renewable and Sustainable Energy Reviews*, 14(2), pp. 557–577. doi: 10.1016/j.rser.2009.10.009.

Bridgwater, a (2003) ‘Renewable fuels and chemicals by thermal processing of biomass’, *Chemical Engineering Journal*, 91(2-3), pp. 87–102. Available at: http://linkinghub.elsevier.com/retrieve/pii/S1385894702001420.

Bridgwater, a. V. (1999) ‘Principles and practice of biomass fast pyrolysis processes for liquids’, *Journal of Analytical and Applied Pyrolysis*, 51(1), pp. 3–22. doi: 10.1016/S0165-2370(99)00005-4.

Briens, C., Piskorz, J. and Berruti, F. (2008) ‘Biomass Valorization for Fuel and Chemicals Production -- A Review’, *International Journal of Chemical Reactor Engineering*, 6(1). doi: 10.2202/1542-6580.1674.

Bye, J. W. *et al.* (2017) ‘Analysis of Mesoscopic Structured 2-Propanol/Water Mixtures Using Pressure Perturbation Calorimetry and Molecular Dynamic Simulation’, *Journal of Solution Chemistry*. Springer US, 46(1), pp. 175–189. doi: 10.1007/s10953-016-0554-y.

Caetano, N. S. *et al.* (2013) ‘Bioethanol from Brewer ’ s Spent Grains : Acid Pretreatment Optimization’, 35, pp. 1021–1026. doi: 10.3303/CET1335170.

Canabarro, N. *et al.* (2013) ‘Thermochemical processes for biofuels production from biomass’, *Sustainable Chemical Processes*, 1(1), p. 22. doi: 10.1186/2043-7129-1-22.

Cao, L. *et al.* (2018) ‘Lignin valorization for the production of renewable chemicals: State-of-the-art review and future prospects’, *Bioresource Technology*. Elsevier, 269(June), pp. 465–475. doi: 10.1016/j.biortech.2018.08.065.

De Caprariis, B. *et al.* (2017) ‘Hydrothermal liquefaction of biomass: Influence of temperature and biomass composition on the bio-oil production’, *Fuel*. Elsevier Ltd, 208, pp. 618–625. doi: 10.1016/j.fuel.2017.07.054.

Carrier, M., Loppinet-Serani, A. and Denux, D. (2011) ‘Thermogravimetric analysis as a new method to determine the lignocellulosic composition of biomass’, *Biomass and Bioenergy*, 35(1), pp. 298–307. doi: 10.1016/j.biombioe.2010.08.067.

Castellví Barnés, M. *et al.* (2017) ‘Wood Liquefaction: Role of Solvent’, *Industrial and Engineering Chemistry Research*, 56(3), pp. 635–644. doi: 10.1021/acs.iecr.6b04086.

Chakar, F. S. and Ragauskas, A. J. (2004) ‘Review of current and future softwood kraft lignin process chemistry’, *Industrial Crops and Products*, 20(2), pp. 131–141. doi: 10.1016/j.indcrop.2004.04.016.

Chen, H. I. and Chang, H. Y. (2004) ‘Homogeneous precipitation of cerium dioxide nanoparticles in alcohol/water mixed solvents’, *Colloids and Surfaces A: Physicochemical and Engineering Aspects*, 242(1-3), pp. 61–69. doi: 10.1016/j.colsurfa.2004.04.056.

Chen, W. T. *et al.* (2014) 'Hydrothermal liquefaction of mixed-culture algal biomass from wastewater treatment system into bio-crude oil', *Bioresource Technology*, 152, pp. 130–139. doi: 10.1016/j.biortech.2013.10.111.

Chen, W.-H. *et al.* (2014) 'Thermochemical conversion of microalgal biomass into biofuels: A review.', *Bioresource technology*, 184, pp. 314–327. doi: 10.1016/j.biortech.2014.11.050.

Cherubini, F. (2010) 'The biorefinery concept: Using biomass instead of oil for producing energy and chemicals', *Energy Conversion and Management*, 51(7), pp. 1412–1421. doi: 10.1016/j.enconman.2010.01.015.

Chimica, I. and Uni, V. (2010) 'Biomass Screening for the Production of Furfural via Thermal Decomposition', pp. 2658–2671.

Crombie, K. *et al.* (2013) 'The effect of pyrolysis conditions on biochar stability as determined by three methods', *GCB Bioenergy*, 5(2), pp. 122–131. doi: 10.1111/gcbb.12030.

Demain, A. L. *et al.* (2005) 'Cellulase, Clostridia, and Ethanol', 69(1), pp. 124–154. doi: 10.1128/MMBR.69.1.124.

Demirbas, A. (2011) 'Competitive liquid biofuels from biomass', *Applied Energy*. Elsevier Ltd, 88(1), pp. 17–28. doi: 10.1016/j.apenergy.2010.07.016.

Demirbaş, A. (2000) 'Mechanisms of liquefaction and pyrolysis reactions of biomass', *Energy Conversion and Management*, 41(6), pp. 633–646. doi: 10.1016/S0196-8904(99)00130-2.

Demirbaş, A. (2001) 'Biomass resource facilities and biomass conversion processing for fuels and chemicals', *Energy Conversion and Management*, 42(11), pp. 1357–1378. doi: 10.1016/S0196-8904(00)00137-0.

Deng, W., Zhang, Q. and Wang, Y. (2015) 'Catalytic transformation of cellulose and its derived carbohydrates into chemicals involving C-C bond cleavage', *Journal of Energy Chemistry*, 24(5), pp. 595–607. doi: 10.1016/j.jechem.2015.08.016.

Déniel, M. *et al.* (2016) 'Energy valorisation of food processing residues and model compounds by hydrothermal liquefaction', *Renewable and Sustainable Energy Reviews*, 54, pp. 1632–1652. doi: 10.1016/j.rser.2015.10.017.

Elliott, D. C. *et al.* (2014) 'Bioresource Technology Hydrothermal liquefaction of biomass : Developments from batch to continuous process', *Bioresource Technology*. Elsevier Ltd, 178, pp. 147–156. doi: 10.1016/j.biortech.2014.09.132.

El-Shafey, E. I. *et al.* (2004) 'Dewatering of Brewer's Spent Grain Using a Membrane Filter Press: A Pilot Plant Study', *Separation Science and Technology*, 39(14), pp. 3237–3261. doi: 10.1081/SS-200028775.

Ezeonu, F. C. and Okaka, a. N. C. (1996) 'Process kinetics and digestion efficiency of anaerobic batch fermentation of brewer's spent grains (BSG)', *Process Biochemistry*, 31(1), pp. 7–12. doi: 10.1016/0032-9592(94)00064-6.

Fan, M., Dai, D. and Huang, B. (2012) 'Fourier Transform Infrared Spectroscopy for Natural Fibres', *Fourier Transform - Materials Analysis*. doi: 10.5772/35482.

Fărcaş, A. *et al.* (2014) 'Brewers ' spent grain – A new potential ingredient for functional foods', *Journal of Agroalimentary Processes and Technologies*, 20(2), pp. 137–141.

Fernando, S. *et al.* (2006) 'Biorefineries: Current Status, Challenges, and Future Direction', *Energy & Fuels*, 20(4), pp. 1727–1737. doi: 10.1021/ef060097w.

Fillaudeau, L., Blanpain-Avet, P. and Daufin, G. (2006) 'Water, wastewater and waste management in brewing industries', *Journal of Cleaner Production*, 14(5), pp. 463–471. doi: 10.1016/j.jclepro.2005.01.002.

Forster-Carneiro, T. *et al.* (2013a) 'Biorefinery study of availability of agriculture residues and wastes for integrated biorefineries in Brazil', *Resources, Conservation and Recycling*. Elsevier B.V., 77, pp. 78–88. doi: 10.1016/j.resconrec.2013.05.007.

Forster-Carneiro, T. *et al.* (2013b) 'Biorefinery study of availability of agriculture residues and wastes for integrated biorefineries in Brazil', *Resources, Conservation and Recycling*. Elsevier B.V., 77, pp. 78–88. doi: 10.1016/j.resconrec.2013.05.007.

G. Peter Van Walsum (2007) 'Effect of Dissolved Co2 on Accumulation of Organic Acids in Liquid Hot Water Pretrheated Biomass Hydrolyzates', 136, pp. 301–312.

Gabrielle, B. *et al.* (2007) 'Life-cycle assessment of straw use in bio-ethanol production : a case-study based on biophysical modelling production : a case-study based on biophysical modelling . Environment and Arable Crops Research Unit , Institut National de la.'

Gai, C. *et al.* (2015) 'Characterization of aqueous phase from the hydrothermal liquefaction of Chlorella pyrenoidosa', *Bioresource Technology*. Elsevier Ltd, 184, pp. 328–335. doi: 10.1016/j.biortech.2014.10.118.

Gallezot, P. (2012) 'Conversion of biomass to selected chemical products', *Chem. Soc. Rev.*, 41(4), pp. 1538–1558. doi: 10.1039/C1CS15147A.

Ganesh D. Saratale (2012) 'Lignocellulosics to ethanol: The future of the chemical and energy industry', *African Journal of Biotechnology*, 11(5), pp. 1002–1013. doi: 10.5897/AJB10.897.

Gao, Y. *et al.* (2011) 'Characterization of products from hydrothermal liquefaction and carbonation of biomass model compounds and real biomass', *Journal of Fuel Chemistry and Technology*. Institute of Coal Chemistry, Chinese Academy of Sciences, 39(12), pp. 893–900. doi: 10.1016/S1872-5813(12)60001-2.

Garcia, R. *et al.* (2013) 'Biomass proximate analysis using thermogravimetry', *Bioresource Technology*. Elsevier Ltd, 139, pp. 1–4. doi: 10.1016/j.biortech.2013.03.197.

García, R. *et al.* (2012) 'Characterization of Spanish biomass wastes for energy use', *Bioresource Technology*, 103(1), pp. 249–258. doi: 10.1016/j.biortech.2011.10.004.

Gaul, M. (2012) 'Energy for Sustainable Development An analysis model for small-scale rural energy service pathways — Applied to Jatropha -based energy services in Sumbawa , Indonesia', *Energy for Sustainable Development*. International Energy Initiative, 16(3), pp. 283–296. doi: 10.1016/j.esd.2012.05.001.

GBEP (2007) 'A Review of the Current State of Bioenergy Development in G8 +5 Countries', *Environment*, pp. 1–276. Available at: www.globalbioenergy.org.

Gollakota, A. R. K., Kishore, N. and Gu, S. (2018) 'A review on hydrothermal liquefaction of biomass', *Renewable and Sustainable Energy Reviews*, 81(April 2017), pp. 1378–1392. doi: 10.1016/j.rser.2017.05.178.

Güngören Madenoğlu, T. *et al.* (2016) 'Hydrothermal gasification of biomass model compounds (cellulose and lignin alkali) and model mixtures', *Journal of Supercritical Fluids*, 115, pp. 79–85. doi: 10.1016/j.supflu.2016.04.017.

Gupta, N. (2007) *EFFECT OF VARIOUS FILLERS ON PHYSICAL AND OPTICAL PROPERTIES OF AGRO-STRAW PAPERS*. THAPAR UNIVERSITY, India.

Harmsen, P. and Huijgen, W. (2010) 'Literature Review of Physical and Chemical Pretreatment Processes for Lignocellulosic Biomass', *Energy*, (September), pp. 1–49. Available at: http://www.ecn.nl/docs/library/report/2010/e10013.pdf.

Hassan, E. B. M. and Shukry, N. (2008) 'Polyhydric alcohol liquefaction of some lignocellulosic agricultural residues', *Industrial Crops and Products*, 27(1), pp. 33–38. doi: 10.1016/j.indcrop.2007.07.004.

Hegner, J. *et al.* (2010) 'Conversion of cellulose to glucose and levulinic acid via solid-supported acid catalysis', *Tetrahedron Letters*. Elsevier Ltd, 51(17), pp. 2356–2358. doi: 10.1016/j.tetlet.2010.02.148.

Hopfgartner, G. (2008) 'Theory and Instrumentation of Mass Spectrometry', in Ramanathan, R. (ed.) *Mass Spectrometry in Drug Metabolism and Disposition: Basic Principles and Applications*, pp. 275–293. doi: 10.1002/9780470409817.

Hu, S. *et al.* (2008) 'Characterization of char from rapid pyrolysis of rice husk', *Fuel Processing Technology*. Elsevier B.V., 89(11), pp. 1096–1105. doi: 10.1016/j.fuproc.2008.05.001.

Huang, H. and Yuan, X. (2015) 'Recent progress in the direct liquefaction of typical biomass', *Progress in Energy and Combustion Science*, 49, pp. 59–80. doi: 10.1016/j.pecs.2015.01.003.

Huang, Y.-B. and Fu, Y. (2013) 'Hydrolysis of cellulose to glucose by solid acid catalysts', *Green Chemistry*, 15(5), p. 1095. doi: 10.1039/c3gc40136g.

Huesemann, M. *et al.* (2010) *Biofuels from Microalgae and Seaweeds, Biomass to Biofuels: Strategies for Global Industries*. doi: 10.1002/9780470750025.ch8.

Iqbal, H. M. N., Kyazze, G. and Keshavarz, T. (2013) 'Advances in the valorization of lignocellulosic materials by biotechnology: An overview', *BioResources*, 8(2), pp. 3157–3176.

Iserentant, D. (1995) 'Beers: Recent Technological Innovation in Brewing', in Piggott, J. R., Lea, A. G. H. (ed.) *Fermented Baverage Production*. First Edit. Chapman & Hall, pp. 45–62. doi: 10.1007/978-1-4615-0187-9_3.

Isikgor, F. H. and Becer, C. R. (2015) 'Lignocellulosic biomass: a sustainable platform for the production of bio-based chemicals and polymers', *Polym. Chem.* Royal Society of Chemistry, 6(25), pp. 4497–4559. doi: 10.1039/C5PY00263J.

J. Sluiter, A. A. S. R. R. C. S. and Templeton, D. (2008) 'Determination of Extractives in Biomass: Laboratory Analytical Procedure (LAP); Issue Date 7/17/2005 - 42619.pdf', *Technical Report NREL/TP-510-42619*, (January), pp. 1–9. doi: NREL/TP-510-42621.

James H. Clark, F. D. (2011) 'Introduction to Chemicals from Biomass (Google eBook)', in, p. 198. Available at: http://books.google.com/books?id=h-57eVISZDIC&pgis=1.

Jazrawi, C. *et al.* (2015) 'Two-stage hydrothermal liquefaction of a high-protein microalga', *Algal Research*. Elsevier B.V., 8, pp. 15–22. doi: 10.1016/j.algal.2014.12.010.

Kanaujia, P. K. *et al.* (2014) 'Review of analytical strategies in the production and upgrading of bio-oils derived from lignocellulosic biomass', *Journal of Analytical and Applied Pyrolysis*. Elsevier B.V., 105, pp. 55–74. doi: 10.1016/j.jaap.2013.10.004.

Kang, Q. *et al.* (2014) 'Bioethanol from Lignocellulosic Biomass: Current Findings Determine Research Priorities', *The Scientific World Journal*, 2014(Ci), pp. 1–13. doi: 10.1155/2014/298153.

Kang, S. *et al.* (2013) 'Hydrothermal conversion of lignin: A review', *Renewable and Sustainable Energy Reviews*, 27, pp. 546–558. doi: 10.1016/j.rser.2013.07.013.

Karagoz, S. *et al.* (2005) 'Comparative studies of oil compositions produced from sawdust , rice husk , lignin and cellulose by hydrothermal treatment', 84, pp. 875–884. doi: 10.1016/j.fuel.2005.01.004.

Karagöz, S. *et al.* (2004) 'Low-temperature hydrothermal treatment of biomass: Effect of reaction parameters on products and boiling point distributions', *Energy and Fuels*, 18(1), pp. 234–241. doi: 10.1021/ef030133g.

Karagöz, S. *et al.* (2005) 'Low-temperature catalytic hydrothermal treatment of wood biomass: Analysis of liquid products', *Chemical Engineering Journal*, 108, pp. 127–137. doi: 10.1016/j.cej.2005.01.007.

Khan, A. A. *et al.* (2009) 'Biomass combustion in fluidized bed boilers: Potential problems and remedies', *Fuel Processing Technology*. Elsevier B.V., 90(1), pp. 21–50. doi: 10.1016/j.fuproc.2008.07.012.

Kleinert, M. and Barth, T. (2008) 'Phenols from lignin', *Chemical Engineering and Technology*, 31(5), pp. 736–745. doi: 10.1002/ceat.200800073.

Kruse, A. (2009) 'Hydrothermal biomass gasification', *Journal of Supercritical Fluids*, 47(3), pp. 391–399. doi: 10.1016/j.supflu.2008.10.009.

Kruse, A. and Dahmen, N. (2015) 'Water - A magic solvent for biomass conversion', *Journal of Supercritical Fluids*, 96, pp. 36–45. doi: 10.1016/j.supflu.2014.09.038.

Kruse, A. and Dinjus, E. (2007) 'Hot compressed water as reaction medium and reactant. Properties and synthesis reactions', *Journal of Supercritical Fluids*, 39(3), pp. 362–380. doi: 10.1016/j.supflu.2006.03.016.

Kubo, S. and Kadla, J. F. (2005) 'Hydrogen bonding in lignin: A fourier transform infrared model compound study', *Biomacromolecules*, 6(5), pp. 2815–2821. doi: 10.1021/bm050288q.

Kumar, M., Olajire Oyedun, A. and Kumar, A. (2018) 'A review on the current status of various hydrothermal technologies on biomass feedstock', *Renewable and Sustainable Energy Reviews*. Elsevier Ltd, 81(May 2017), pp. 1742–1770. doi: 10.1016/j.rser.2017.05.270.

Kumar, R. *et al.* (2016) 'Recent updates on lignocellulosic biomass derived ethanol - A review', *Biofuel Research Journal*, 3(1), pp. 347–356. doi: 10.18331/BRJ2016.3.1.4.

Kumar, S. and Gupta, R. B. (2008) 'Hydrolysis of Microcrystalline Cellulose in Subcritical and Supercritical Water in a Continuous Flow Reactor', pp. 9321–9329.

Lai, F. ying *et al.* (2018) 'Liquefaction of sewage sludge in ethanol-water mixed solvents for bio-oil and biochar products', *Energy*, 148, pp. 629–641. doi: 10.1016/j.energy.2018.01.186.

Laine, C. (2015) 'Hydrothermal refining of biomass — an overview and future perspectives', *Tappi Journal*, 14(3), pp. 195–207.

Lange, J. P. *et al.* (2012) 'Furfural-A promising platform for lignocellulosic biofuels', *ChemSusChem*, 5(1), pp. 150–166. doi: 10.1002/cssc.201100648.

Laskar, D. D. *et al.* (2013) 'Pathways for biomass-derived lignin to hydrocarbon fuels †', pp. 602–626. doi: 10.1002/bbb.

Lee, H. V, Hamid, S. B. a and Zain, S. K. (2014) 'Conversion of Lignocellulosic Biomass to Nanocellulose: Structure and Chemical Process', 2014. doi: 10.1155/2014/631013.

Lehr, V. *et al.* (2007) 'Catalytic dehydration of biomass-derived polyols in sub- and supercritical water', *Catalysis Today*, 121(1-2), pp. 121–129. doi: 10.1016/j.cattod.2006.11.014.

Li, R. *et al.* (2014) 'Mesoscopic structuring and dynamics of alcohol/water solutions probed by terahertz time-domain spectroscopy and pulsed field gradient nuclear magnetic resonance', *Journal of Physical Chemistry B*, 118(34), pp. 10156–10166. doi: 10.1021/jp502799x.

Limayem, A. and Ricke, S. C. (2012) 'Lignocellulosic biomass for bioethanol production: Current perspectives, potential issues and future prospects', *Progress in Energy and Combustion Science*, 38(4), pp. 449–467. doi: 10.1016/j.pecs.2012.03.002.

Liu, H. M. *et al.* (2013) 'Understanding the mechanism of cypress liquefaction in hot-compressed water through characterization of solid residues', *Energies*, 6(3), pp. 1590–1603. doi: 10.3390/en6031590.

Liu, W. *et al.* (2012) 'Efficient Conversion of Cellulose to Glucose, Levulinic Acid, and Other Products in Hot Water Using SO 2 as a Recoverable Catalyst', *Industrial and Engineering Chemistry Research*, 51, pp. 15503–15508. doi: 10.1021/ie302317t.

Liu, Z. and Zhang, F.-S. (2008) 'Effects of various solvents on the liquefaction of biomass to produce fuels and chemical feedstocks', *Energy Conversion and Management*, 49(12), pp. 3498–3504. doi: 10.1016/j.enconman.2008.08.009.

Lynch, K. M., Steffen, E. J. and Arendt, E. K. (2016) 'Brewers' spent grain: a review with an emphasis on food and health', *Journal of the Institute of Brewing*, 122(4), pp. 553–568. doi: 10.1002/jib.363.

M.Schwanninnger (2004) 'Effect of short-time vibratory ball milling on the shape of FT-IR spectra of wood and cellulose', *Vibrational Spectroscopy*, (36), pp. 23–40. doi: 10.15713/ins.mmj.3.

Mahmood, A. S. N. *et al.* (2013) 'The intermediate pyrolysis and catalytic steam reforming of Brewers spent grain', *Journal of Analytical and Applied Pyrolysis*, 103, pp. 328–342. doi: 10.1016/j.jaap.2012.09.009.

Mahmood, A. S. N. *et al.* (2013) 'The intermediate pyrolysis and catalytic steam reforming of Brewers spent grain', in *Journal of Analytical and Applied Pyrolysis*, pp. 328–342.

Maity, S. K. (2015) 'Opportunities, recent trends, and challenges of integrated biorefinery: Part I', *Renewable Sustainable Energy Rev.* Elsevier, 43, pp. 1427–1445. doi: 10.1016/j.rser.2014.11.092.

Malomo, O. (2013) 'The Use of Brewer′S Spent Grains in the Cultivation of Some Fungal Isolates', *International Journal of Nutrition and Food Sciences*, 2(1), p. 5. doi: 10.11648/j.ijnfs.20130201.12.

McGregor, J. *et al.* (2015) 'Structure and dynamics of aqueous 2-propanol: A THz-TDS, NMR and neutron diffraction study', *Physical Chemistry Chemical Physics*. Royal Society of Chemistry, 17(45), pp. 30481–30491. doi: 10.1039/c5cp01132a.

Mckendry, P. (2002) 'Energy production from biomass (Part 1): Overview of biomass', 83(February), pp. 37–46. doi: 10.1016/S0960-8524(01)00118-3.

McKendry, P. (2002a) 'Energy production from biomass (part 1): Overview of biomass', *Bioresource Technology*, 83(1), pp. 37–46. doi: 10.1016/S0960-8524(01)00118-3.

McKendry, P. (2002b) 'Energy production from biomass (part 2): Conversion technologies', *Bioresource Technology*, 83(1), pp. 47–54. doi: 10.1016/S0960-8524(01)00119-5.

Meneses, N. G. T. *et al.* (2013) 'Influence of extraction solvents on the recovery of antioxidant phenolic compounds from brewer's spent grains', *Separation and Purification Technology*. Elsevier B.V., 108, pp. 152–158. doi: 10.1016/j.seppur.2013.02.015.

Mika, T. L., Edit, C. and Horvath, I. T. (2015) 'The role of water in catalytic biomass-based technologies to produce chemicals and fuels', *Catalysis Today*, 247, pp. 33–46. doi: 10.1016/j.cattod.2014.10.043.

Miles, T. R. *et al.* (1996) 'Boiler deposits from firing biomass fuels', *Biomass and Bioenergy*, 10(2-3), pp. 125–138. doi: 10.1016/0961-9534(95)00067-4.

Milne, T. A. and Evans, R. J. (1998) 'Biomass Gasifier " Tars ": Their Nature , Formation , and Conversion Biomass Gasifier " Tars ": Their Nature , Formation , and Conversion', (November).

Mohanty, P. *et al.* (2014) 'Synthesis of green fuels from biogenic waste through thermochemical route – The role of heterogeneous catalyst: A review', *Renewable and Sustainable Energy Reviews*, 38, pp. 131–153. doi: 10.1016/j.rser.2014.05.011.

Mussatto, S. I. *et al.* (2010) 'Production, characterization and application of activated carbon from brewer's spent grain lignin.', *Bioresource technology*. Elsevier Ltd, 101(7), pp. 2450–7. doi: 10.1016/j.biortech.2009.11.025.

Mussatto, S. I. (2014) 'Brewer's spent grain: a valuable feedstock for industrial applications.', *Journal of the science of food and agriculture*, 94(7), pp. 1264–75. doi: 10.1002/jsfa.6486.

Mussatto, S. I., Dragone, G. and Roberto, I. C. (2006) 'Brewers' spent grain: generation, characteristics and potential applications', *Journal of Cereal Science*, 43(1), pp. 1–14. doi: 10.1016/j.jcs.2005.06.001.

Mussatto, S. I. and Roberto, I. C. (2005) 'Acid hydrolysis and fermentation of brewer's spent grain to produce xylitol', *Journal of the Science of Food and Agriculture*, 85(December 2004), pp. 2453–2460. doi: 10.1002/jsfa.2276.

Nagy, M. (2009) *Biofuels from lignin and novel biodiesel analysis*. Georgia Institute of Technology.

Nanda, S. *et al.* (2013) 'Characterization of North American Lignocellulosic Biomass and Biochars in Terms of their Candidacy for Alternate Renewable Fuels', *Bioenergy Research*, 6(2), pp. 663–677. doi: 10.1007/s12155-012-9281-4.

Nazari, L. *et al.* (2015) 'Hydrothermal liquefaction of woody biomass in hot-compressed water: Catalyst screening and comprehensive characterization of bio-crude oils', *Fuel*. Elsevier Ltd, 162, pp. 74–83. doi: 10.1016/j.fuel.2015.08.055.

Nigam, P. S. and Singh, A. (2011) 'Production of liquid biofuels from renewable resources', *Progress in Energy and Combustion Science*. Elsevier Ltd, 37(1), pp. 52–68. doi: 10.1016/j.pecs.2010.01.003.

Nizamuddin, S. *et al.* (2017) 'An overview of e ff ect of process parameters on hydrothermal carbonization of biomass', 73(December 2016), pp. 1289–1299. doi: 10.1016/j.rser.2016.12.122.

Özbay, N. *et al.* (2001) 'Biocrude from biomass: pyrolysis of cottonseed cake', *Renewable Energy*, 24(3-4), pp. 615–625. doi: 10.1016/S0960-1481(01)00048-9.

Pasangulapati, V. *et al.* (2012) 'Effects of cellulose, hemicellulose and lignin on thermochemical conversion characteristics of the selected biomass', *Bioresource Technology*, 114, pp. 663–669. doi: 10.1016/j.biortech.2012.03.036.

Pathak, B., Chaudhari, S. and Fulekar, M. H. (2013) 'Biomass - Resource for Sustainable Development', 2(6), pp. 271–289.

Pavlovič, I., Knez, Ž. and Škerget, M. (2013) 'Hydrothermal reactions of agricultural and food processing wastes in sub- and supercritical water: A review of fundamentals, mechanisms, and state of research', *Journal of Agricultural and Food Chemistry*, 61(34), pp. 8003–8025. doi: 10.1021/jf401008a.

Perkin Elmer (2004) 'Thermogravimetric Analysis (TGA)', *Perkin Elmer*, (June), pp. 3–19. doi: 10.1198/tech.2005.s328.

Peterson, A. a. *et al.* (2008) 'Thermochemical biofuel production in hydrothermal media: A review of sub- and supercritical water technologies', *Energy & Environmental Science*, 1(1), p. 32. doi: 10.1039/b810100k.

Peterson, A. A. *et al.* (2008) 'Thermochemical biofuel production in hydrothermal media: A review of sub- and supercritical water technologies', *Energy & Environmental Science*, 1(1), p. 32. doi: 10.1039/b810100k.

Peterson, A. A., Lachance, R. P. and Tester, J. W. (2010) 'Kinetic evidence of the maillard reaction in hydrothermal biomass processing: Glucose-glycine interactions in high-temperature, high-pressure water', *Industrial and Engineering Chemistry Research*, 49(5), pp. 2107–2117. doi: 10.1021/ie9014809.

Pileidis, F. D. and Titirici, M. M. (2016) 'Levulinic Acid Biorefineries: New Challenges for Efficient Utilization of Biomass', *ChemSusChem*, 9(6), pp. 562–582. doi: 10.1002/cssc.201501405.

Pińkowska, H., Wolak, P. and Złocińska, A. (2012) 'Hydrothermal decomposition of alkali lignin in sub- and supercritical water', *Chemical Engineering Journal*, 187, pp. 410–414. doi: 10.1016/j.cej.2012.01.092.

Poerschmann, J. *et al.* (2014) 'Bioresource Technology Characterization of biocoals and dissolved organic matter phases obtained upon hydrothermal carbonization of brewer ' s spent grain', *Bioresource Technology*, 164, pp. 162–169. doi: 10.1016/j.biortech.2014.04.052.

Quispe, C. a. G., Coronado, C. J. R. and Carvalho Jr., J. a. (2013) 'Glycerol: Production, consumption, prices, characterization and new trends in combustion', *Renewable and Sustainable Energy Reviews*. Elsevier, 27, pp. 475–493. doi: 10.1016/j.rser.2013.06.017.

Ragauskas, A. J. *et al.* (2006) 'The path forward for biofuels and biomaterials.', *Science (New York, N.Y.)*, 311(5760), pp. 484–489. doi: 10.1126/science.1114736.

Reddy, N. and Yang, Y. (2005) 'Biofibers from agricultural byproducts for industrial applications', *Trends in Biotechnology*, 23(1), pp. 22–27. doi: 10.1016/j.tibtech.2004.11.002.

Relvas, F. M., Morais, A. R. C. and Bogel-Lukasik, R. (2015) 'Selective hydrolysis of wheat straw hemicellulose using high-pressure CO_2 as catalyst', *RSC Adv.* Royal Society of Chemistry, 5(90), pp. 73935–73944. doi: 10.1039/C5RA14632A.

Del Río, J. C., Prinsen, P. and Gutiérrez, A. (2013) 'Chemical composition of lipids in brewer's spent grain: A promising source of valuable phytochemicals', *Journal of Cereal Science*, 58(2), pp. 248–254. doi: 10.1016/j.jcs.2013.07.001.

Rodríguez-Gutiérrez, G. *et al.* (2014) 'Properties of lignin, cellulose, and hemicelluloses isolated from olive cake and olive stones: Binding of water, oil, bile acids, and glucose', *Journal of Agricultural and Food Chemistry*, 62(36), pp. 8973–8981. doi: 10.1021/jf502062b.

Van Rossum, G. *et al.* (2014) 'Liquefaction of lignocellulosic biomass: Solvent, process parameter, and recycle oil screening', *ChemSusChem*, 7(1), pp. 253–259. doi: 10.1002/cssc.201300297.

Rubin, E. M. (2008) 'Genomics of cellulosic biofuels.', *Nature*, 454(7206), pp. 841–845. doi: 10.1038/nature07190.

Russ, W., Mörtel, H. and Meyer-Pittroff, R. (2005) 'Application of spent grains to increase porosity in bricks', *Construction and Building Materials*, 19(2), pp. 117–126. doi: 10.1016/j.conbuildmat.2004.05.014.

Saisu, M. *et al.* (2003) 'Conversion of lignin with supercritical water-phenol mixtures', *Energy and Fuels*, 17(4), pp. 922–928. doi: 10.1021/ef0202844.

Saldarriaga, J. F. *et al.* (2015) 'Fast characterization of biomass fuels by thermogravimetric analysis (TGA)', *Fuel*. Elsevier Ltd, 140, pp. 744–751. doi: 10.1016/j.fuel.2014.10.024.

Samuelsson, R., Burvall, J. and Jirjis, R. (2006) 'Comparison of different methods for the determination of moisture content in biomass', *Biomass and Bioenergy*, 30(11), pp. 929–934. doi: 10.1016/j.biombioe.2006.06.004.

Saxena, R. C., Adhikari, D. K. and Goyal, H. B. (2009a) 'Biomass-based energy fuel through biochemical routes: A review', *Renewable and Sustainable Energy Reviews*, 13(1), pp. 167–178. doi: 10.1016/j.rser.2007.07.011.

Saxena, R. C., Adhikari, D. K. and Goyal, H. B. (2009b) 'Biomass-based energy fuel through biochemical routes: A review', *Renewable and Sustainable Energy Reviews*, 13(1), pp. 167–178. doi: 10.1016/j.rser.2007.07.011.

Sežun, M. *et al.* (2011) 'Anaerobic digestion of brewery spent grain in a semi-continuous bioreactor: Inhibition by phenolic degradation products', *Acta Chimica Slovenica*, 58(1), pp. 158–166.

Sills, D. L. and Gossett, J. M. (2012) 'Using FTIR to Predict Saccharification From Enzymatic Hydrolysis of Alkali-Pretreated Biomasses', 109(2), pp. 353–362. doi: 10.1002/bit.23314.

Silva, J. P. *et al.* (2004) 'Adsorption of acid orange 7 dye in aqueous solutions by spent brewery grains', *Separation and Purification Technology*, 40(3), pp. 309–315. doi: 10.1016/j.seppur.2004.03.010.

Singh, R. *et al.* (2015) 'Conversion of rice straw to monomeric phenols under supercritical methanol and ethanol.', *Bioresource technology*. Elsevier Ltd, 188, pp. 280–6. doi: 10.1016/j.biortech.2015.01.001.

Sneddon, J., Masuram, S. and Richert, J. C. (2007) 'Gas Chromatography-Mass Spectrometry-Basic Principles, Instrumentation and Selected Applications for Detection of Organic Compounds', *Analytical Letters*, 40(6), pp. 1003–1012. doi: 10.1080/00032710701300648.

Stocker, M. (2013) 'Catalytic Hydrotreatment of Bio-Oils for High-Quality Fuel Production', (Chapter 11), pp. 351–396. Available at: https://doi.org/10.1016/B978-0-444-56330-9.00011-5.

Stöcker, M. (2008) ‘Biofuels and biomass-to-liquid fuels in the biorefinery: catalytic conversion of lignocellulosic biomass using porous materials.’, *Angewandte Chemie (International ed. in English)*, 47(48), pp. 9200–11. doi: 10.1002/anie.200801476.

Stojceska, V. *et al.* (2008) ‘The recycling of brewer’s processing by-product into ready-to-eat snacks using extrusion technology’, *Journal of Cereal Science*, 47(3), pp. 469–479. doi: 10.1016/j.jcs.2007.05.016.

Stuart, B. H. (2004) *Infrared Spectroscopy: Fundamentals and Applications*, *Wiley*. doi: 10.1002/0470011149.

Sumit Sharma *et al.* (2014) ‘Biomass Conversion Technologies for Renewable Energy and Fuels: A Review Note.’, *IOSR Journal of Mechanical and Civil Engineering (IOSR-JMCE)*, 11(2), pp. 28–35. Available at: http://www.iosrjournals.org/iosr-jmce/papers/vol11-issue2/Version-3/C011232835.pdf.

Sun, Y. and Cheng, J. (2002) ‘Hydrolysis of lignocellulosic materials for ethanol production: A review’, *Bioresource Technology*, 83, pp. 1–11. doi: 10.1016/S0960-8524(01)00212-7.

Suryanarayana, C. (2001) ‘Mechanical alloying and milling’, *Progress in Materials Science*, 46(1-2), pp. 1–184. doi: 10.1016/S0079-6425(99)00010-9.

Tan, H. W., Abdul Aziz, a. R. and Aroua, M. K. (2013) ‘Glycerol production and its applications as a raw material: A review’, *Renewable and Sustainable Energy Reviews*, 27, pp. 118–127. doi: 10.1016/j.rser.2013.06.035.

Tanger, P. *et al.* (2013) ‘Biomass for thermochemical conversion: targets and challenges’, *Frontiers in Plant Science*, 4(July), pp. 1–20. doi: 10.3389/fpls.2013.00218.

Technical Association of Pulp and Paper Industry (1997) ‘T204 cm-97. Solvent extractives of wood and pulp.’, *TAPPI test methods*, p. 12. doi: 10.5772/916.

Tekin, K., Karagöz, S. and Bektaş, S. (2014) ‘A review of hydrothermal biomass processing’, *Renewable and Sustainable Energy Reviews*, 40, pp. 673–687. doi: 10.1016/j.rser.2014.07.216.

Telmo, C. and Lousada, J. (2011) ‘The explained variation by lignin and extractive contents on higher heating value of wood’, *Biomass and Bioenergy*, 35(5), pp. 1663–1667. doi: 10.1016/j.biombioe.2010.12.038.

Thomas, K. R. and Rahman, P. K. S. M. (2006) ‘Brewery wastes . Strategies for sustainability . A review’, *Aspects of Applied Biology*, 80, pp. 147–153.

Titirici, M. M. and Antonietti, M. (2010) ‘Chemistry and materials options of sustainable carbon materials made by hydrothermal carbonization’, *Chemical Society Reviews*, 39(1), pp. 103–116. doi: 10.1039/b819318p.

Toor, S. S., Rosendahl, L. and Rudolf, A. (2011) 'Hydrothermal liquefaction of biomass: A review of subcritical water technologies', *Energy*, 36(5), pp. 2328–2342. doi: 10.1016/j.energy.2011.03.013.

Tucker, M. P. *et al.* (2001) 'Fourier transform infrared quantitative analysis of sugars and lignin in pretreated softwood solid residues', *Applied Biochemistry and Biotechnology - Part A Enzyme Engineering and Biotechnology*, 91-93, pp. 51–61. doi: 10.1385/ABAB:91-93:1-9:51.

Vanreppelen, K. *et al.* (2014) 'Activated carbon from pyrolysis of brewer's spent grain: Production and adsorption properties', *Waste Management and Research*, 32(7), pp. 634–645. doi: 10.1177/0734242X14538306.

Vassilev, S. V. *et al.* (2010) 'An overview of the chemical composition of biomass', *Fuel*, 89(5), pp. 913–933. doi: 10.1016/j.fuel.2009.10.022.

Wahyudiono *et al.* (2007) 'Decomposition of a lignin model compound under hydrothermal conditions', *Chemical Engineering and Technology*, 30(8), pp. 1113–1122. doi: 10.1002/ceat.200700066.

Wahyudiono, Sasaki, M. and Goto, M. (2008) 'Recovery of phenolic compounds through the decomposition of lignin in near and supercritical water', *Chemical Engineering and Processing: Process Intensification*, 47(9-10), pp. 1609–1619. doi: 10.1016/j.cep.2007.09.001.

Waters, D. M. *et al.* (2012) 'Fibre, protein and mineral fortification of wheat bread through milled and fermented brewer's spent grain enrichment', *European Food Research and Technology*, 235(5), pp. 767–778. doi: 10.1007/s00217-012-1805-9.

Watkins, D. *et al.* (2015) 'Extraction and characterization of lignin from different biomass resources', *Journal of Materials Research and Technology*. Korea Institute of Oriental Medicine, 4(1), pp. 26–32. doi: 10.1016/j.jmrt.2014.10.009.

Weger, A. *et al.* (2014) 'Solid Biofuel Production by Mechanical Pre-Treatment of Brewers ' Spent Grain', 37, pp. 661–666. doi: 10.3303/CET1437111.

Weingarten, R., Conner, W. C. and Huber, G. W. (2012) 'Production of levulinic acid from cellulose by hydrothermal decomposition combined with aqueous phase dehydration with a solid acid catalyst', *Energy and Environmental Science*, 5(6), pp. 7559–7574. doi: 10.1039/c2ee21593d.

Werpy, T. and Petersen, G. (2004) 'Top Value Added Chemicals from Biomass Volume I — Results of Screening for Potential Candidates from Sugars and Synthesis Gas Top Value Added Chemicals From Biomass Volume I : Results of Screening for Potential Candidates', *Other Information: PBD: 1 Aug 2004*, p. Medium: ED; Size: 76 pp. pages. doi: 10.2172/15008859.

White, J. S., Yohannan, B. K. and Walker, G. M. (2008) 'Bioconversion of brewer's spent grains to bioethanol', *FEMS Yeast Research*, 8(7), pp. 1175–1184. doi: 10.1111/j.1567-1364.2008.00390.x.

Xiros, C. and Christakopoulos, P. (2009) 'Enhanced ethanol production from brewer's spent grain by a Fusarium oxysporum consolidated system.', *Biotechnology for biofuels*, 2(1), p. 4. doi: 10.1186/1754-6834-2-4.

Xu, C. C. et. al (2014) *Application of Hydrothermal Reactions to Biomass Conversion*. Edited by F. Jin. Springer. doi: 10.1007/978-3-642-54458-3.

Xu, F. *et al.* (2013) 'Qualitative and quantitative analysis of lignocellulosic biomass using infrared techniques: A mini-review', *Applied Energy*, 104, pp. 801–809. doi: 10.1016/j.apenergy.2012.12.019.

Yin, S., Mehrotra, A. K. and Tan, Z. (2011) 'Alkaline hydrothermal conversion of cellulose to bio-oil: Influence of alkalinity on reaction pathway change', *Bioresource Technology*, 102(11), pp. 6605–6610. doi: 10.1016/j.biortech.2011.03.069.

Yin, S., Pan, Y. and Tan, Z. (2011) 'Hydrothermal conversion of cellulose to 5-hydroxymethyl furfural', *International Journal of Green Energy*, 8(2), pp. 234–247. doi: 10.1080/15435075.2010.548888.

Yin, S. and Tan, Z. (2012) 'Hydrothermal liquefaction of cellulose to bio-oil under acidic, neutral and alkaline conditions', *Applied Energy*, 92, pp. 234–239. doi: 10.1016/j.apenergy.2011.10.041.

Yinxin, Z., Jishi, Z. and Yi, M. (2015) 'Preparation and Application of Biochar from Brewery ` s Spent Grain and Sewage Sludge', pp. 14–19.

Yip, J. *et al.* (2009) 'Comparative study of liquefaction process and liquefied products from bamboo using different organic solvents', *Bioresource Technology*, 100(24), pp. 6674–6678. doi: 10.1016/j.biortech.2009.07.045.

Yong, T. L. K. and Yukihiko, M. (2013) 'Kinetic analysis of guaiacol conversion in sub- and supercritical water', *Industrial and Engineering Chemistry Research*, 52(26), pp. 9048–9059. doi: 10.1021/ie4009748.

Yu, Y., Liu, D. and Wu, H. (2012) 'Characterization of water-soluble intermediates from slow pyrolysis of cellulose at low temperatures', *Energy and Fuels*, 26(12), pp. 7331–7339. doi: 10.1021/ef3013097.

Yu, Y., Lou, X. and Wu, H. (2008) 'Some Recent Advances in Hydrolysis of Biomass in Hot-Compressed Water and Its Comparisons with Other Hydrolysis Methods', *Energy and Fuels*, 22(1), pp. 46–60. doi: 10.1021/ef700292p.

Zakzeski, J. *et al.* (2010) 'The catalytic valorization of lignin for the production of renewable chemicals', *Chemical Reviews*, 110(6), pp. 3552–3599. doi: 10.1021/cr900354u.

Zhang, J. and Wang, Q. (2016) 'Sustainable mechanisms of biochar derived from brewers ' spent grain and sewage sludge for ammonia e nitrogen capture', *Journal of Cleaner Production*, 112, pp. 3927–3934. doi: 10.1016/j.jclepro.2015.07.096.

Zhang, Q. *et al.* (2007) 'Review of biomass pyrolysis oil properties and upgrading research', *Energy Conversion and Management*, 48(1), pp. 87–92. doi: 10.1016/j.enconman.2006.05.010.

Zhang, Y. (2010) *Hydrothermal Liquefaction to Convert Biomass into Crude Oil*, *Biofuels from Agricultural Wastes and Byproducts*. doi: 10.1002/9780813822716.ch10.

Zhao, Y. P. *et al.* (2013) 'Synergic effect of methanol and water on pine liquefaction', *Bioresource Technology*. Elsevier Ltd, 142, pp. 504–509. doi: 10.1016/j.biortech.2013.05.028.

Zhao, Y.-P. *et al.* (2013) 'Synergic effect of methanol and water on pine liquefaction.', *Bioresource technology*, 142, pp. 504–9. doi: 10.1016/j.biortech.2013.05.028.

Zheng, C. Y., Tao, H. X. and Xie, X. A. (2013) 'Distribution and characterizations of liquefaction of celluloses in sub- and super-critical ethanol', *BioResources*, 8(1), pp. 648–662.

Zhou, C.-H. *et al.* (2011) 'Catalytic conversion of lignocellulosic biomass to fine chemicals and fuels.', *Chemical Society reviews*, 40(11), pp. 5588–617. doi: 10.1039/c1cs15124j.

Zhu, J. Y. and Pan, X. J. (2010) 'Woody biomass pretreatment for cellulosic ethanol production: Technology and energy consumption evaluation', *Bioresource Technology*. Elsevier Ltd, 101(13), pp. 4992–5002. doi: 10.1016/j.biortech.2009.11.007.

Zhu, J. Y., Pan, X. and Zalesny, R. S. (2010) 'Pretreatment of woody biomass for biofuel production: Energy efficiency, technologies, and recalcitrance', *Applied Microbiology and Biotechnology*, 87(3), pp. 847–857. doi: 10.1007/s00253-010-2654-8.

Zhu, Z. *et al.* (2009) 'Analysis of product distribution and characteristics in hydrothermal liquefaction of Barley Straw in Subcritical and Supercritical water', *Environmental Progress*, 28(3), pp. 404–409.

Zhu, Z. *et al.* (2015) 'Influence of alkali catalyst on product yield and properties via hydrothermal liquefaction of barley straw', *Energy*, 80, pp. 284–292. doi: 10.1016/j.energy.2014.11.071.